GENE EDITING IN RICE AND PEANUT: MULTIPLEX EDITING, PROTOPLAST VALIDATION, AND PRIME EDITING

A Dissertation

by

SUDIP BISWAS

Submitted to the Graduate and Professional School of
Texas A&M University
in partial fulfillment of the requirements for the degree of

DOCTOR OF PHILOSOPHY

Chair of Committee,	Endang M. Septiningsih
Committee Members,	Michael Thomson
	Keerti Rathore
	Dmitry Kurouski
Head of Department,	David D. Baltensperger

May 2022

Major Subject: Plant Breeding

ABSTRACT

CRISPR-Cas9 is a powerful and versatile genome-editing tool for introducing genetic changes for studying gene expression and improving crops, including rice (*Oryza sativa* L.) and peanut (*Arachis hypogaea L.*). Resistant starch is a starch product that is not easily digestible and absorbed in the stomach or small intestine and instead is passed on directly to the large intestine. Cereals high in resistant starch are beneficial to improve human health and reduce the risk of diet-related chronic diseases. It was previously reported through chemical mutagenesis and RNA interference studies that some of the starch branching enzymes (*SBEs*) may play a major role in developing higher levels of resistant starch in crops. To test the specific roles of all four rice *SBE* genes in rice, a CRISPR-Cas9 vector construct with four *SBE* gene sgRNAs was transformed into the U.S. rice variety Presidio using *Agrobacterium*-mediated transformation. Targeted mutations were identified, and several *SBE* edited lines showed significantly increased resistant starch content up to 15% higher than the parental cultivar, Presidio. This study demonstrated an example of developing lines with high resistant starch through multiplex CRISPR-Cas9-mediated genome editing. Likewise, improving peanut production and nutrition will require new technologies to enable novel trait development. To test multiplex CRISPR-Cas9 genome editing in peanut, an efficient protoplast editing system was developed to knock out a major allergen gene with the help of an endogenous tRNA-processing system. Peanut protoplast isolation and transformation were successfully optimized and two sgRNAs for an allergen gene, *Ara h 2*, were designed, tested with in vitro digestion with Cas9, and validated by PEG-mediated transformation in protoplasts, resulting in the identification of knockout mutations. Thus, the protoplast transformation system

can serve as a rapid and effective tool for gRNA validation in peanut. Lastly, prime editing, a new technique providing a wide range of precise mutation types, was tested in rice and peanut. Although more optimizations will be needed, a mutant GFP was successfully edited using prime editing in both rice and peanut protoplasts. These studies pave the way for more efficient and precise gene editing for rice and peanut improvement.

DEDICATION

To my wife (Roly Malaker) and my parents.

ACKNOWLEDGEMENTS

I am grateful to everyone who has helped me in my struggle to achieve my dream of earning a Ph.D. degree. First, I would like to thank Dr. Endang M. Septiningsih and Dr. Michael Thomson for their continual support and guidance of my graduate studies with endless patience. My sincere thanks to my other committee members, Dr. Keerti Rathore and Dr. Dmitry Kurouski, who have given much time, effort and knowledge to aid in the completion of this dissertation.

I would also like to thank Dr. John Cason for providing the seeds for the peanut research in this dissertation. I would like to acknowledge Marco Molina-Risco and Mayra Faion-Molina from the Texas A&M AgriLife Research Multi Crop Transformation Facility Lab for helping me by generating rice plants through transformation. The faculty, staff, and students in the Soil and Crop Sciences Department also deserve recognition, as well as LeAnn Hague and Taylor L. Atkinson, for helping me deal with document processing and unexpected situations as an international student. Many thanks go to all the current and previous lab members as well as undergraduate students of the Texas A&M AgriLife Research Crop Genome editing lab who helped me a lot in my thesis work. I would also like to thank the Soil and Crop Sciences Department for all the support for my graduate studies. Finally, I express my gratitude to my family for all of the love and support they have sent my way along this journey.

CONTRIBUTORS AND FUNDING SOURCES

Contributors

This work was supervised by a dissertation committee consisting of Professors Endang M. Septiningsih, Michael Thomson, and Keerti Rathore of the Department of Soil and Crop Sciences, and Professor Dmitry Kurouski of the Department of Biochemistry and Biophysics.

The data for Chapter 3 were published in the International Journal of Molecular Sciences (2021). Dr. Endang Septiningsih designed the experiment and supervised the research and data analysis. All other work conducted for the thesis was completed by the student independently.

Funding Sources

Graduate study was supported by a graduate research assistantship and teaching assistantship from Texas A&M University and Texas A&M AgriLife Research and research funding from Texas A&M AgriLife Research and USDA-NIFA.

NOMENCLATURE

ABE	Adenine base editor
BE	Base editing
Cas9	CRISPR associated protein 9
CBE	Cytosine base editor
CRISPR	Clustered Regularly Interspaced Short Palindromic Repeats
CTAB	Cetyl Trimethylammonium Bromide
ddPCR	Droplet digital polymerase chain reaction
FDA	Fluorescein diacetate
GFP	Green fluorescence protein
gRNA	Guide RNA
nCas9	Catalytically impaired Cas9 endonuclease
PEG	Polyethylene Glycol
pegRNA	Prime editing guide RNA
PTG	Polycistronic tRNA-gRNA
RNP	Ribonucleotide protein
RS	Resistant starch
RT	Reverse transcriptase
RT	Room temperature
SBE	Starch branching enzyme
TE	Transformation Efficiency

TABLE OF CONTENTS

Page

LIST OF FIGURES

Page

LIST OF TABLES

Page

1. INTRODUCTION

According to the Food and Agriculture Organization (FAO), by 2050, we will need to increase our food production up to 60 percent to feed a world population of 9.3 billion (Tilman et al., 2011). To meet the demand, scientists and plant breeders need to continuously develop new technologies to increase agricultural productivity and accelerate sustainable agricultural development. Conventional plant breeding, marker-assisted selection, mutagenesis, transgenesis, and gene editing are some of the available technologies that can be used for crop improvement.

Traditional plant breeding, or cross-breeding, has played an important role in improving agricultural productivity that involves crossing selected plants to combine desirable traits of interest. Although significant progress has been made with major crops, the low availability of suitable parental lines, low genetic variability in specific crop germplasm, and extra time, effort and expenses still limit the genetic gains provided by this technique (Hedgecock and Davis, 2007). Likewise, marker-assisted selection and genomic selection have made great strides, but are ultimately limited by the effects provided by natural variation.

Mutation breeding has created novel genetic variation by introducing random mutations using chemical mutagens or physical irradiation (Pacher and Puchta, 2017). However, these methods have several drawbacks, including the non-specific nature of the generated mutations, a large number of nucleotides simultaneously mutated, and sometimes the deletion, duplication, or rearrangement of large genomic fragments. In contrast to the random nature of mutagenesis to provide beneficial alleles, the transgenic method involves the precise transfer of desired foreign

genes into elite background varieties through plant transformation techniques, including *Agrobacterium*-method and biolistic delivery systems, which can provide novel traits not available in the crop gene pool. However, public acceptance and lengthy and costly regulatory evaluation processes of genetically modified products are the major drawbacks of this technique (Prado et al., 2014).

CRISPR-Cas9 genome editing is a promising technology that can enable efficient targeted modification of crops to accelerate crop improvement with the added benefit of providing a non-transgenic approach. It has recently become a widely adopted, easy-to-use targeted genetic manipulation tool that has been applied to many crops through continuous improvements of CRISPR-Cas technology, such as alternate nucleases (such as CRISPR-Cpf1/Cas12a), base editing, and prime editing (Li et al., 2013; Shan et al., 2015; Alok et al., 2020; Bharat et al., 2020; Lin et al., 2020).

The aim of this dissertation is to optimize and apply new CRISPR-Cas9 technologies in both rice and peanut for crop improvement. In Chapter 2, gene editing was performed to improve resistant starch content in the U.S. rice, Presidio, by disrupting four SBE genes through CRISPR-Cas9 gene editing. The results from this study may enable the improvement of the nutritional properties of rice grains for better human health. In Chapter 3, a simple and efficient protocol for isolation of peanut protoplasts and its application for transient gene expression studies and gene editing was described. In Chapter 4, prime editing in both rice and peanut protoplasts was optimized by transiently targeting mutant GFP with a prime editing system to recover a functional GFP. Three promoters were used to develop the vectors with different combinations and their efficiency was tested in both crops.

2. INCREASING THE LEVEL OF RESISTANT STARCH IN THE RICE CULTIVAR PRESIDIO THROUGH MULTIPLEX CRISPR-CAS9 GENE EDITING OF STARCH BRANCHING ENZYME GENES

2.1. Introduction

Rice is one of the major staple food crops consumed by half of the world's population, and about 4.5 million hectares of rice are grown each year globally (Sun et al., 2017). To ensure food security for nine billion people by 2050, there is a dire need to increase rice production congruent with the population growth (Prosekov and Ivanova, 2018). Moreover, diet-related chronic diseases are prevalent in both developed and developing countries (Chen et al., 2012). Hence simultaneously increasing yield and improving grain quality and nutrition for a healthier rice diet will be essential to meet the needs of a growing population.

Rice grains largely consist of starch, which is normally hydrolyzed by enzymes in the human digestive tract to be converted into glucose that cells directly use to produce energy. Amylopectin and amylose are two components of starch, polymerized through α-1, 4 and α-1, 6 linkages. Amylose is a linear polymer of α -1, 4 linkages linked with few α-1, 6 linkages and average degree of polymerization (DP). In contrast, amylopectin is a large, highly branched polysaccharide with higher DP (Morrison and Karkalas, 1990). In cooked rice, amylose molecules rapidly precipitate and form complexes resistant to digestion, while the amylopectin molecules form complexes slowly and are more readily digestible. Therefore, rice grains with high amylose content (AC) tend to have higher levels of resistant starch (RS), which is not easily digestible or absorbed in the stomach or small intestine and passes directly into the large intestine (ASP, 1992), leading to

various human health benefits (Zhu et al., 2012; Regina et al., 2015). Consumption of RS reduces the risk of colorectal cancer through the promotion of fermentation by beneficial microbiota in the large intestine (Birt et al., 2013) and by reducing dietary protein-induced colonocyte DNA damage (Conlon et al., 2012).

Starch branching enzyme (SBE) catalyzes the formation of α-1,6-glucosidic linkages during starch biosynthesis resulting in amylopectin. Therefore SBE plays a significant role in the formation of a distinct fine structure of amylopectin (Nakamura et al., 2010). There are at least four SBE isozymes in cereal endosperm: SBEI, IIa, IIb and III (Pandey et al., 2012b). SBEI and SBEII generate ά-(1–6) linkages by cleaving internal ά-(1–4) bonds to form the branched structure of the amylopectin molecule. SBEII proteins transfer shorter chains and show a higher affinity towards amylopectin than the SBEI, which demonstrates higher rates of branching with amylose (Nakamura et al., 2010). Another enzyme isoform, SBEIII, has also been reported (Chen et al., 2004), which plays an important role in the synthesis of 1–6 branching. It has been hypothesized that the inhibition of SBEs in normal cereal endosperm decreases the branching degree, prolongs the branch-chain length of amylopectin, and significantly increases amylose content in starch, ultimately contributing to elevated levels of RS (Wang et al., 2017). For example, in barley, simultaneous RNAi suppression of all the *SBE* genes led to a barley producing pure amylose (Carciofi et al., 2012). In wheat, a line combining mutations in all *SBE* genes increased the level of resistant starch (Schönhofen et al., 2017).

CRISPR-Cas9-mediated gene editing technology has tremendous scope to greatly expedite plant breeding through improvement of major agronomic traits and development of novel germplasm in crop plants. This technology has been optimized and used in various crops, including wheat, maize,

peanut, soybean, cotton, tomato, sorghum, potato (Jacobs et al., 2015; Svitashev et al., 2016; Gao et al., 2017; Li et al., 2018b; Johansen et al., 2019; Liu et al., 2019; Jouanin et al., 2020; Biswas et al., 2022), and is already well established in rice (Mishra et al., 2018; Liang et al., 2021; Molina-Risco et al., 2021). In rice, genome editing through CRISPR-Cas9 has been applied towards yield-related genes such as those controlling grain number (*OsGn1a*), grain size (*OsGS3*), grain weight (*GW2, OsGW5, OsGLW2, or TGW6*), panicle size (*OsDEP1, TaDEP1*), and tiller number (*OsAAP3*) (Li et al., 2016a; b; Xu et al., 2016; Zhang et al., 2016, 2018; Liu et al., 2017b; Lu et al., 2018; Chen et al., 2019). Resistant starch has also been a key target for rice crop improvement via the CRISPR-Cas9 system. Edited rice with increased RS levels by knocking out the *SBEIIb* gene has been previously reported (Baysal et al. 2016; 2020; Sun et al. 2017; Guo et al. 2020). However, disruption of different combinations of *SBE* genes to improve RS content in rice via CRISPR-Cas9 has not been previously reported. The aim of the current study is to improve the levels of resistant starch in the US rice cultivar Presidio by disrupting four *SBE* genes through CRISPR-Cas9 gene editing. The results of this study may provide insight into the relationship between resistant starch and amylose content in rice grains, as well as enable improvement of rice grain's nutritional properties for better human health.

2.2. Material and methods

2.2.1. Plant material

The rice cultivar Presidio was used for this study. Presidio is a semi-dwarf *tropical japonica* rice cultivar, high yielding, and has high grain quality. In addition, this variety is one of the best varieties to be planted as ratoon rice in Texas and Louisiana, which could provide additional

income for rice growers (McClung, 2005). Additionally, tissue culture and transformation of this variety have been optimized recently (Molina-Risco et al. 2021).

2.2.2. Design of the sgRNAs for the construct

Four *SBE* genes, *SBE1(SBEI), SBE2, SBE3 (SBEIIb)* and *SBE4* (*SBEIIa),* were targeted for this research project, and sgRNAs were designed for the coding region of each gene target. For this purpose, the targeted exons of each gene were amplified, cloned, sequenced, and checked for similarities with the rice reference sequences. DNA was isolated from young leaves using the CTAB method (Doyle and Doyle, 1987). A total of 100 ng of the genomic DNA was used as a template for a PCR reaction using the Phusion® High-Fidelity DNA Polymerase master mixer using the designed primers. PCR was performed with initial denaturation step at 98°C for 30 s, followed by 30 cycles of 98°C for 30 s, 56-58°C for 30 s, and 72°C for 30 s, followed by a final extension at of 72°C for 7 min. Afterward, PCR products were ligated using the Zero Blunt™ TOPO™ PCR Cloning Kit (Invitrogen™, Waltham, MA) as per manufacturer's specifications and then sequenced by the Sanger method. Based on the sequencing result, gRNAs were readily designed using the CRISPR-P2 database (Liu et al., 2017a) and CRISPR-DIRECT (Naito et al., 2015).

2.2.3. *In vitro* efficiency test of sgRNAs

The efficiency of the sgRNAs in performing the edits was checked using the *in vitro* ribonucleoprotein (RNP) digestion of DNA with Cas9 Nuclease (NEB) provided by the manufacturer with a few modifications. In this case, a 27 µl reaction mixture containing 30 nM of synthesized sgRNA (Synthego), 30 nM of Cas9 Nuclease (NEB), and 3 µl of 10x NEB buffer 3.1

were pre-incubated for 10 minutes at 25ºC. Afterward, 100 ng purified PCR product was added to make a total reaction volume 30 µl and incubated at 37°C for 1h. After adding 1 µl of Proteinase K, the reaction mixture was kept for 10 minutes at 56°C, and fragment analysis was performed using gel electrophoresis.

2.2.4. Development of the CRISPR-Cas9 construct and *Agrobacterium*-mediated transformation

Multiple sgRNAs for the four *SBE* genes were expressed through the polycistronic tRNA-gRNA (PTG) gene under the *OsU3* promoter (Xie et al., 2015), which was synthesized and incorporated into pUC57 (Genscript Biotech Ltd., Piscataway, NJ, USA). pUC57_tRNA-gRNA (PTG) was cloned into a binary destination vector (pRGEB32) according to the protocol of (Čermák et al., 2017). In this construct, *OsCAS9* was expressed under the control of rice ubiquitin promoter. The constructed binary vector containing all sgRNAs was transformed into NEB 5-alpha competent *E. coli* (NEB, Ipswich, MA, USA). Plasmids were isolated using QIAprep® Spin Miniprep Kit (Qiagen. Hilden, Germany) and positive clones were confirmed by Sanger sequencing and finally transformed into *Agrobacterium tumefaciens EHA105*. After that, the *Agrobacterium* containing the desired construct was transformed into the regenerating calli of presidio rice varieties using the modified protocol of (Hiei and Komari, 2008). The transformed calli was selected using hygromycin (50 mg/L). Transformed explants was then be regenerated, transferred to soil, and finally, the transformed progenies screened to identify desired edits.

2.2.5. Screening of transformed progenies

Genomic DNA of the transformed plants were extracted according to the protocol (Doyle and Doyle, 1987) with minor modifications. The positively transformed plants of T_o and T_1 generation were confirmed by PCR using CAS9 and tRNA-gRNA specific primers (Appendix Table 1). PCR was conducted with an initial denaturation step of 98°C for 30 s, followed by 32 cycles of 98°C for 30 s, 55°C (CAS9) or 58°C (tRNA-gRNA) for 30 s, and 72°C for 30 s, and a final extension of 72°C for 5 min.

Deep amplicon sequencing was used to identify the edits in the positive T_0 and T_1 transformed lines (Chen et al., 2018). The Cas9-sgRNAs target sites of DNA segments were amplified with Phusion polymerase using pairs of four SBE primers listed in (Appendix Table 1). PCR was performed with an initial denaturation step of 98°C for 30 s, followed by 32 cycles of 98°C for 30 s, 55-58°C for 30 s, and 72°C for 30 s, and a final extension of 72°C for 7 min. The PCR product was then purified by gel extraction. The site-specific primer was designed and used for the first-round amplicon PCR using the KAPA HiFi Hot Start ReadyMix PCR Kit (Millipore Sigma, Burlington, MA, USA) (Appendix Table 1). PCR was performed with an initial denaturation step of 98°C for 30 s, followed by 25 cycles of 98°C for 30 s, 55°C for 30 s, and 72°C for 30 s, and a final extension of 72°C for 5 min. Next, forward and reverse barcodes for amplicon library construction were added to the PCR products for the second round of PCR with an initial denaturation step of 98 °C for 30 s, followed by eight cycles of 98°C for 30 s, 55°C for 30 s, and 72°C for 30 s, and a final extension of 72°C for 5 min. Each sample corresponded to a unique pair of barcodes. The products of 1st and 2nd round amplicon PCR were purified using CleanNGS kit according to the manufactural protocol. The libraries were pooled into equimolar concentrations

for multiplexed sequencing on the Illumina MiSeq platform (Illumina, San Diego, CA) with 2×150 run parameters at Texas A&M Institute for Genome Sciences and Society (TIGSS) lab TAMU (https://genomics.tamu.edu/). The obtained next-generation sequencing data were analyzed using CRIS.py (Connelly and Pruett-Miller, 2019). Indels or base substitutions located around the Cas9 cleavage site (3 bp upstream of the protospacer–adjacent motif sequence) were identified as mutations induced by Cas9.

Droplet digital PCR (ddPCR) was used to identify the copy number of the transgene at $T_{0,}$ which is a simpler and less expensive molecular technique than southern hybridization (Collier et al., 2017). A single copy of the transgene is more desirable for making transgene-free genome-edited plants because transgene will be segregated out in the next generation. For ddPCR, genomic DNA was quantified using a Qubit fluorometer using the dsDNA quantification kit according to the manufacturer protocol (Thermo Fisher Scientific, Waltham, MA, USA). Prior to ddPCR, DNA was digested with *Hind*III restriction enzyme for 15 min. *OsPLD* was used as the reference gene probe, labeled with 5′ FAM™ (6-fluorescein), and hptII was used as the transgene probe, labeled with 5′ HEX™ (hexachloro-fluorescein). Both types of probes were tagged with ZEN™ and Iowa Black Hole Quencher® 1 (Integrated DNA Technologies, USA) double-quenchers. A solution of 25 µL ddPCR cocktail was prepared with 12.5 µL 2 × ddPCR Supermix (no dUTP; product # 186-3024; Bio-Rad Laboratories), 450 nM of each primer pair (for the endogenous reference gene and the transgene), 250 nM of each probe, digested genomic DNA and sterile ultrapure water. For droplet generation, 20 µL ddPCR cocktail mix was added with 70 µL Bio-Rad Droplet Generation Oil (product # 186-3005) and droplet was made in the microcapillary droplet generator cartridge (product # 186-4008) following the manufacturer's instructions (Bio-Rad). After droplet

generation, the PCR plate was sealed and placed into the thermocycler for ddPCR. ddPCR was performed following protocol: initial 95°C denaturation for 10 min, followed by 40 cycles of 94°C (30 s), 57°C for 1 min with a temperature ramp rate of 2°C sec^{-1} and final step at 98°C for 10 min. The plate was then transferred to a QX200 droplet reader (Bio-Rad) for droplet counting. Droplet counts were measured, and transgene copy numbers were calculated using the Bio-Rad QuantaSoft™ software (v1.6.6.0320).

Edited plants were selected for generation advancement based on the transgene presence (one copy of transgene) and type of edits (homozygous and bi-allelic heterozygous) at T_0 generation. At T_1 generation, approximately 15 seeds/line were used to check the presence of transgenes and mutation patterns by PCR and amplicon-based deep sequencing. T_2 seeds from such T_1 plants were used for subsequent phenotypic analysis.

2.2.6. Phenotypic analysis and starch content measurement

A stereomicroscope was used to take photomicrographs of T_2 generations whole grain samples. The granular morphology of starch was examined by scanning electron microscopy (SEM). Grain samples were transversely cut and photographed by TESCAN VEGA SEM (TESCAN Czech Republic) at TAMU (Microscopy and Imaging Center 2257 TAMU). The percent of total starch, amylose content (AC) and resistant starch (RS) in the rice flour of *SBE* mutants and WT was measured with the starch assay kits (Sun et al., 2017) according to the manufacturer protocol.

2.3. Results

2.3.1. *SBE*-targeting guide RNA design, validation, and vector construction

The first exon in each of the *SBE1*, *SBE2* and *SBE3* genes and the 3rd exon for *SBE4* were targeted for designing sgRNAs (Figure 2.1A). An *in vitro* ribonucleoprotein (RNP) assay for the four gRNAs targeting a PCR amplicon flanking the target site of the *SBE1*, *SBE2*, *SBE3* and *SBE4* was performed using the RNP complexes with purified Cas9 (Invitrogen, Waltham, MA, USA) and synthetic gRNAs (Synthego, Menlo Park, CA, USA). The negative controls had uncut PCR products, while three bands were seen for the cut amplicon with all sgRNAs, indicating that all four sgRNAs were efficiently cut their target nucleotide sequences (Figure 2.1B). The polycistronic tRNA-gRNA (PTG) construct bearing all sgRNAs was cloned into a destination vector pRGEB32 (Figure 2.1C and Figure 2.1D).

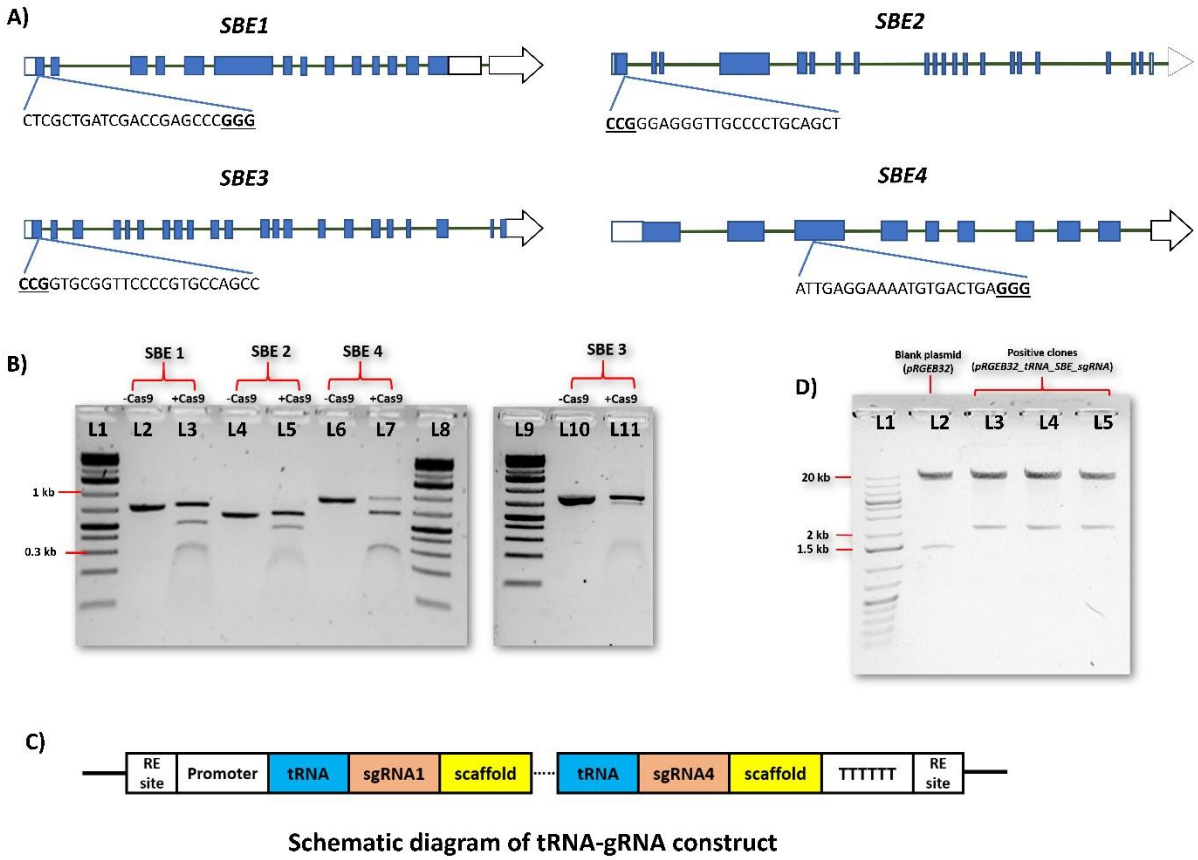

Figure 2.1 Target regions of gRNA targets of four *SBE* genes, tRNA-sgRNAs construct of *SBE* genes, *in vitro*-digestion of gRNAs and cloning of the *tRNA_gRNA* construct. A) Schematic map of the gRNA target sites on the genomic regions of *SBE1, SBE2, SBE3 and SBE4,* B) *In vitro* RNP digestion of *SBE1*, *SBE2*, *SBE3* and *SBE4* genes PCR amplified product. L1, L8 and L9: 1kb^{+} ladders; L2: uncut *SBE1* target region; L3: *SBE1* target region digested with Cas9 and sgRNA1 (expected bands of 466 bp and 246 bp); L4: uncut *SBE2* target region; L5: *SBE2* target region digested with Cas9 and sgRNA2 (expected bands of 447 bp and 168 bp); L6: uncut *SBE4* target region; L7: *SBE4* target region digested with Cas9 and sgRNA4 (expected bands of 643 bp and 256 bp); L10: uncut *SBE*3 target region; L9: *SBE*3 target region digested with Cas9 and sgRNA3 (expected bands of 682 bp and 127 bp). C) Schematic diagram of tRNA-gRNA construct. D) Cloning of of *tRNA-gRNA* construct into destination vector pRGEB32. L1: 1kb^{+} ladder, L2:

blank plasmid digested with specific restriction enzymes; L3-L5: positive clones of *pRGEB32_tRNA_gRNAs* digested with specific restriction enzymes.

2.3.2. Targeted mutagenesis in transgenic rice plants

The CRISPR-Cas9 vector containing four *SBE* gRNAs was transformed into rice immature embryo-derived calli through *Agrobacterium*-mediated transformation and generated transgenic lines after six rounds of hygromycin selection with the help of the Multi Crop Transformation Facility Lab, TAMU. For acclimation, the putative transformed rice seedlings were first kept into hydroponic solution for 10 days and then transferred to soil (Appendix Figure 1A). PCR was used to detect the presence of the transgene (Appendix Figure 1B) and to amplify the target *SBE* gene sequences in the transformed plants. Genomic DNA was extracted from eight plants. All eight plants showed positive PCR results with both CAS9 and tRNA-gRNA specific primers (Appendix Figure 1C), indicating positive transformation. To detect the editing pattern and efficiency, targeted deep sequencing was performed for PCR products of *SBE1, SBE2, SBE3* and *SBE4* obtained from the isolated genomic DNA from each of 8 transformed plants. The most common mutation was biallelic (i.e. two different mutant alleles at the same locus), followed by monoallelic (i.e. one mutant allele alongside the wild type allele), and chimeric (i.e. three or more alleles were identified), while one plant had one locus (*SBE3*) with fixed homozygous mutant alleles (Appendix Figure 2A). The most common mutations were deletions, followed by substitutions, and a few insertions (Appendix Figure 2B). Predicted knockout mutations were identified at all four *SBE* genes, although with varying zygosity and in different plants, due to frameshift mutations leading to premature stop codons (Appendix Figure 3).

Specifically, for the *SBE1* gene, six lines (P1-P4, P7 and P8) showed biallelic mutations. Among them, four lines (P1-P4) had one allele with a 3 bp deletion and the other allele had a 23 bp deletion, while two lines (P7 and P8) had a 4 bp deletion in one allele and a 22 bp insertion in the other allele (Appendix Table 2A). Monoallelic mutations were found in line P5 (23 bp deletion) and line P6 (24 bp deletion). For *SBE2*, two lines (P7 and P8) had biallelic mutations (11 bp and 15 bp deletions) and one line (P4) had a monoallelic mutation (1 bp deletion); however, five lines (P1, P2, P3, P5 and P6) showed chimeric mutations (Appendix Table 2B). For the *SBE3* gene target, four lines (P4-P7) contained a homozygous mutation (1 bp deletion only), while three other lines (P1, P2 and P3) has monoallelic mutations (1 bp deletion and wild type), and one line (P8) did not have any edits (Appendix Table 2C). For *SBE4*, seven lines (P1-P5, P7 and P8) showed biallelic mutations: lines P1-P5 had a 1 bp deletion in one allele and 1 bp substitution (C to G) in the other allele, while P7 and P8 had a 4 bp deletion on one allele and a combination of 4 bp deletion and 1 bp substitution in the other allele, while no edit was found in the P6 line (Appendix Table 2D).

2.3.3. Copy number detection of transformants

Five independent transgenic edited T_0 rice lines were selected to detect the transgene copy number using ddPCR (Figure 2.2). ddPCR is a novel technology that provides precise data from a single reaction mixture and has been established in multiple crop species, including rice, wheat, potato, tomato and maize (Collier et al., 2017). Our T_0 transgenic rice lines were analyzed using ddPCR with primers and probes designed to detect the *OsPLD* reference gene and the *hptII* transgene. The *OsPLD* gene was used as a reference gene which is a single copy and constitutively expressed gene within the rice genome (Mazzara, 2007). We did not see any droplet generation from the

negative control (no genomic DNA template) for both probes (*hpt*II and *OsPLD*) and from the wild type (WT) control for the transgene *hpt*II probe (Figure 2.2A). Our ddPCR results showed that four lines (P1-P4) contained a single copy and one line (P5) contains two copies of the *hpt*II transgene (Figure 2.2D).

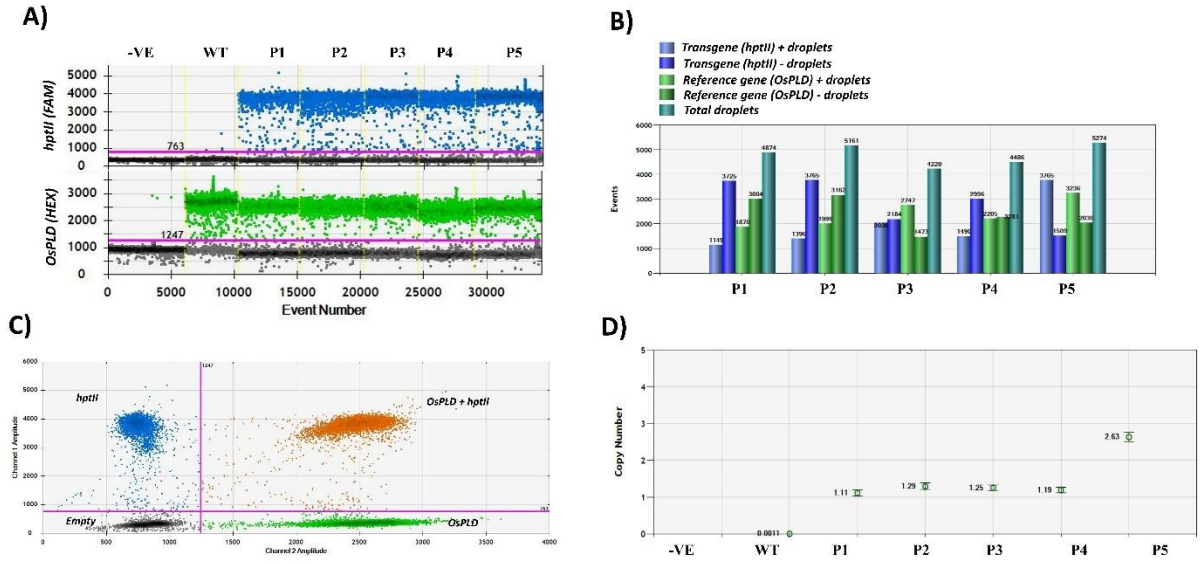

Figure 2.2 Droplet digital polymerase chain reaction (ddPCR) results from QuantaSoft™ software demonstrating quantitative analysis for the *hpt*II (transgene copy number) and *OsPLD* (reference housekeeping gene) from wild type (WT) and five T_0 transgenic rice lines. A) One-dimensional plot of droplets measured for fluorescence signal (amplitude indicated on *y*-axis) emitted from the transgene *hpt*II (FAM™ labeled; positive droplets are blue) or endogenous housekeeping reference gene *OsPLD* (HEX™ labeled; positive droplets are green). Negative droplets are shown in black. B) Droplet data are further displayed from the same five lines in a bar graph to highlight the relative abundance of droplets scored as positive (1st and 3rd bar in each group; green for reference gene *OsPLD*, blue for transgene *hpt*II) or negative (2nd and 4th bar in each group, same color scheme) compared with the total number of droplets (5th bar in each group, teal color). C) The droplets visualized in two dimensions for line P1. The colors are

as described in (A), except that droplet containing both fluorescent probes are orange. D) Calculated transgene *hpt*II copy number in T_0 transgenic rice lines after copy number variation processing in QuantaSoft™ where the reference gene *OsPLD* was determined as single copy and it is a homozygous gene in a diploid genome. The error bars represent the maximum and minimum Poisson distribution for the 95% confidence interval generated by the QuantaSoft™ software.

2.3.4. Identification of transgene inheritance and detection of mutations in the T_1 generation

Four one-copy transgene-containing T_o mutant plants, with mutations at the four SBE loci (Figure 2.3), were self-pollinated and the resulting T_1 plants were used for segregation analysis for both transgene inheritance and mutation frequency. We randomly selected 11 to 14 T_1 progenies derived from each T_o plant for genotyping analysis. To determine transgene presence (*Cas9* and *tRNA-gRNA*) at the T_1 generation, we performed PCR amplification using the *Cas9* and *tRNA-gRNA* specific primer sets as were used to validate the T_o transformants. We successfully recovered transgene-free mutants (i.e. no *CAS9* and *tRNA-gRNA*) at the T_1 generation: 3 plants from the P1 line, 5 plants from the P2 line, 5 plants from the P3 line, and 5 plants from the P4 line (Figure 2.4).

For transgene inheritance calculation, all lines followed the Mendelian segregation ratio (3:1, $\chi 2$ test, $P > 0.05$) (Table 2.1).

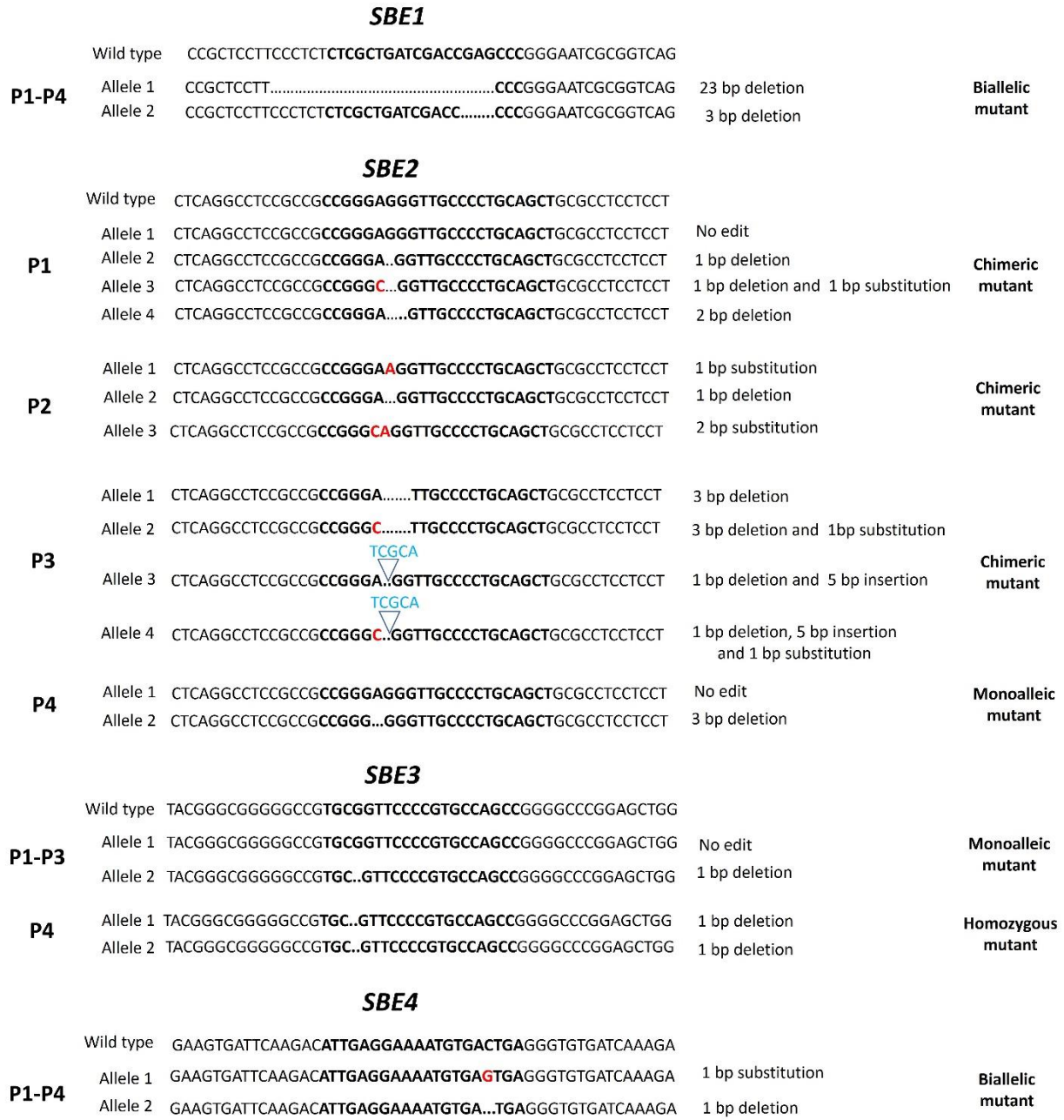

Figure 2.3 Deep sequencing results in four of the edited *SBE* genes in the T_0 generation. The four selected plants were advanced to the T_1 generation for further analysis.

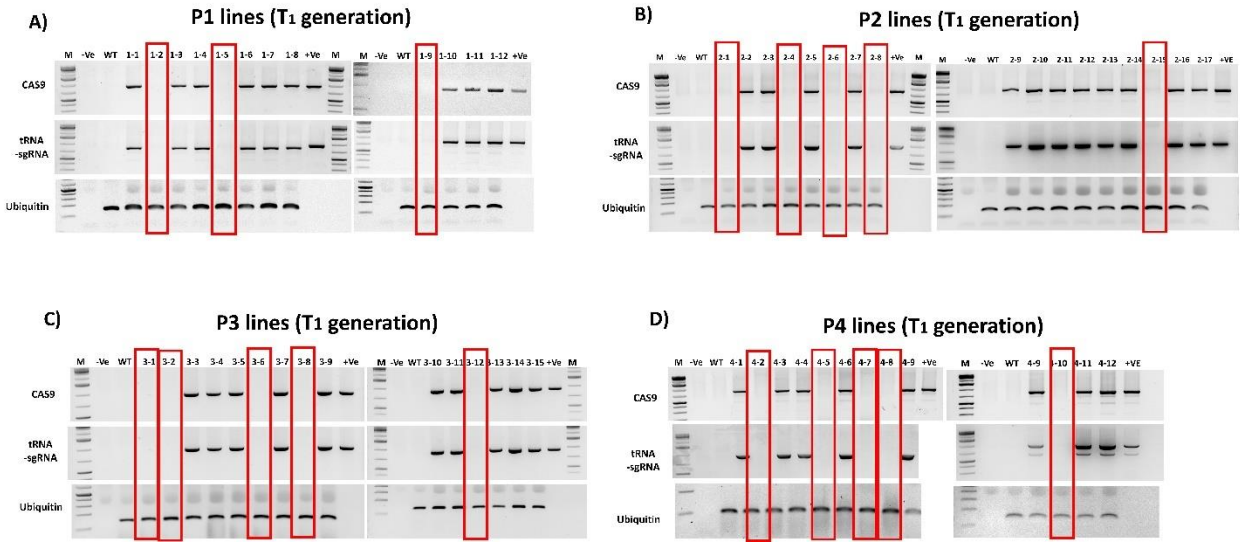

Figure 2.4 Identification of transgene-free T_1 plants from four (P1-P4) *mutant* lines. DNA fragments of Cas*9* and *tRNA-gRNA* were not detected in a number of T_1 plants, namely: A) P1 lines (1-2, 1-5 and 1-9); B) P2 lines (2-1, 2-4, 2-6, 2-8, 2-15); C) P3 lines (3-1, 3-6, 3-8 and 3-12); and D) P4 lines (4-2, 4-7, 4-8 and 4-10). The control PCR product was amplified from the endogenous *Ubiquitin g*ene, indicating that the genomic DNAs used have sufficient quality for PCR. WT, wild type DNA control. -ve (negative), water control and +ve (positive), plasmid control.

Table 2.1 Transgene and mutation segregation of *SBE* edited plants from T0 to T1.

Gene	Line	Mutation at T_0	Zygosity	No. T_1 plants	Mutation at T_1	Expected segre-gation	Chi-square P value
SBE1	P1	d23/d3	Biallelic	10	0 d23, 8 d23/d3 and 2 d3	1:2:1	0.35
	P2	d23/d3	Biallelic	15	3 d23, 10 d23/d3 and 2 d3	1:2:1	0.77*
	P3	d23/d3	Biallelic	13	4 d23, 7 d23/d3, 2 d3	1:2:1	0.95*
	P4	d23/d3	Biallelic	9	1 d23, 4 d23/d3, 4 d3	1:2:1	0.80*
SBE2	P1	Chimeric (WT/d3/d1)	Chimeric	10	5 chimeric, 2 WT, 1 WT/d1, 2 d1	NA	NA
	P2	Chimeric (s1/d1/s2)	Chimeric	15	8 s1/d1, 5 S1, 2 d1	NA	NA
	P3	Chimeric (d3/d3-s1/d1-5i/d1-S1-i5)	Chimeric	13	7 d3/d1-5i, 4 d3, 2 d1-i5	NA	NA
	P4	WT/d1	Monoallelic	9	3 WT/d1, 4 chimeric, 1 d1, 1 d1/ 1 i1	1:2:1	NA
SBE3	P1	WT/d1	Monoallelic	10	6 WT/d1, 4 chimeric	NA	NA
	P2	WT/d1	Monoallelic	15	6 WT/d1, 6 chimeric, 2 WT, 1 d1	NA	NA
	P3	WT/d1	Monoallelic	13	3 WT/d1, 5 chimeric, 4 WT, 1d1	NA	NA
	P4	d1/d1	Homozygous	9	9 d1	NA	NA
SBE4	P1	s1/d1	Biallelic	10	1 s1, 5 s1/d1, 4 d1	1:2:1	0.77*
	P2	s1/d1	Biallelic	15	3 s1, 12 s1/d1	1:2:1	0.15
	P3	s1/d1	Biallelic	13	3 s1, 10 s1/d1	1:2:1	0.27
	P4	s1/d1	Biallelic	9	7 s1 and 2 s1/d1	1:2:1	0.004

Note: i, d, s, and WT represent insertion, deletion, substitution/inversion, and no mutation detected, respectively; plants noted with an asterisk (*) followed the Mendelian law of inheritance.

We also checked the mutation segregation analysis after deep sequencing analysis at the T_1 generation. For biallelic heterozygous mutants, three lines (P2-P4) for *SBE1* and one line (P1) for *SBE4* were consistent with the predicted Mendelian segregation (1:2:1, $\chi 2$ test, $P > 0.05$) (Table 2.1, Appendix Table 3A-3P). Only one line (P4), which showed biallelic homozygous mutation for *SBE3* were also found homozygous with the same type mutations for all plants at T_1 generation

(Table 2.1, Appendix table 3O). However, we also detected some extra mutations and chimeric mutations in several lines for *SBE2* and *SBE3* genes at the T_1 generation.

2.3.5. Effect of *SBE* genes mutation on grain morphology

T_1 and T_2 *SBE* mutant lines derived from 4 T_0 lines were used to analyze the grain and starch granule morphology. The mutant *SBE* seeds were opaque and blurred, but wild type (WT) seeds looked more translucent under a light microscope (Figure 2.5A). Under the scanning electron microscope, starch granules from *SBE* mutant lines were rounded and heterogeneous in size and shape and separated by large gaps. On the other hand, the WT starch grains are homogeneous, compact, and angular, with few interstitial spaces (Figure 2.5B). Interestingly P4-2, P4-3, P4-4, P4-5, P4-8 derived from P4 lines were more uniformly opaque than other lines (Appendix Figure 4A). The length, width, and thickness of grains from *SBE* mutant lines were significantly lower than those of wild type (Appendix Figure 4B-4D).

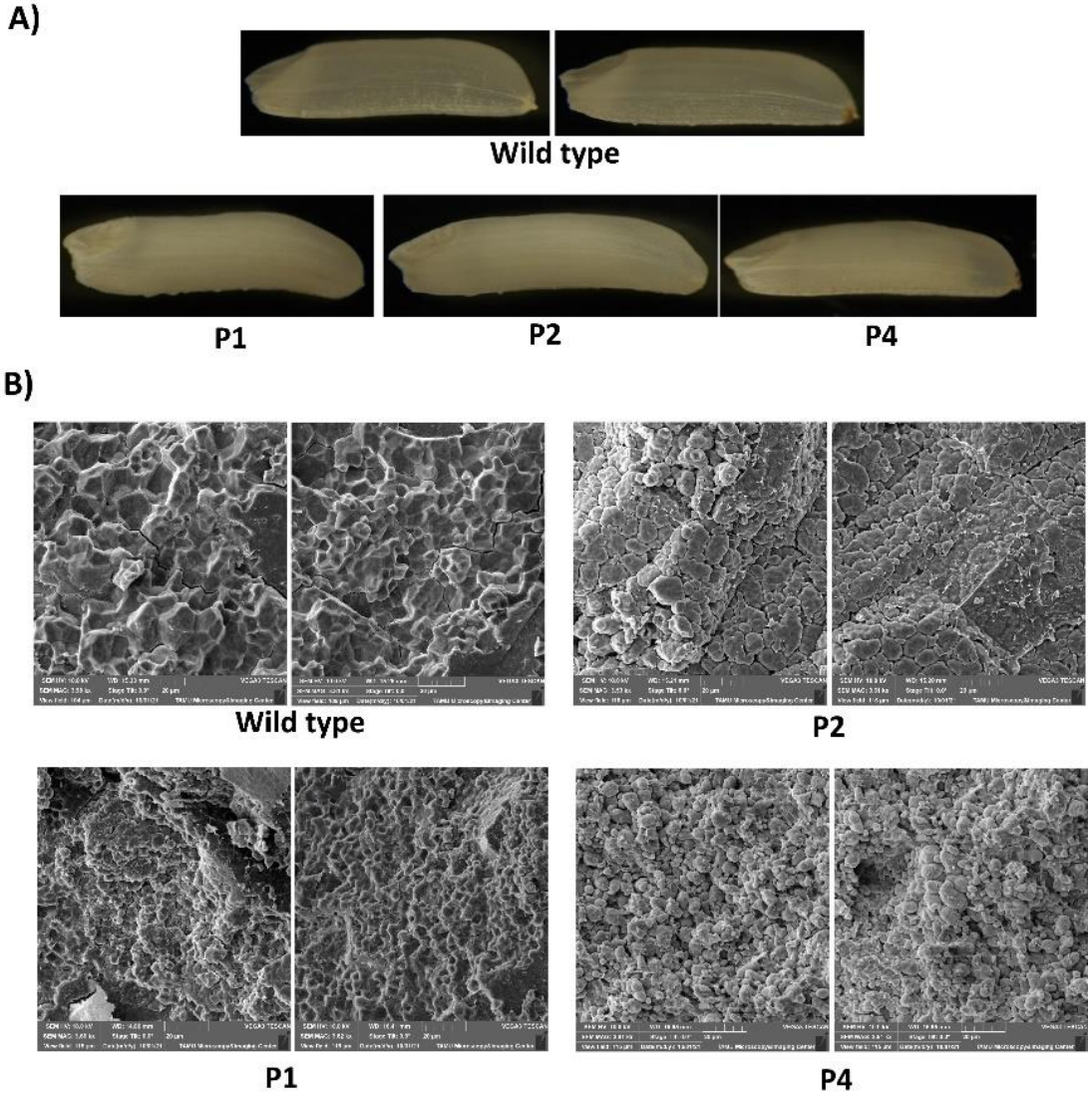

Figure 2.5 Grain and starch granule morphology of the *SBE* mutant lines at the T_1 generation. A) Morphologies of the WT and mutant seed under light microscope. Bars = 1 mm. B) Scanning electron microscopy images of starch in wild type and *SBE* mutant seeds (P1, P2 and P4). Bars = 10 mm. The WT starch grains are homogeneous, compact, and angular, with few interstitial spaces, whereas *SBE* mutants are rounded rather than angular, and separated by large gaps.

2.3.6. Amylose and resistant starch content in *SBE* edited lines

We measured the content of amylose, resistant starch, and total starch according to the starch assay kits Megazyme K-STAR, K-AMYL and K-RSTAR (Megazyme, Wicklow, Ireland). The endosperm amylose content of the T_2 seeds in *SBE* edited lines was significantly higher (19%-42%) than wild-type seeds (17%). Among them, P4-8 line showed 42% of amylose content which was 2.4-fold higher than the wild type (Figure 2.6A). Resistant starch (RS) content was also significantly increased in *SBE* mutant lines. Likewise, P4 lines also contained higher percentage of RS (10%-15%) than other lines (Figure 2.6B). We also found some lines with significantly decreased total starch than the WT (Figure 2.6C).

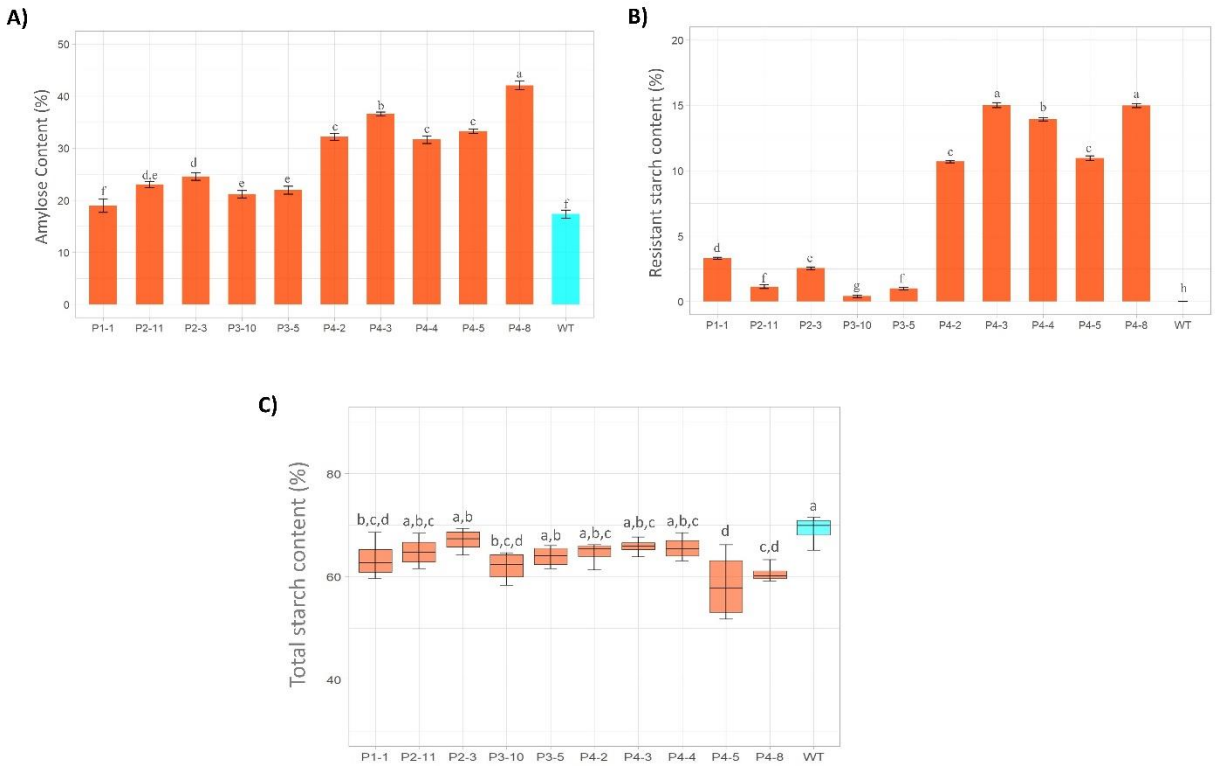

Figure 2.6 Rice grain content analysis. A) Percent amylose content; B) percent resistant starch content; and C) percent total starch content using the starch assay kits in the grain of wild type (WT) and *SBE*-edited plants. Values represent means ± SE (n = 4). The different letters indicate significant differences at $p < 0.05$.

2.4. Discussion

SBE genes have been targeted for altered starch composition using different strategies in several cereal crops. For example, the loss of function of *SBEI* contributes to an altered branching pattern for amylopectin and amylose and reduced coleoptile growth during germination in maize, but has no effect on starch granule morphology (Xia et al., 2011). In wheat, mutation in both copies (A and B genome) in *SBE4* increased amylose content and led to a 115% increase in resistant starch content (Hazard et al., 2012). The downregulation of *OsSBE3* by RNAi and artificial microRNA

in rice (Nipponbare) showed increased resistant starch content up to 9.5% (Butardo et al., 2011). By targeting the same gene (*SBE3* or *SBEIIb*) via CRISPR-Cas9, edited rice lines having higher RS content have also been obtained, up to 6% (Guo et al. 2020) and 9.8% (Sun et al. 2017). *SBEI* was also targeted for CRISP-Cas9 editing; however, no obvious differences were observed between the mutants and wild type (Sun et al. 2017). It had been reported that multiple gene mutations in the SBE family significantly improved results in both AC content and grain physiology. For instance, in potato, simultaneous downregulation of both *SBE1* and *SBE3* genes are required to significantly increase the amylose content (Schwall et al., 2000; Tuncel et al., 2019), whereas reduction in *SBE3* alone altered only granule size without changing amylose content. In the current study, we targeted four *SBE* genes simultaneously in one gene construct to evaluate the effects of different combinations of *SBE* gene mutations on starch composition in rice grains.

Detection of transgene copy numbers is a key step in plant genome editing. It is important to detect single-copy transgene-containing transformants at T_0 generation, so the Cas9-gRNA cassette can be segregated out from the genome in the T_1 generation (Xu et al., 2015; Aliaga-Franco et al., 2019). In this study, we successfully identified four transformed lines with a single-copy transgene at the T_o generation through droplet digital PCR (ddPCR) and subsequently found multiple transgene-free edited lines at the T_1 generation. The ddPCR assay is an accurate, precise, timesaving tool for the detection and evaluation of the transgene copy number in gene editing experiments.

Due to the natural preference of plant DNA repair systems for the error-prone non-homologous end joining (NHEJ) mechanism, short insertion and deletions (INDELs) are the most common type of mutations generated by the CRISPR-Cas9 editing system (Bortesi and Fischer 2015). Deep

sequencing results of eight T_o transformation plants showed that we had a higher percentage of deletion mutations compared to insertions and substitutions mutations. Moreover, we saw a higher percentage of biallelic heterozygous mutations in *SBE1*, *SBE2* and *SBE4*; however, we also detected more chimeric mutations at the *SBE3* gene target. Chimeric mutations have also been reported previously in other genome-edited studies, including *Arabidopsis*, tomato, and rice (Zhang et al., 2014, 2020). We also detected additional mutations or chimeric mutations in *SBE2* and *SBE3* targets at the T_1 generation. This is partly due to the continued presence of the CRISPR-Cas9 cassette in those lines, which created an additional mutation in the target gene. It has been reported that CRISPR-Cas9 will likely modify the wild-type allele of the target gene in the progeny if the parent plants still contained a wild-type allele and the Cas9-gRNA expression cassette (Zhang et al., 2020). However, the biallelic heterozygous lines for *SBE1* and *SBE2* followed the Mendelian segregation ratio at the T_1 generation. We did not detect any extra mutations in our transgene-free edited lines at the T_1 generation. P4, the only biallelic homozygous line for *SBE3*, showed the same type of mutation in all plants in the next generation.

The length, width, and thickness of grains of mutant lines were significantly lower than those of wild type. This trend was also previously reported for *SBE3* rice mutants (Sun et al., 2017). The morphological analysis also revealed that the mutant seeds were opaque, and the starch grains were different in size, shape, and distribution compared to wild-type grains. In general, *SBE* mutants also have higher resistant starch and amylose content along with lower total starch content. However, P4-line plants showed a significantly higher percentage of resistant starch and amylose content than other lines. This, in part, might be due to biallelic homozygous mutations in the *SBE3* gene target in all the P4-line-derived plants. It has been reported that *SBE3* is the crucial gene for

the starch biosynthesis pathway, and mutation of this gene gave high resistant starch and amylose content in a previous study (Sun et al., 2017). Notably, P4 edited lines showed higher RS content (Sun et al. 2017; Guo et al. 2020) or similar (Baysal et al. 2020) than previously reported edited lines. Even so, it is possible that the disruption of other *SBE* genes also contributes to high RS in addition to the *SBE3* gene, but this needs further investigation. *In silico* analysis revealed that all four *SBE* genes in the P4-2 line had premature stop codons in the coding sequence due to deletions, which would be expected to lead to a non-functional truncated protein. However, except for SBE3 in the P4 lines, most of the lines were not fixed for knockout mutations at the other loci, and therefore further studies will be needed in subsequent generations.

3. OPTIMIZATION OF PROTOPLAST ISOLATION AND TRANSFORMATION AND ESTABLISHMENT FOR A PILOT STUDY OF GENOME EDITING SYSTEM IN PEANUT BY TARGETING THE ALLERGEN GENE ARA H 2*

3.1. Introduction

Cultivated peanut or groundnut (*Arachis hypogaea L.*) is an allotetraploid (2n = 4x = 40) with a large reservoir of seed oil (~46–58%) and high-quality protein (~22–32%) (Janila et al., 2016). In 2018, about 45.95 million tons of peanut were produced across 28.51 million ha worldwide (FAO, 2018). China and India are the leading peanut producers globally, while the USA is fifth. Traditional peanut breeding has been a lengthy process with difficulties due to polyploidy and sterility barriers (Wilson et al., 2019). However, the availability of the recently published complete peanut genome (Bertioli et al., 2019; Zhuang et al., 2019) and bioinformatics resources, such as the peanut genome database (Dash et al., 2016), has enabled more rapid progress in peanut genetics, genomics and molecular breeding (- Advances in Genetics and Genomics for Sustainable Peanut Production, 2011; Pandey et al., 2012a, 2020; Stalker et al., 2013; Liang et al., 2017, 2018, 2020; Ozias-Akins et al., 2017; Bhat et al., 2021) 1. Furthermore, the implementation of functional genomics combined with biotechnology, especially DNA recombinant technology, has served as an essential toolbox that further enables the discovery and characterization of genes of agronomic importance and speeds up the progress in peanut breeding efforts. Unlike Arabidopsis and rice,

*Reprinted with permission from "Optimization of Protoplast Isolation and Transformation for a Pilot Study of Genome Editing in Peanut by Targeting the Allergen Gene Ara h 2" by Biswas, S., Wahl, N.J., Thomson, M.J., Cason, J.M., McCutchen, B.F. and Septiningsih, E.M., 2022. *International Journal of Molecular Sciences*, 23, p.837,

making transgenic peanut plants through *Agrobacterium* transformation has been known to be more challenging and low efficiency (Sun et al., 2013). In this case, *Agrobacterium rhizogenes* has been frequently used for transformation of hairy roots in peanut (Liu et al., 2016), but there is no report found to develop mature plants from the transformed root. Although, some products of transgenic research on peanuts have been developed, including varieties having resistance to various biotic stresses, such as viruses (Mehta et al., 2013), insects (Keshavareddy et al., 2013) and fungus (Prasad et al., 2013), and different abiotic stresses, such as drought and salt tolerance (Banavath et al., 2018), as well as improved grain quality and allergen-free peanut (Dodo et al., 2008).

Among the most recent techniques in biotechnology, genome editing is the most promising technology to study gene functions and help speed up crop improvement. Gene editing is a versatile technology that can be used to more precisely knock out the function of a gene (Liang et al., 2021; Molina-Risco et al., 2021), inactivate undesirable chromosomal DNA (Zhou et al., 2014), regulate endogenous genes (Fang et al., 2019), and to introduce novel coding sequences (Ref). Thus far, three genome editing techniques have been established: zinc finger nucleases (ZFN), transcription activator-like effector nucleases (TALENs), and clustered regularly interspaced short palindromic repeats associated with nuclease *Cas9 (CRISPR-Cas9)* (Razzaq et al., 2019). Among them, *CRISPR/Cas9* genome editing has proven to be the most popular and widely used for its precision effectiveness and ease; moreover, this technology can be applied in both diploid and polyploid plants (Wilson et al., 2019).

Despite the economic importance, peanut is less amenable to genome editing technology than other crops, such as rice, maize, and wheat; therefore, testing and evaluating this technology in such

crops is deemed an important step. As generating stable genome-edited plants is complex and labor-intensive (Lin et al., 2018), it is necessary to evaluate the most effective *Cas9-gRNA* beforehand. To evaluate the potential of CRISPR-Cas9 system in peanut, a reproducible system for the design, construction, and delivery of Cas9-gRNA need to be developed and validated via *in vitro* and *in vivo* systems. For *in vivo* assay, protoplast transformation can be used as a tool to express genes transiently as well as evaluate the genome-editing efficacy.

Allergenicity to peanuts is one of the most life-threatening food allergies and one of the most challenging problems faced by peanut breeders and researchers. This problem negatively impacts the peanut and food industries, and its significant health consequences demonstrate the dire need to find a cure for this problem. A total of 16 proteins are potentially involved in peanut allergenicity, four of which have been identified as the most important based on clinical tests (Mueller et al., 2014). Here we targeted a major allergen gene *Ara h 2* for optimizing gene editing in peanut protoplast. However, since the initial successful isolation of peanut protoplasts about four decades ago (Oelck et al., 1982), there have been limited reports on the application of protoplasts in peanut, primarily due to relatively low yields of the protoplasts. In this study, we describe a simple and efficient protocol for the isolation of peanut protoplasts and its application for transient gene expression studies.

3.2. Materials and Methods

3.2.1. Plant material

Schubert, a peanut genotype developed by Texas A&M AgriLife Research (Burow et al., 2014), was used in this study. Schubert is a high-yielding, high-oleic acid, early maturing Spanish-type

peanut cultivar with improved shell-out. The peanut seedlings were grown in a greenhouse with a temperature of 32/26 °C (day/night) and a 16/8 h light-dark cycle.

3.2.2. Plasmid preparation and constructs

The *35S:GFP* and *CmYLCV:GFP* vectors were used for checking the transformation efficiency in this study. Three intermediate module plasmids A, B and C were prepared for the construction of CRISPR-Cas9 vector of *Ara h 2* (Čermák et al., 2017). For module A, *CmYLCV* promoter from pMOD_A3003 (Addgene #91043) was inserted into pMOD_A0101 (Addgene #90998) in place of 35S promoter via restriction digestion and cloned using T4 Ligase (NEB) (Figure S1A and S1B). The pMOD_B2303 vector was used for module B. The Polycistronic *tRNA-gRNA (PTG)* Gene containing two sgRNAs sequences for *Ara h 2* (Xie et al., 2015) were synthesized and incorporated commercially into pUC57 (Genscript Biotech Ltd.). The synthesized pUC57-PTG was digested with *PstI* and *XhoI* and cloned into the *PstI* and *XhoI* -digested pMOD_B2303 vector (Addgene #91068) using T4 Ligase (NEB) following the manufacturer's recommendations (Appendix Figure 5A and 5C). Modified pMOD_A0101, Modified pMOD_B2303, and empty vector pMOD_C0000 (Addgene #91081) were assembled into a non-binary vector, pTRANS_100 (Addgene #91198) by simple Golden Gate protocol using the *AarI* enzyme (Xie et al., 2015) (Appendix Figure 5A and 5D).

3.2.3. In vitro efficiency test of sgRNAs

All steps were performed according to the manufacturer's instructions for *in vitro* digestion of DNA with Cas9 Nuclease (NEB) with a few modifications. In this case, a 27 µl reaction mixture containing 30 nM of synthesized sgRNA, 30 nM of Cas9 nuclease, and 3 µl of 10x NEB buffer

3.1 were pre-incubated for 10 minutes at 25ºC. Afterward, 100 ng substrate purified PCR product was added to make a total reaction volume of 30 µl and incubated at 37°C for 1 h. After adding 1 µl of Proteinase K, the reaction mixture was kept for 10 minutes at 56°C, and fragment analysis was then performed using gel electrophoresis.

3.2.4. Protoplast isolation from peanut

Protoplasts were isolated from different tissues of 5 and 10 days old peanut seedlings according to previously published protocols (Li et al., 1995; Shan et al., 2014) with some modifications. Briefly, tissues were cut into latitudinal strips using a sharp razor and transferred the strips into a 150-ml conical flask containing 20 ml of filter-sterilized enzyme solution (Table 3.1) and wrapped the flask with aluminum foil. The strips with cell wall–dissolving enzymes were vacuum-infiltrated by applying a vacuum (~380–508 mmHg) for 30 min in the dark. Next, the strips were incubated in the dark for 5 h with gentle shaking (50 r.p.m.) at room temperature (RT). After enzymatic digestion, 25 ml of W5 solution were added to the conical flask and then shaken gently by hand for 10 s to release the protoplasts. The protoplasts were collected into three or four 50-ml round-bottomed centrifuge tubes after filtering the mixture through 40-µm nylon meshes and washing the strips on the surface of the nylon mesh 3–5 times with W5 solution. The solution containing protoplast was centrifuged at 100×g for 2 min at RT in a swinging bucket rotor, and the supernatant was removed by pipetting. Protoplasts were resuspended in 10 ml of W5 solution and then collected into a 50-ml round-bottomed tube. Afterward, they were centrifuged at 100×g for 2 min at RT, supernatant was removed by pipetting, and the protoplasts were then resuspended in 4 ml of MMG solution and ready for further evaluation.

Table 3.1 Solutions used for peanut protoplast isolation and transformation.

Solution Name	Composition
Enzyme solution	3% cellulase RS (Yakult, Tokyo, Japan), 0.1% macroenzyme, 0.5% pectinase, 0.4 M Mannitol, 20 mM KCl, 20 mM MES (pH 5.7), 10 mM CaCl2, 0.1% BSA Special instructions: MES, mannitol, H_2O, cellulase RS, macroenzyme and pectinase were stirred and incubated at 55 °C for 10 min. The solution was cooled to room temperature, and $CaCl_2$ and BSA were added in and gently mixed
W5 solution	154 mM NaCl, 125 mM $CaCl_2$, 5 mM KCl and 2 mM MES (pH 5.7)
Washing and Incubation Solution (WS1)	0.5 M Mannitol, 20 mM KCl and 4 mM MES (pH 5.7)
MMG Solution	0.4 M Mannitol, 15 mM MgCl2 and 4 mM MES (pH 5.7)
PEG-$CaCl_2$ solution	0.2 M Mannitol, 0.1 M $CaCl_2$, 20-80% of PEG 4000

3.2.5. Protoplast counting and viability test

The total number of protoplasts was counted under a microscope (×100) using a hemocytometer (XB. K.25, QiuJing, Shanghai, China). Ten microliters of protoplast in MMG solution were added on the surface of the hemocytometer and carefully covered with a glass slide to avoid bubbles formation. The number of intact protoplasts in the four corners of the grid was counted under the microscope. The protoplast density was calculated as follows: Protoplasts number (g^{-1} fresh weight leave tissue) = the average count of protoplast per square× 10^4.

Fluorescein diacetate (FDA) and propidium bromide staining (Sigma) were used to determine the protoplast viability according to the manufactural protocol. In this case, 1 mL each of fluorescein diacetate and propidium bromide were added to a tube containing 98 mL of water or PBS. After that, 10 mL of the 10X stain solution was added to 90 mL of protoplast cells and mixed well by gently tapping. After incubation for 2 min, the viability of protoplasts was determined with Echo revolve-microscope under ultraviolet light. The viable protoplasts were stained green, whereas the dead cells and cell debris were not stainable. The viable protoplasts ratio was calculated as follows: percentage of viable protoplasts = (fluorescing protoplasts determined under fluorescence microscope)/ (total protoplasts observed under the bright field).

3.2.6. Protoplast transfection

PEG-mediated transfection was performed following a previously published method (Li, 2011) with some modifications. The 15 ml conical bottom tubes were coated with 5% FBS (fetal bovine serum), spun at 100×g for 2 min, and the FBS was removed. Next, 100 µl DNA (20-300 µg of plasmid DNA) were added to 400 µL of protoplasts suspension (2×10^6 total cells), gently flicked

and inverted to mix thoroughly. Afterward, 460μL of PEG-$CaCl_2$ solution was added, and the tube was gently inverted several times until fully mixed and incubated at room temperature in the dark for 5-50 min. After incubation, 3 mL of W5 solution were added to stop the reaction, inverted several times gently until fully mixed, and centrifuged at 100×g for 2 min, and the protoplast pellet was then recovered by carefully removing the supernatant. The protoplast pellet was then resuspended with gentle inversions and minimal pipetting in 200μL WS1 solution and incubated in the dark at room temperature. Then protoplast viability was measured using light microscopy, and the transformation efficiency with GFP plasmid was calculated using a fluorescence microscope on a hemocytometer after 24h and 48h of transformation.

3.2.7. Deep amplicon sequencing

At four days post-transfection under dark conditions, the peanut protoplasts were collected by centrifugation at 13000 RPM, and genomic DNA was then extracted with the CTAB protocol (Doyle and Doyle, 1987). The Cas9-sgRNAs target sites of DNA segments were amplified with Phusion polymerase using pairs of allele-specific primers listed in Table S1. PCR was performed with an initial denaturation step of 98°C for 30 s, followed by 32 cycles of 98°C for 30 s, 55-58°C for 30 s, and 72°C for 30 s, and a final extension of 72°C for 7 min. The PCR product was then purified by gel extraction. The site-specific primer was designed and used for the first-round amplicon PCR using the KAPA HiFi HotStart ReadyMix PCR Kit (KAPA BIOSYSTEMS) (Table S1). This PCR was done with an initial denaturation step of 98°C for 30 s, followed by 25 cycles of 98°C for 30 s, 55°C for 30 s, and 72°C for 30 s, and a final extension of 72°C for 5 min Next, forward and reverse barcodes for amplicon library construction were added to the PCR products for the second round of PCR with a protocol with an initial denaturation step of 98°C for 30 s,

followed by 8 cycles of 98 °C for 30 s, 55°C for 30 s, and 72 °C for 30 s, and a final extension of 72 °C for 5 min. Each sample corresponded to a unique pair of barcodes. The products of 1st and 2nd round amplicon PCR were purified using CleanNGS kit according to the manufactural protocol. The libraries were pooled into equimolar concentrations for multiplexed sequencing on the Illumina MiSeq platform (Illumina, San Diego, CA) with 2×150 run parameters at Texas A&M Institute for Genome Sciences and Society (TIGSS) lab TAMU (https://genomics.tamu.edu/)). The obtained next-generation sequencing data were analyzed using CRIS.py (Connelly and Pruett-Miller, 2019). Indels located around the Cas9 cleavage site (3 bp upstream of the protospacer–adjacent motif sequence) were considered to be mutations induced by Cas9.

3.3. Results

3.3.1. An efficient method of protoplasts isolation from peanut seedlings

Protoplasts offer a convenient and reliable system to optimize gene editing in plants (Lin et al., 2018). Selecting the proper source of plant tissue is the first critical step for obtaining a high yield of protoplasts. In this study, we isolated protoplast from three different tissues of 10 days old peanut seedlings (Figure 3.1A). The yield of cells from fully expanded leaves (section i) was higher than those of unexpanded leaves (section ii) and hypocotyl (section iii), but the shape of the protoplast from section i was spherical (Figure 3.1C). From both sections ii and iii, we found oval-shaped protoplasts, although the protoplast yields were much lower, especially from section iii. Moreover, we also compared the protoplast yields of the unexpanded leave from 5 days old peanut seedlings (Figure 3.1B). The results showed that the yield of protoplasts isolated from 5 days old seedlings was higher than that of the 10 days old peanut seedlings (Figure 3.1D). Considering

protoplast yield and shape, unexpanded leaves from 5 days old seedlings have been the most suitable source of plant tissue.

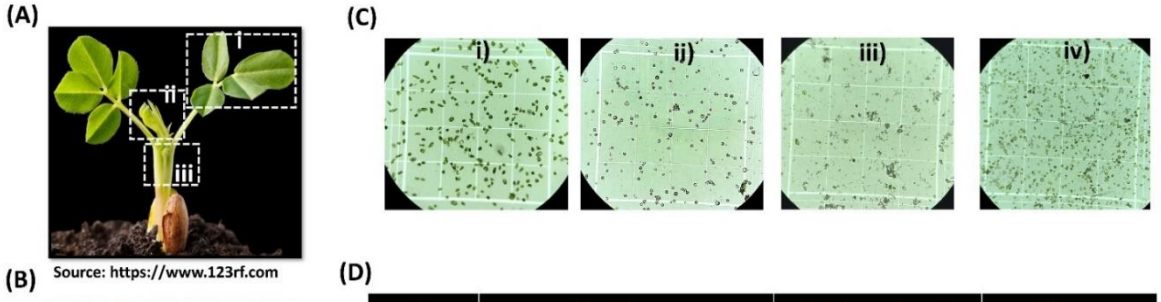

(D)

No	Plant tissue	Total number of cells g^{-1} ($\times 10^4$)	Shape
i	Fully expanded leaves (10 days old)	130	Spherical
ii	Unexpanded leaves (10 days old)	90	Oval
iii	Hypocotyl (10 days old)	5	Oval
iv	Unexpanded leaves (5 days old)	240	Oval

Figure 3.1 Protoplast isolation from different tissues and ages of peanut seedlings: A) 10 days old, B) 5 days old peanut seedlings; C) protoplast from different tissues (i, ii, iii and iv) of A and B; D) the total number of protoplast and their shapes from different tissues of peanut seedling.

3.3.2. Temperature effect on protoplast viability

Temperature plays a crucial role in protoplast viability. We kept and tested the protoplast viability at three different temperatures (4°C, 13°C and 23°C) after isolation. The result showed that the number of both total and viable protoplast decreased as the temperature increased (Figure 3.2). There were more viable protoplasts at 4°C than other temperatures. Unfortunately, all the protoplasts died at 23°C for 48h. The protoplast at 13°C for 24h showed a similar viability rate as 4°C, although the viability was considerably decreased after 48h. For further experiments, we

selected the condition at 13°C for 24h as an ideal condition for peanut protoplast transformation because we found the highest transformation efficiency and viability with *CmYLCV:GFP* plasmid (data not shown). Although the protoplast showed the highest viability at 4°C, we did not find any GFP expression even after 96h of transformation.

We also tested the two constitutive promoters' activity (*35S* and *CmYCLV* promoters) in peanut protoplast and found that protoplast transformed with *CmYLCV:GFP* gave higher transformation efficiency than *35S:GFP* based on the number the GFP expressing protoplast (Appendix Figure 6). Thereby, *CmYLCV:GFP* plasmid was used for further optimization.

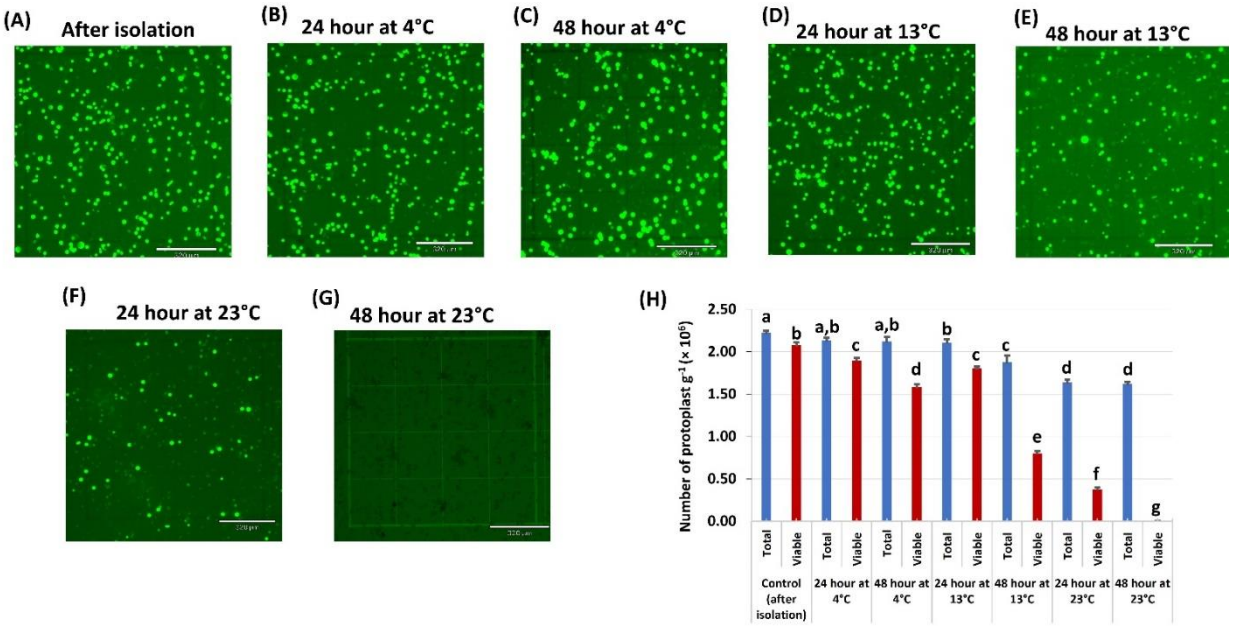

Figure 3.2 Protoplast viability test under different temperature, A)-G) Micrograph of viable protoplasts stained with FDA under fluorescence field kept at three temperature points (4°C, 13°C and 23°C) for 24h and 48h. H) The effects of temperature on the number of protoplasts. The number of total protoplasts and viable protoplasts was counted after 24 h and 48 h cultivation.

Values represent means ± SE (n = 7). The different letters indicate significant differences at $P < 0.05$.

3.3.3. Effects of PEG concentration on protoplast transformation efficiency and viability

Polyethylene glycol (PEG) is widely used to directly deliver DNA or plasmid into individual plant cells or protoplast. We tested the effects of different PEG 4000 concentrations on protoplast transformation efficiency, with concentrations (w/v) ranging from 20% to 80% (Figure 3.3 and Appendix Figure 7). In each treatment, the different PEG concentrations were tested with the optimal DNA and 5-min DNA incubation time. Additionally, the effect of PEG concentrations on protoplast viability was also tested. After 5 min PEG incubation and 24 h cultivation, it was evident that the 50% PEG concentration gave the highest transformation efficiency (TE) up to 7% (Figure 3.3A) based on GFP expressed protoplasts. The numbers of total intact and viable protoplasts decreased as the PEG concentration increased (Fig. 3.3B), which partly might be caused by the PEG-induced high permeability. Based on our observation, the 50% PEG concentration also gave the highest TE up to 7% and proper viable protoplasts.

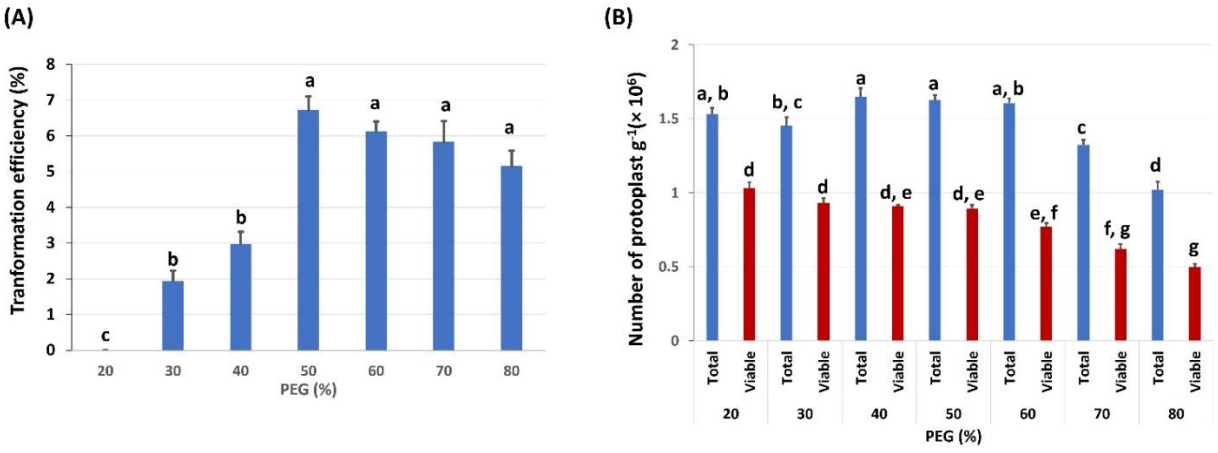

Figure 3.3 Effect of PEG concentration on protoplast transfection; A) transformation efficiency (TE) of protoplasts cultivated with various concentrations of PEG. TE was calculated after 24 h cultivation. B) The effects of PEG concentration on the number of protoplasts. The number of total protoplasts and viable protoplasts counted after 24 h cultivation. Values represent means ± SE (n = 7). The different letters indicate significant differences at $P < 0.05$.

3.3.4. Effects of plasmid concentrations on transformation efficiency

The amount of plasmid concentration is also critical for protoplast TE. Using the optimized conditions (50% PEG, incubated for 5 min), we examined the effects of different concentrations of *CmYLCV:GFP* plasmid on TE of peanut protoplasts (Figure 3.4 and Appendix Figure 8). The results showed that TE increased up to 7% with the increasing amount of plasmids from 20 to 300 µg, and the concentrations between 250 – 300 µg plasmids gave the highest TE (Figure 3.4). It is worth mentioning that the viability of protoplasts does not change due to the increase of plasmid concentration (data not shown).

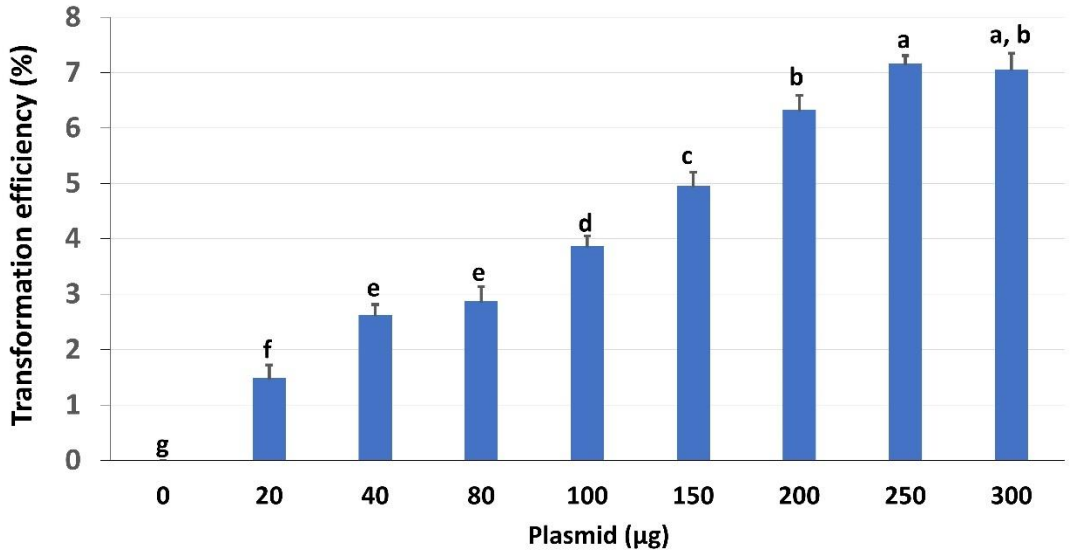

Figure 3.4 Effects of plasmid concentrations on protoplast transfection. The transformation efficiency (TE) of protoplasts cultivated with various concentrations of plasmids. The protoplast TE was evaluated after incubation in 50% PEG solution for 10 min. Values represent means ± SE (n = 7). The different letters indicate significant differences at $P < 0.05$.

3.3.5. Effects of PEG incubation time on protoplast transformation efficiency

To identify the optimum PEG incubation time, we examined the effect of different PEG incubation times on TE and protoplast viability (Figure 3.5 and Appendix Figure 8). The results showed that the TE was the highest (up to 7%) after incubation for 5 min with the 50% PEG concentration (Figure 3.5A), and afterward (> 5 mins) TE decreased. The total protoplasts and viable protoplasts from these various incubation times also had a similar trend (Figure 3.5B). Therefore, we inferred that 5 min was the optimal PEG incubation time.

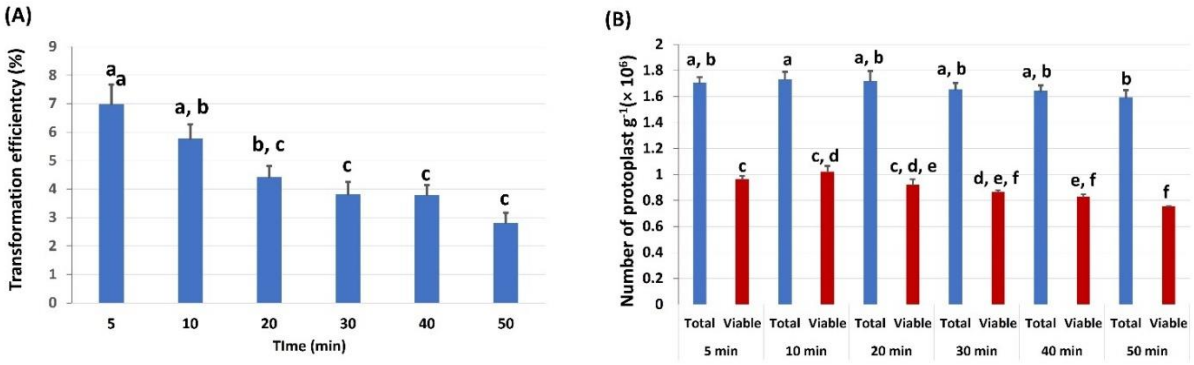

Figure 3.5 Effects of PEG incubation time on protoplast transfection. A) The transformation efficiency (TE) of protoplasts cultivated with various PEG incubation time. B) The effects of PEG incubation time on the number of protoplasts. The number of total protoplasts and viable protoplasts was counted after 24 h

cultivation. The protoplasts TE was evaluated after incubation in 50% PEG solution. Values represent means ± SE (n = 7). The different letters indicate significant differences at $P < 0.05$.

3.3.6. Selection of DNA sequence of *Ara h 2* gene target and vector construction

The coding sequence of *Ara h 2* (NM_001376217.1) was used to search for homologous sequences within the reference peanut genome database (http://peanutbase.org), and two copies of *Ara h 2 (Ara h 2A and Ara h 2B)* were identified in the A and B genomes (Figure 3.6 A). The conserved regions for both copies were identified, amplified with allele-specific primers (Appendix Table 4), and sequenced. To increase the chance of disrupting the *Ara h 2* gene sequence, two distinct *gRNAs (gRNA1 and gRNA2)* were designed. The CRISPR-P program was used to identify gRNAs with the highest efficacy and the least off-target potential (Liu et al., 2017a). The Polycistronic *tRNA-gRNA (PTG)* construct bearing the two *sgRNAs* was cloned into a nonbinary vector (pTrans_100). (Appendix Figure 5 and Figure 3.6 B). The *Cas9* gene *and tRNA-gRNA (PTG)* were expressed under the control of the *CmYLCV* promoter (Appendix Figure 5 and Figure 3.6B).

3.3.7. In vitro test of sgRNA efficiency

In vitro ribonucleoprotein (RNP) assay for the two gRNAs targeting a PCR amplicon flanking the target site of the peanut *Ara h 2* gene was performed using the RNP complexes with purified *Cas9* (Invitrogen) and synthetic *gRNAs* (Synthego). The negative controls had uncut PCR products, while three bands were seen for the cut amplicon with *gRNA1* and *gRNA2*, indicating that both sgRNAs efficiently cut their target nucleotide sequences in the *Ara h 2* gene copies (Figure 3.6C).

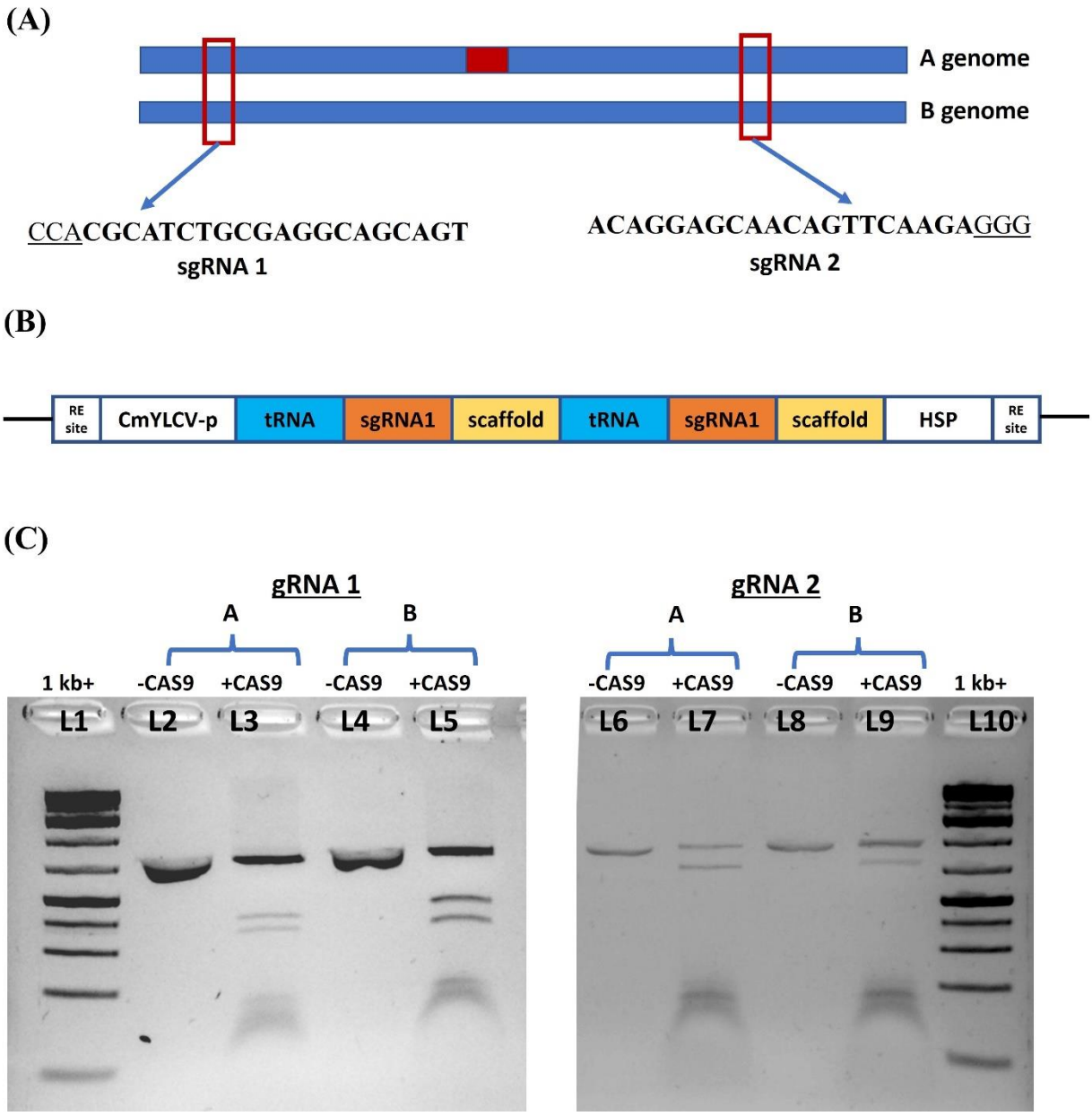

Figure 3.6 Schematic diagram of the peanut *Ara h 2* target gene copies, tRNA-sgRNAs of *Ara h 2* and in vitro digestion of *Ara h 2* gene targets; A) Schematic diagram representation of peanut *Ara h 2* gene copies at A and B genome and gRNA target regions. B) Schematic diagram representation of tRNA-sgRNAs of Ara h 2; C) In vitro digestion of Ara h 2. L1 and L10: 1kb^{+} ladders; L2: uncut Ara h 2A target region (genome A); L3: Ara h 2A target region digested with Cas9 and sgRNA1 (expected bands of 399 bp and

376 bp); L4: uncut Ara h 2B target region (genome B); L5: Ara h 2B target region digested with Cas9 and sgRNA1 (expected bands of 396 bp and 380 bp); L6: uncut Ara h 2A target region (genome A); L7: Ara h 2A target region digested with Cas9 and sgRNA2 (expected bands of 596 bp and 199 bp); L8: uncut Ara h 2B target region (genome B); L9: Ara h 2B target region digested with Cas9 and sgRNA2 (expected bands of 564 bp and 212 bp).

3.3.8. Editing of *Ara h 2* gene in peanut protoplast

To test the gene-editing efficacy of CRISPR-Cas9 vector for *Ara h 2*, peanut protoplasts was transformed with our optimized protocol. Genomic DNA was extracted to amplify the DNA fragment containing the target site. Targeted deep sequencing of targeted PCR products obtained from the isolated genomic DNA from each protoplast pool was used to detect the editing efficiency and patterns. The sequencing results revealed various indel mutation frequencies ranging from 0.13% to 0.8% for each *CRISPR sgRNA* sample (Table 3.2). Notably, on plant sample S2, both *sgRNAs* cut both genomic copies of *Ara h 2* and deleted several nucleotides of the target genes. On the other hand, on plant sample S1, the two sgRNAs only edited genome A of *Ara h 2* gene.

Table 3.2 Mutation analysis by targeted deep sequencing in *Ara h 2 gene.*

Plant no	*Ara h 2* gRNA target region (5'-3')	Type of edit	Editing Efficiency
	Ara h 2A (genome A) *gRNA1* NGS results		
WT	GCTGCCCA**CGCATCTGCGAGGCAGCAGT**GGGAACTCCAA		
S1	GCTGCCCA**CGC------TGCGAGGCAGCAGT**GGGAACTCCAA	3 bp deletion	0.8%
S2	GCTGCCCA**CG----------GCGAGGCAGCAGT**GGGAACTCCAA	5 bp deletion	0.37%
	Ara h 2B (genome B) *gRNA1* NGS results		
WT	GCTGCCCA**CGCATCTGCGAGGCAGCAGT**GGGAACTCCAA		
S1	GCTGCCCA**CGCATCTGCGAGGCAGCAGT**GGGAACTCCAA	No edit	
S2	GCTGCCCA**CGC--------GCGAGGCAGCAGT**GGGAACTCCAA	4 bp deletion	0.20%
	Ara h 2A (genome A)*gRNA2* NGS results		
WT	GGGAGGCA**ACAGGAGCAACAGTTCAAGA**GGGAGCTCAG		
S1	GGGAGGCA**ACAGGAGCAAC----------AGA**GGGAGCTCAG	6 bp deletion	0.14%
S2	GGGAGGCA**ACAGGAGCAACAG------AAGA**GGGAGCTCAG	3 bp deletion	0.13%
	Ara h 2B (genome B) *gRNA2* NGS results		
WT	GGGAGGCA**ACAGGAGCAACAGTTCAAGA**GGGAGCTCAG		
S1	GGGAGGCA**ACAGGAGCAACAGTTCAAGA**GGGAGCTCAG	No edit	
S2	GGGAGGCA**ACAGGAGCAACAG------AAGA**GGGAGCTCAG	3 bp deletion	0.16%

3.4. Discussion

Isolation of high yield and good quality protoplasts depends on the proper tissue materials and age of the plants (Wang et al., 2021). For leguminous crops like chickpea and soybean, fully expanded leaves are the best choice for protoplasts isolation (Wu and Hanzawa, 2018; Cheng and Nakata, 2020). However, our results on peanut protoplast demonstrated that the best tissue for protoplast isolation was unexpanded leave from 5 days old seedling (Figure 3.1). Using such type of leaf tissues, oval-shaped cells were identified and being used successfully in PEG-mediated transformation. Spherical-shaped cells were recovered from the isolation of the expanded leaves of the peanut plants; however, this type of cells failed to be used in the PEG-mediated

transformation. This may indicate that the oval-shaped cells were the true protoplasts, while the spherical-shaped cells were presumably spheroplasts (Taiz and Jones, 1971).

Temperature is another crucial factor for maintaining the viability of the isolated protoplasts. Most plant protoplasts are stable at room temperature (23°C-28°C) (Reed and Bargmann, 2021). In contrast, however, our experiments showed that all the peanut protoplasts died at 23°C after 48h. Next, we tested the viability of protoplasts at 4°C and 13°C and showed that the 13°C was the ideal temperature for the PEG-mediated transformation. The optimum concentration of PEG and the duration of the PEG incubation time are other criteria that need to be considered for increasing transformation efficiency in protoplasts; it varies from plant to plant (Lin et al., 2018; Reed and Bargmann, 2021). Our data showed that 50% of PEG and 5 min incubation time were ideal for peanut protoplast transformation. The concentration of the plasmid is also a key factor in protoplast transformation. Different amounts of plasmids, such as 15 µg for wheat (total volume 460µl) , 20 µg for rice (total volume 460µl), 30 µg sugarcane (total volume 230 µl), have been reported to be the optimal amounts of DNA in their optimized protocols with approximately TE 70-80% for protoplast transformation, respectively (Shan et al., 2014; Brandt et al., 2020; Wang et al., 2021). Moreover, 2.73% transformation efficiency was achieved in oil palm protoplast using 40% PEG and 50 µg plasmid, which was highest for this plant (Masani et al., 2014). However, we obtained 7% transformation efficiency after using 250-300 µg of *CmYLCV* plasmid in our experiment.

Gene editing technology has not yet been used widely in peanut. Thus far, the only reported study of gene editing in peanut was the knocking out of the *FAD2* gene using the *CRISPR/Cas9* system through the *Agrobacterium rhizogenes* mediated hairy root transformation (Yuan et al., 2019). However, there has been major limitation of the hairy root-regenerated transformants, which is the integration of unwanted pRi T-DNA (Hudzieczek et al., 2019). The presence and expression of the

oncogenes in pRi T-DNA may cause some problems in analyzing the phenotypic evaluations of the transgenic lines. The major limitation of this approach is that since shoots are not transformed and mature complete plants is not possible either by vegetative propagation or self-fertilization. The use of *Agrobacterium tumefacient*-mediated transformation may overcome such problems (Gelvin, 2003); however, the effectiveness of *Cas9-gRNAs* of the target gene needs to be evaluated first before generating stable transformants to increase the chance of our success. For this purpose, PEG-mediated protoplast transformation can be used, such as conducted in this study.

In order to increase our chance of success, two *gRNAs* were designed to disrupt allergen gene function in the peanut cultivar Schubert. Due to the natural preference of DNA repaired system for the non-homologous end joining (NHEJ), insertion and deletions (INDELs) are the most common type of mutations that occurred by CRISPR-Cas9 editing system (Bortesi and Fischer, 2015). We verified that all the *gRNAs* efficiently cut their respective allergen target site through in vitro digestion with Cas9 protein and identified two edited samples after transformation with *CRISPR_Cas9* plasmid. In silico analysis revealed that all the edited plants had different nucleotide changes due to deletions. For the edited sample S2, premature stop codons were generated in the coding sequence of both gene copies. Meanwhile, for the edited sample S1, the coding sequences of *Ara h 2A* completely changed due to the deletions in the two *gRNA* regions (Appendix Figure 8).

4. OPTIMIZATION OF PRIME EDITING IN RICE AND PEANUT PROTOPLASTS BY RESTORATION OF GFP ACTIVITY

4.1. Introduction

Precise gene editing promises to be a crucial tool for functional genomics studies and crop improvement. Precise sequence deletions, insertions, and replacements have been performed by homology-directed repair (HDR) of double-stranded breaks (DSBs) through the presence of a donor DNA template (Xu et al., 2020a). However, HDR used in basic plant research and crop improvement is still very limited because of its low efficiency and the difficulty of DNA template delivery (Molla and Yang, 2020). Yet, this technique is important in plant breeding for large sequence insertion/precise knock-in and complex DNA modification (Lu et al., 2020).

Base editing (BE) is recognized as an alternative tool to HDR-mediated replacement that greatly enhances crop breeding opportunities for allele modifications where base substitutions are needed (Li et al., 2017; Lu and Zhu, 2017; Veillet et al., 2019). Base editing can perform up to 100-fold higher efficiency than HDR in obtaining desired mutations (Molla and Yang, 2019). Cytosine and adenine base editors (CBEs and ABEs) are the two groups of base editors widely used that can install C•G-to-T•A and A•T-to-G•C transitions, respectively (Mishra et al., 2020). For CBE, the Cas9 nickase (nCas9) or catalytically dead Cas protein (dCas9) is fused with a cytidine deaminase that converts the original C to T in the targeted DNA region (Komor et al., 2016). In ABE, nCas9 or dCas9 is fused with adenosine deaminase, which permits A·T to G·C base substitutions in the target DNA sequence (Nishida et al., 2016). Both CBEs and ABEs have been well established in

various crops, including rice, wheat, maize, tomato, and cotton (Shimatani et al., 2017; Zong et al., 2017; Kang et al., 2018; Li et al., 2018a; Qin et al., 2020).

Although base editors in plants are highly efficient, they can perform only four types of base changes; however, manipulation of many agronomic traits may require the other eight nucleotide substitutions (A•T-to-C•G, C•G-to-A•T, T•A-to-A•T and G•C-to-C•G), or precise deletions and insertions (Xu et al., 2020b). Prime editing systems have the capability to perform efficient and precise genome editing in these circumstances (Anzalone et al. 2019). There are three prime editor systems (PPEs): PPE2, PPE3, and PPE3b. PPE2 consists of a nCas9 (H840A) fused to an engineered M-MLV reverse transcriptase (RT), and a pegRNA composed of a primer binding site (PBS) and an RT template. PPE3 adds nicking single guide RNA (sgRNA) to cleave the non-edited strand, facilitating favorable DNA repair. In PPE3b, this nicking sgRNA targets the edited sequence, thereby preventing nicking of the non-edited strand until after editing occurs, resulting in fewer indels in mammalian cells (Anzalone et al., 2019).

Some studies using prime editing have been recently published in plants, including rice, wheat, maize, potato, and tomato (Jiang et al., 2020; Lin et al., 2020; Tang et al., 2020; Veillet et al., 2020; Xu et al., 2020a; Lu et al., 2021). In wheat, the frequencies of single nucleotide substitutions, including A-to-T, C-to-G, G-to-C, T-to-G, and C-to-A reached up to 1.4% (Lin et al., 2020). Interestingly, using dual PEG and designing perfect PBS, prime editing efficiency was increased up to 17% in rice (Lin et al., 2021) . Considering the usefulness of this technology, prime editing efficiency needs to be further improved in different crops. This study aimed to further optimize prime editing in both rice and peanut protoplasts by transiently targeting a mutant GFP to restore

functionality. We used three promoters to develop the vectors with different combinations and tested their efficiency in both rice and peanut.

4.2. Materials and methods

4.2.1. Plant material

The temperate *japonica* rice cultivar Nipponbare was used for this study. For peanut, a cultivar developed by Texas A&M AgriLife Research, Schubert, was used (Burow et al., 2014). The peanut seedlings were grown in a greenhouse with a temperature of 32/26 °C (day/night) and a 16/8 h light–dark cycle.

4.2.2. Prime editing vector construction

CmYLCV_GFP_HSP and *35S_GFP_NOS* vectors were used for active *GFP* expression in protoplasts. For the development of the prime editing vectors, we used three intermediate module plasmids A, B, and C and one backbone vector, *pTRANS_100* (Čermák et al., 2017) (Figure 4.1).

For making a mutant GFP vector, a stop codon (TAG) (changing C to G at 202 positions) was inserted in the coding sequence of GFP by overlapping PCR and cloned into *CmYLCV_GFP_HSP* vector by removing active GFP sequence through restriction digestion cloning with T4 DNA ligase (NEB, Ipswich, MA, USA). *CmYLCV_mutant_GFP_HSP* was modified as Module A (Figure 4.1A).

For making pegRNAs, four gRNAs were designed at the mutated GFP position. The efficiency of the gRNAs was checked using the *in vitro* digestion of DNA with Cas9 Nuclease (NEB, Ipswich,

MA, USA) provided by the manufacturer with a few modifications. In this case, a 27 µl reaction mixture containing 30 nM of synthesized sgRNA, 30 nM of Cas9 nuclease, and 3 µl of 10x NEB buffer 3.1 were pre-incubated for 10 minutes at 25 ºC. Afterward, 100 ng purified PCR product was added to make a total reaction volume 30 µl and incubated at 37 °C for 1h. After adding 1 µl of Proteinase K, the reaction mixture was kept for 10 minutes at 56 °C, and fragment analysis was performed using gel electrophoresis.

To target the GFP mutation, two single pegRNAs were designed using pegFinder (Chow et al., 2021), and one dual pegRNA was designed using PlantPegDesigner (Lin et al., 2021). An endogenous tRNA processing system was used for the dual pegRNA expression (Xie et al., 2015). All pegRNAs were synthesized and cloned into pMOD_2515b/pMOD_B2303 where pegRNAs were driven by the *OsU6/CmYLCV* promoter (Figure 4.1B). The *nCAS9* and *M-MLV RT* were amplified from nCas9-PPE plasmid (Addgene #140445) and cloned into the *35S_GFP_NOS* vector by removing the GFP. For making *CmYLCV_nCAS9 + M-MLV_NOS*, *CmYLCV* was placed by removing 35S promoter from *35s_nCAS9 + M-MLV_NOS* plasmid (Figure 4.1C). The *CmYLCV_mutant_GFP_HSP* (module A), and pMOD_2515b/pMOD_B2303_pegRNA (Module B) and *35S*/*CmYLCV*_nCAS9+M-MLV_NOS (Module C) were cloned into a non-binary pTRANS_100 through golden gate assembly cloning (Čermák et al., 2017) (Figure 4.1D).

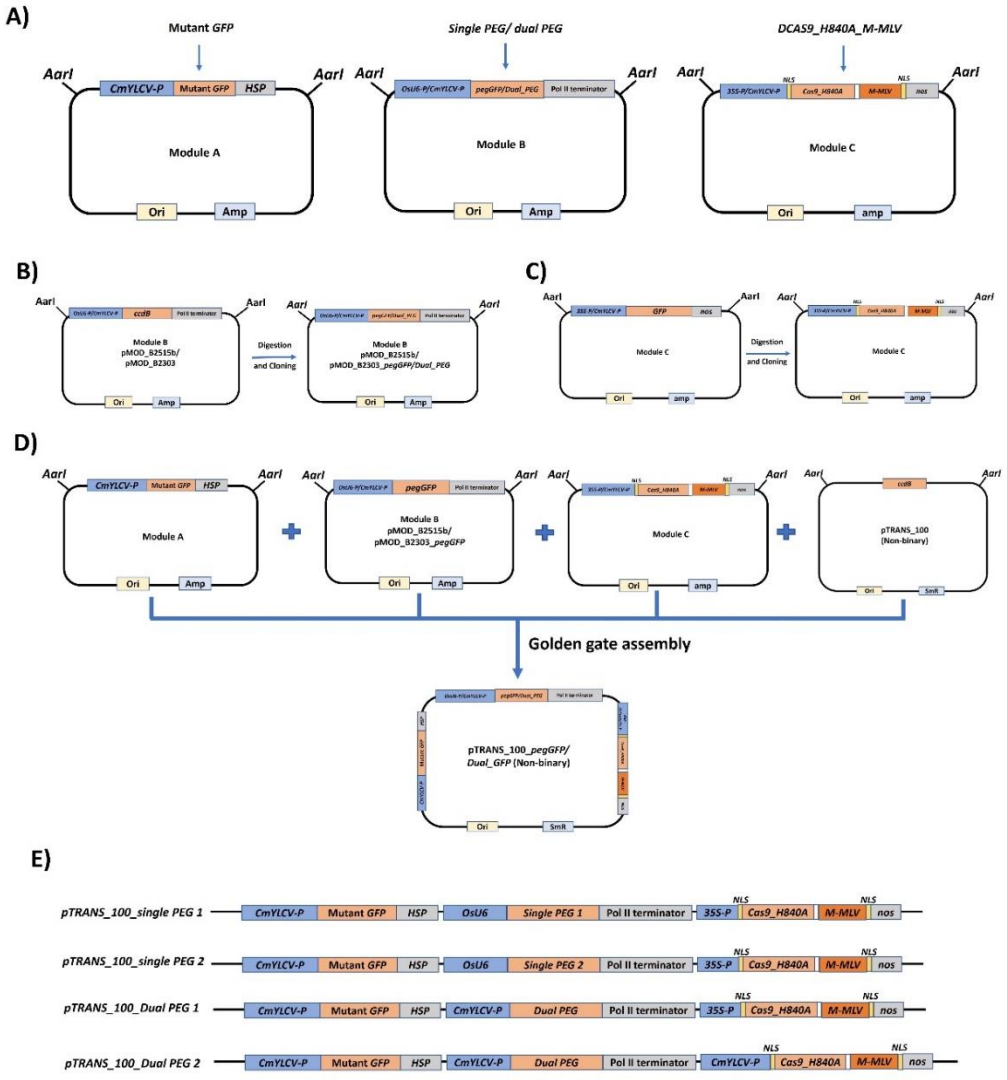

Figure 4.1 Schematic diagram of cloning strategies of the prime editing vector in this study. A) Vector modules used for the prime editing vector, CmYLCV-P_mutant_GFP_HSP was used as module A, OsU6-P/CmYLCV-P_single PEG/dual PEG_Pol II terminator was used as module B and 35S-P/CmYLCV-P_nCAS9_M_MLV_NOS was used as module C; B) Cloning of OsU6-P/CmYLCV-P_single PEG/dual PEG_Pol II terminator vector; C) Cloning of 35S-P/CmYLCV-P_nCAS9_M_MLV_NOS; D) Making of prime editing vectors using golden gate assembly; E) Schematic representation of different prime editing vectors used in this study.

4.2.3. Protoplast isolation and transfection

Rice protoplasts were isolated from the stems of 10-12 days old rice seedlings according to established protocols (Li et al., 1995; Shan et al., 2014) with some modifications. Briefly, the stems and sheaths of ~30 rice seedlings per trial (total 100–120 seedlings) were cut into latitudinal strips. The strips were transferred into a 150-ml conical flask containing 50 ml of filter-sterilized enzyme solution (1.5% (w/v) Cellulase RS, 0.1% (w/v) Macerozyme R-10, 0.4 M Mannitol, 20 mM KCl and 20 mM MES (pH 5.7)) and the flask was wrapped with aluminum foil. The strips with cell wall–digesting enzymes were vacuum-infiltrated by applying a vacuum (~380–508 mmHg) for 30 min in the dark. Next, the strips were incubated in the dark for 5 h with gentle shaking (50 rpm) at room temperature. After enzymatic digestion, 50 ml of W5 solution (154 mM NaCl, 125 mM $CaCl_2$, 5 mM KCl, 2 mM MES (pH 5.7) was added to the conical flask and then shaken gently by hand for 10 s to release the protoplasts. The protoplasts were collected into three or four 50-ml round-bottomed centrifuge tubes after filtering the mixture through 40-µm nylon mesh and washing the strips on the surface of the nylon mesh 3–5 times with W5 solution. The solution containing protoplasts was centrifuged at 250 g for 3 min at room temperature (RT) in a swinging bucket rotor, and the supernatant was removed by pipetting. The protoplasts were resuspended in 10 ml of W5 solution, collected into a 50-ml round-bottomed tube, and centrifuged at 250 g for 3 min at room temperature. The supernatant was removed by pipetting, and the protoplasts were resuspended in 4 ml of MMG solution (0.4 M Mannitol, 15 mM $MgCl_2$ and 4 mM MES (pH 5.7)). The density of protoplasts was determined under a microscope (×100) with a hemocytometer. Rice protoplast transfection with the prime editing vectors was performed using PEG

(polyethylene glycol) according to Shan et al., 2014. Peanut protoplasts and transformation were performed according to the protocol by Biswas et al., 2022.

4.2.4. Microscopy analysis

The total, viable, and GFP-expressed protoplasts were counted with the microscope under normal light and fluorescent light (ECHO Revolve). The transformation efficiency of each prime editing vector was calculated after the 24h of transformation.

4.2.5. Mutant analysis

After 4–5 days post-transfection under dark conditions, both rice and peanut protoplasts were collected by centrifugation at 13000 rpm. RNA was extracted following the protocol of the Zymo plant RNA isolation kit (Zymo, Irvine, CA, USA). Next, cDNA was synthesized according to the manufacturer's protocol (RevertAid First Strand cDNA Synthesis Kit, ThemoFiser Scientific, Waltham, MA). The targeted edited region of GFP was amplified with the Phusion Taq polymerase by primer sets (Forward_GFP: 5'-GTCCCAATTCTTGTTGAATTAGATG-3' and reverse_GFP: 5'-ACAGGTAATGGTTGTCTGGTAAAAG-3') as following protocol: with an initial denaturation step of 98°C for 30 s, followed by 30 cycles of 98°C for 30 s, 58°C for 30 s, and 72 °C for 30 s, and a final extension of 72°C for 7 min. PCR products of GFP were purified by gel extraction and cloned into a TOPO vector (ThemoFiser Scientific, Waltham, MA). The positive clones were sequenced through the Sanger sequencing.

4.3. Results

4.3.1. Design of mutant GFP and sgRNA test for PEG RNAs

One stop codon (ATG) was inserted in the coding region of GFP by changing C to G at position 202 (Figure 4.2A). Four gRNAs were designed using CRISPR-P2 and their efficiency was tested by *in vitro* digestion with Cas9 RNPs. All four gRNAs cut the target GFP sequence efficiently (Figure 4.2C). Out of four, two gRNAs were used for pegRNA design depending on to close proximity of the mutation site (Figure 4.2B).

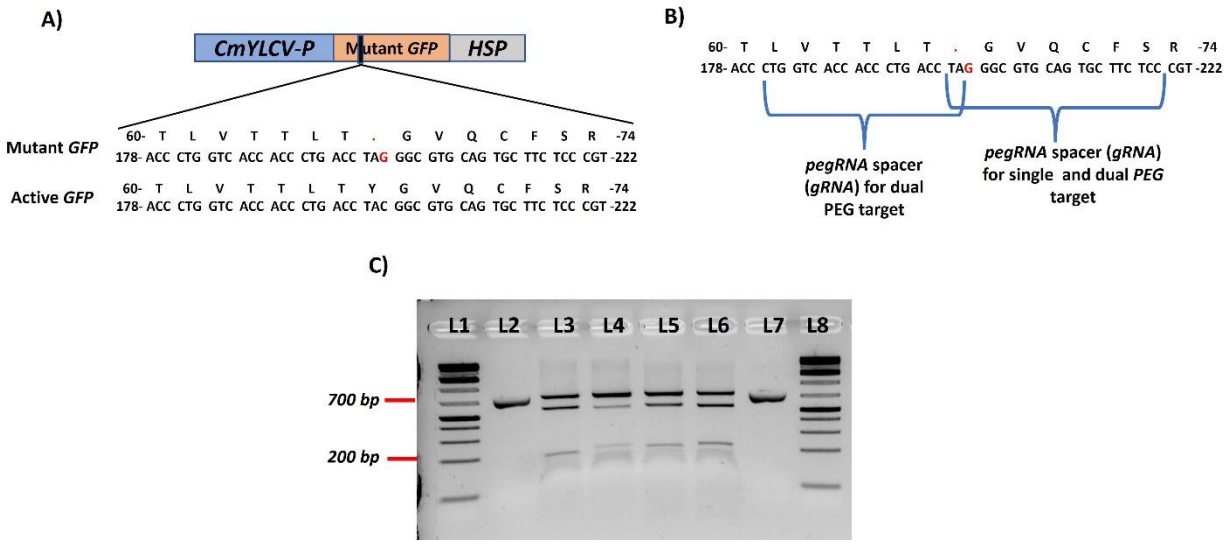

Figure 4.2 A) Map of mutant GFP, B) position of pegRNA spacer/gRNA for single pegRNA and dual pegRNA and C) invitro-digestion of gRNAs. L1 and L8: 1kb^{+} ladders; L2 and L7: uncut mutant *GFP* target region; L3: mutant *GFP* target region digested with Cas9 and sgRNA4 (expected bands of 531 bp and 190 bp); L4: mutant *GFP* region digested with Cas9 and sgRNA3 (expected bands of 518 bp and 203

bp);); L5: mutant *GFP* region digested with Cas9 and sgRNA2 (expected bands of 522 bp and 199 bp);); L6: mutant *GFP* region digested with Cas9 and sgRNA1 (expected bands of 521 bp and 200 bp);

4.3.2. Making of Mutant GFP vector and test in protoplasts

An expression vector containing the mutant GFP sequence driven by the CmYLCV promoter was developed (Figure 4.3A). For introducing a stop codon in the GFP coding sequence, overlapping PCR was performed, and the mutant GFP was inserted into module A vector by removing active GFP through restriction digestion cloning. The mutant GFP vector was then tested in both rice and peanut protoplasts along with the active GFP expression vector as a control. After 48 h of transformation, no GFP expression was seen in both rice and peanut protoplasts. In contrast, a high level of GFP expression was seen in rice and peanut protoplasts with the active GFP vector (Figure 4.3B). The result showed that the activity of GFP was successfully terminated by the insertion of a stop codon (TAG).

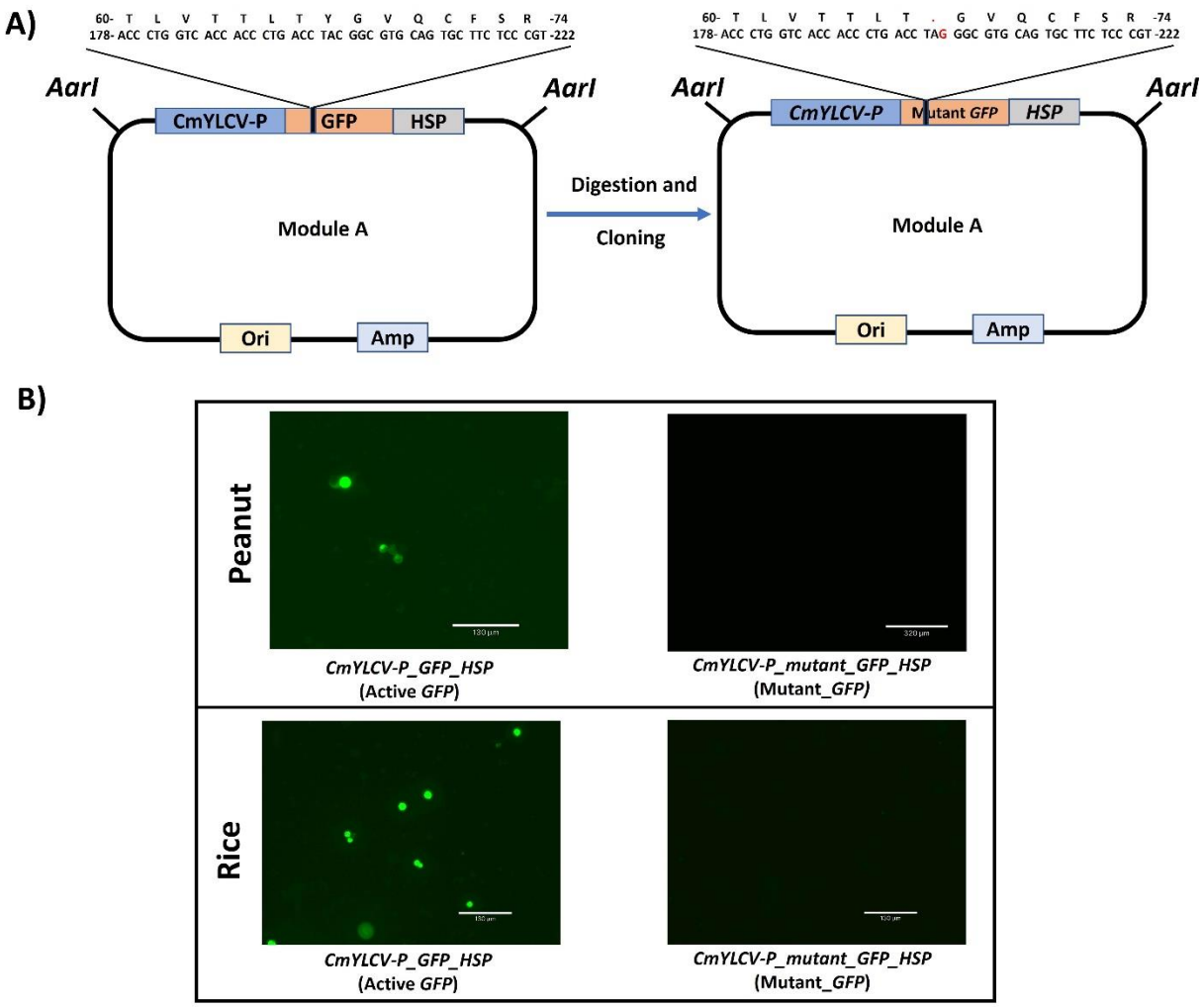

Figure 4.3 A) Cloning of mutant GFP and B) Test of active GFP and mutant GFP in both peanut and rice protoplast. Micrographs of protoplasts expressing *active GFP and mutant GFP* under GFP field for both peanut and rice. For peanut, the condition was 50% PEG, 5 min PEG incubation time and 300µg plasmid DNA of each vector. For rice, the condition was 40% PEG, 20 min PEG incubation time and 20µg plasmid DNA of each vector.

4.3.3. Test of prime editing vectors in rice and peanut

Four types of prime editing vectors were used to test the efficiency of prime editing in both rice and peanut protoplasts, and GFP expressions were then evaluated at 24h after post-transformation (Figure 4.4). Both single pegRNAs containing vectors showed low GFP expression in rice protoplasts (Figure 4.4). However, both dual pegRNAs containing vectors gave significantly higher expression than the single pegRNAs vectors (Figure 4.4). This result demonstrated that dual pegRNAs vectors had higher prime editing efficiency (16 times) than the single pegRNAs vectors in rice. We did not see any GFP expression in the negative control (Figure 4.4A), but higher GFP expression/transformation efficiency (60%) was found in rice protoplasts transformed with the CmYLCV_GFP expression vector (Figure 4.4F). We successfully obtained edits of mutant GFP position (G to C) in rice protoplast using the dual pegRNA1 containing vectors through Sanger sequencing (Figure 4.4H).

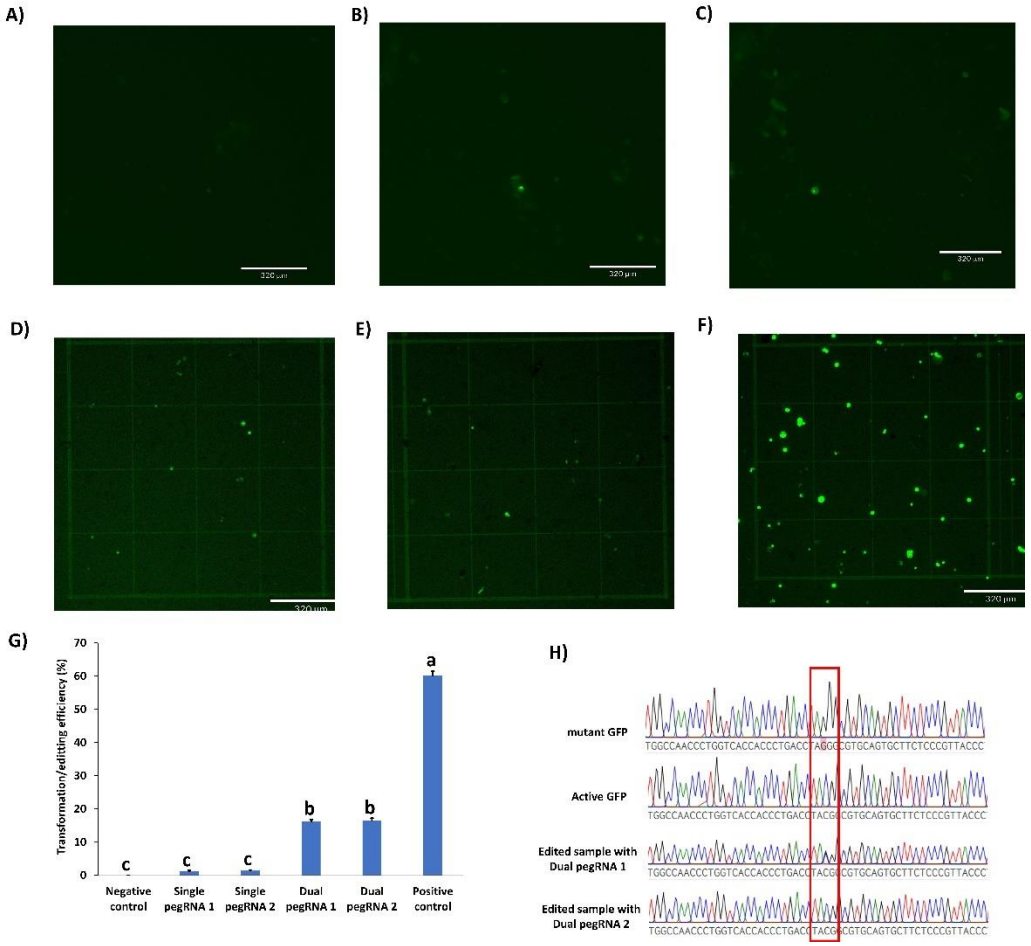

Figure 4.4 Prime editing results in rice protoplasts using single and dual pegRNAs containing vectors. Micrograph of A) negative control (no GFP plasmid/prime editing vectors); B) protoplasts with single pegRNA 1 containing editing vector; C) protoplasts with single pegRNA 2 containing editing vector; D) protoplasts with dual pegRNA 1 containing editing vector; E) protoplasts with dual pegRNA 2 containing editing vector F) positive control (protoplasts with *CmYLCV_GFP* vector); G) The transformation efficiency (TE) of protoplasts transformed with different prime editing vectors; The protoplasts TE was evaluated after incubation in 40% PEG solution with 20µg plasmid DNA of each prime editing vector. Values represent means ± SE (n = 6). The different letters indicate significant differences at $P < 0.05$. H) Sanger sequencing result of active GFP, mutant GFP and sample transformed dual pegRNA 1 containing vector.

GFP expressions were also evaluated at 24h after post-transformation in peanut protoplasts (Figure 4.5). Unfortunately, we did not get any GFP expression in peanut protoplasts with two single pegRNAs and one dual pegRNA containing prime editing vectors (Figure 4.5B, 4.5C, 4.5D). But one dual pegRNA vector where all the genes (nCAS9-M_MLV, dual pegRNA and mutant GFP) were expressed by CmYLCV promoter showed lower GFP expression in peanut protoplast (Figure 4.5E, 4.5G). As expected, there was no GFP expression in the negative control (Figure 4.5A); however, we found good GFP expression in peanut protoplasts with the positive control (CmYLCV_GFP) (Figure 4.5F).

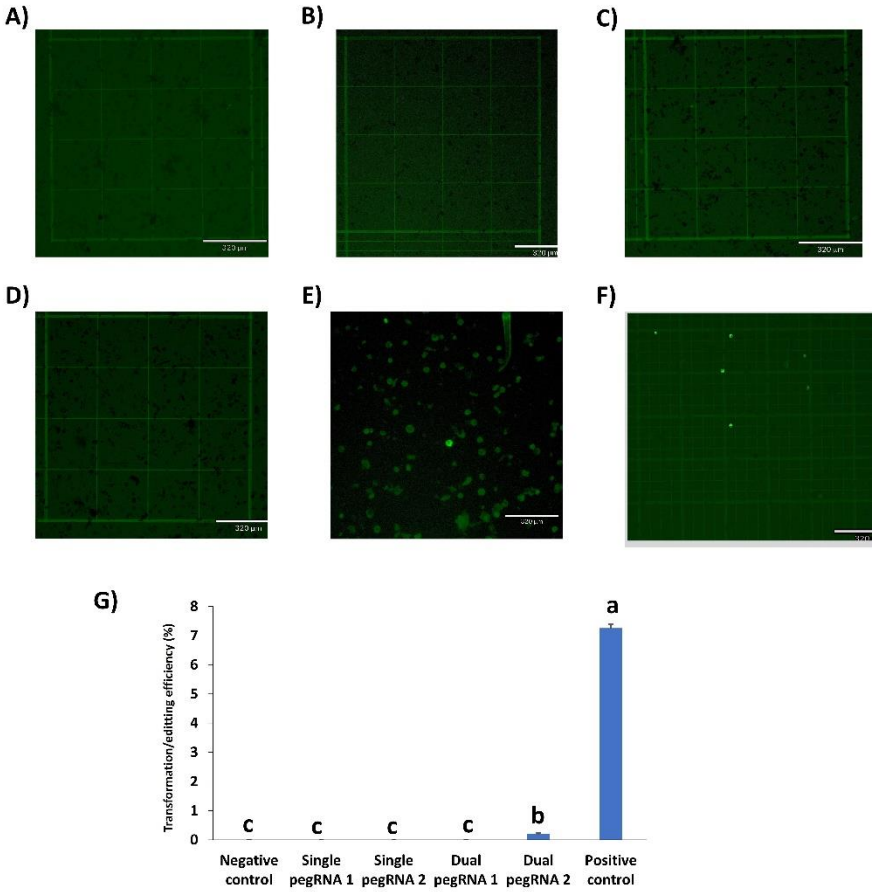

Figure 4.5 Prime editing results in peanut protoplasts using single and dual pegRNAs containing vectors. Micrograph of A) negative control (no GFP plasmid/prime editing vectors); B) protoplasts with single pegRNA 1 containing editing vector; C) protoplasts with single pegRNA 2 containing editing vector; D) protoplasts with dual pegRNA 1 containing editing vector; E) protoplasts with dual pegRNA 2 containing editing vector F) positive control (protoplasts with *CmYLCV_GFP* vector); G) The transformation efficiency (TE) of protoplasts transformed with different prime editing vectors. The protoplasts TE was evaluated after incubation in 50% PEG solution with 300µg plasmid DNA of each prime editing vector. Values represent means ± SE (n = 6). The different letters indicate significant differences at $P < 0.05$.

4.4. Discussion

Although the CRISPR-Cas9 system creates revolutionary changes in the field of agriculture, precise genome editing still remains a challenge in plants. In plants, the homology-directed repair is limited due to low efficiency and challenges in delivering the template DNA to make precise edits (Ali et al., 2020). The first set of base editors, cytosine and adenine base editors (CBEs and ABEs) have several drawbacks, including lower efficiency, the possibility of off-target mutations effects, and their limitation in editing only four types of base changes (Rees and Liu, 2018). Prime editing, however, has a more versatile capability for broader applications in crop improvement through making more precise edits through insertions, deletions and substitutions with all types of possible combinations of bases (Hassan et al., 2020).

Although the first prime editing prototypes were also limited by the low editing efficiency, recently, by using two prime editing guide (peg) RNA (dual PEG) in trans direction for the same target location, up to 17% editing efficiency was obtained (Lin et al., 2021). In this study, we successfully developed vectors for prime editing through Golden Gate assembly and demonstrated

their efficacy in one monocot and one dicot plant. I found higher editing efficiency (16%) in rice, similar to previously published data (Lin et al., 2021), where up to 60% transformation efficiency was found with the positive control (35S_GFP plasmid). However, we obtained a lower percentage of edits in peanuts, which partly might be due to the lower transformation efficiency in protoplast to start with, which is about 7% (Biswas et al., 2022).

Testing of the CRISPR-Cas system can be performed relatively easily in protoplasts due to the convenience of protoplast isolation and transfection in different plants (Lin et al., 2018). For instance, validation of Cas codon-optimization or modification, sgRNA, identification of the best promoter and analysis of different vector designs can be performed in protoplasts through transient expression (Yue et al., 2021; Biswas et al. 2022). Therefore, protoplasts present the ideal platform for the determination of prime editing vector efficiency in a relatively short period of time. In this study, we successfully isolated and transformed protoplasts with our developed prime editing vector in both rice and peanut.

Despite the economic importance, gene editing technologies have not yet been used widely in peanut. In vivo assays and protoplast transformation can be used as a tool to express prime editing cascade transiently as well as to evaluate the prime editing efficacy. In this study, we obtained only 0.2% editing efficiency with dual PEG RNA containing prime editing where all the genes (mutant GFP, nCAS9_M-MLV and PEG RNA) were expressed by the CmYLCV promoter, but we did not get any GFP expressed plasmid after transformation with other prime editing vectors, although the positive control (CmYLCV_GFP transformed protoplast) reached up to 7% transformation efficiency. But for rice, we found 16% editing efficiency with both dual pegRNA containing prime editing vectors, although 60% transformation efficiency was reached with the

positive control (CmYLCV_GFP transformed protoplast). These results showed that promoter activity plays a significant role in the prime editing vector efficiency. In this study, we used three different types of promoters: CAMV 35S, CmYLCV and OsU6. All three promoters worked better in rice protoplasts, but only CmYLCV gave up to 7% transformation efficiency in peanut. Other parameters that are crucial for prime editing success are sgRNA position for nCAS9 and R.T. (reverse transcriptase) and PBS (primer binding site) length (Lin et al., 2021). Further optimizations will be required, such as using appropriate promoters and modifying those parameters to improve the editing efficiency.

5. CONCLUSION

The use of CRISPR-Cas systems makes genome editing a powerful tool for precise crop improvement via gene knockout, knock-in, replacement, point mutations, specific gene regulation, and other modifications at any gene locus in almost any crop.

In summary, the resistant starch project showed the feasibility of using multiplex CRISPR-Cas9 genome editing to simultaneously target multiple *SBE* genes and efficiently developed transgene-free high amylose and higher resistant starch-containing rice plants. The results of our study will potentially contribute to providing a better diet option to rice consumers and help reduce the prevalence of diet-related diseases. Although it has been known that *SBE3* gene plays a crucial role in starch biosynthesis, further investigation is needed to better understand the contribution of the rest of *SBE* genes, especially in combination with other *SBE* gene modifications. Future studies can explore this further once additional lines with different combinations of *SBE* gene edits become available. These lines would also help further differentiate the relationship between high amylose and high resistant starch content in rice grains. As extremely high amylose content is undesirable for cooked rice texture and quality, it will be important to explore combinations of gene-edited alleles that lead to high resistant starch while keeping the amylose content in a desirable range for cooked rice quality. Alternatively, rice with very high amylose content and resistant starch could be used for further processed rice products, such as rice flour.

An efficient gene editing platform in peanut needs to be established not only to assist in basic research in trying to understand gene functions and molecular pathways, but also to help accelerate breeding programs in developing peanut with improved yield and quality and tolerance to various

abiotic and biotic stresses. Our study describes the success in developing an efficient protoplast isolation protocol in peanut as a testbed for optimizing genome editing using the CRISPR-Cas9 system with the allergen gene *Ara h 2* as a test case. This strategy provides an efficient pipeline to develop gene editing constructs for various genes or peanut transformation. Once optimized, stable transformants can be developed using *Agrobacterium*-mediated transformation or alternative delivery systems. Additionally, further optimization of the CRISPR-Cas9 system in peanut can be explored using other editing techniques, including allele replacement, to widen the target traits and speed up the breeding progress.

In our prime editing project, we successfully developed vectors for prime editing through Golden Gate assembly and demonstrated their efficacy in monocot and dicot protoplasts. We found higher editing efficiency (16%) in rice, although we obtained a lower percentage of edits in peanut. However, efficiencies are likely to be higher in stably transformed plants. Further optimization will be required, including using appropriate promoters and modifying with R.T. template and PBS length. It is possible to make prime editing a useful biotechnological tool for precise genome editing in plant research and breeding through further refinement.

REFERENCES

Advances in Genetics and Genomics for Sustainable Peanut Production. 2011

Ali, Z., A. Shami, K. Sedeek, R. Kamel, A. Alhabsi, M. Tehseen, N. Hassan, H. Butt, A. Kababji, S.M. Hamdan, and M.M. Mahfouz. 2020. Fusion of the Cas9 endonuclease and the VirD2 relaxase facilitates homology-directed repair for precise genome engineering in rice. Commun. Biol. 3. doi:10.1038/s42003-020-0768-9

Aliaga-Franco, N., C. Zhang, S. Presa, A.K. Srivastava, A. Granell, D. Alabadí, A. Sadanandom, M.A. Blázquez, and E.G. Minguet. 2019. Identification of Transgene-Free CRISPR-Edited Plants of Rice, Tomato, and Arabidopsis by Monitoring DsRED Fluorescence in Dry Seeds. Front. Plant Sci. 10. doi:10.3389/fpls.2019.01150

Alok, A., D. Sandhya, P. Jogam, V. Rodrigues, K.K. Bhati, H. Sharma, and J. Kumar. 2020. The Rise of the CRISPR/Cpf1 System for Efficient Genome Editing in Plants. Front. Plant Sci. 11. doi:10.3389/fpls.2020.00264

Anzalone, A. V., P.B. Randolph, J.R. Davis, A.A. Sousa, L.W. Koblan, J.M. Levy, P.J. Chen, C. Wilson, G.A. Newby, A. Raguram, and D.R. Liu. 2019. Search-and-replace genome editing without double-strand breaks or donor DNA. Nature 576. doi:10.1038/s41586-019-1711-4

ASP, N.-G. 1992. Resistant starch. Proceeding from the second plenary meeting of EURESTA: European FLAIR concerted action no. 11 on physiological inplications of the consumption of resistant starch in man. J Eur, J. Clin, Nutr. 46:S1

Banavath, J.N., T. Chakradhar, V. Pandit, S. Konduru, K.K. Guduru, C.S. Akila, S. Podha, and C.O.R. Puli. 2018. Stress inducible overexpression of AtHDG11 leads to improved drought and salt stress tolerance in peanut (Arachis hypogaea L.). Front. Chem. 6. doi:10.3389/fchem.2018.00034

Bertioli, D.J., J. Jenkins, J. Clevenger, O. Dudchenko, D. Gao, G. Seijo, S.C.M. Leal-Bertioli,

L. Ren, A.D. Farmer, M.K. Pandey, S.S. Samoluk, B. Abernathy, G. Agarwal, C. Ballén-Taborda, C. Cameron, J. Campbell, C. Chavarro, A. Chitikineni, Y. Chu, S. Dash, M. El Baidouri, B. Guo, W. Huang, K. Do Kim, W. Korani, S. Lanciano, C.G. Lui, M. Mirouze, M.C. Moretzsohn, M. Pham, J.H. Shin, K. Shirasawa, S. Sinharoy, A. Sreedasyam, N.T. Weeks, X. Zhang, Z. Zheng, Z. Sun, L. Froenicke, E.L. Aiden, R. Michelmore, R.K. Varshney, C.C. Holbrook, E.K.S. Cannon, B.E. Scheffler, J. Grimwood, P. Ozias-Akins, S.B. Cannon, S.A. Jackson, and J. Schmutz. 2019. The genome sequence of segmental allotetraploid peanut Arachis hypogaea. Nat. Genet. 51:877–884. doi:10.1038/s41588-019-0405-z

Bharat, S.S., S. Li, J. Li, L. Yan, and L. Xia. 2020. Base editing in plants: Current status and challenges. Crop J. 8. doi:10.1016/j.cj.2019.10.002

Bhat, R.S., K. Shirasawa, V. Sharma, S.N. Isobe, H. Hirakawa, C. Kuwata, M.K. Pandey, R.K. Varshney, and M.V.C. Gowda. 2021. Population Genomics of Peanut

Biswas, S., N.J. Wahl, Thomson M.J., Cason J.M., McCutchen B.F., and Septiningsih E.M. 2022. Optimization of Protoplast Isolation and Transformation for a Pilot Study of Genome Editing in Peanut by Targeting the Allergen Gene Ara h 2. Int. J. Mol. Sci.

Bortesi, L., and R. Fischer. 2015. The CRISPR/Cas9 system for plant genome editing and beyond. Biotechnol. Adv. 33:41–52. doi:10.1016/j.biotechadv.2014.12.006

Brandt, K.M., H. Gunn, N. Moretti, and R.S. Zemetra. 2020. A Streamlined Protocol for Wheat (Triticum aestivum) Protoplast Isolation and Transformation With CRISPR-Cas Ribonucleoprotein Complexes. Front. Plant Sci. 11. doi:10.3389/fpls.2020.00769

Burow, M.D., M.R. Baring, N. Puppala, C.E. Simpson, J.L. Ayers, J. Cason, A.M. Schubert, A. Muitia, and Y. López. 2014. Registration of ‘Schubert’ Peanut. J. Plant Regist. 8. doi:10.3198/jpr2013.07.0042crc

Butardo, V.M., M.A. Fitzgerald, A.R. Bird, M.J. Gidley, B.M. Flanagan, O. Larroque, A.P.

Resurreccion, H.K.C. Laidlaw, S.A. Jobling, M.K. Morell, and S. Rahman. 2011. Impact of down-regulation of starch branching enzyme IIb in rice by artificial microRNA-and hairpin RNA-mediated RNA silencing. J. Exp. Bot. 62. doi:10.1093/jxb/err188

Carciofi, M., A. Blennow, S.L. Jensen, S.S. Shaik, A. Henriksen, A. Buléon, P.B. Holm, and K.H. Hebelstrup. 2012. Concerted suppression of all starch branching enzyme genes in barley produces amylose-only starch granules. BMC Plant Biol. 12. doi:10.1186/1471-2229-12-223

Čermák, T., S.J. Curtin, J. Gil-Humanes, R. Čegan, T.J.Y. Kono, E. Konečná, J.J. Belanto, C.G. Starker, J.W. Mathre, R.L. Greenstein, and D.F. Voytas. 2017. A multipurpose toolkit to enable advanced genome engineering in plants. Plant Cell 29. doi:10.1105/tpc.16.00922

Chen, K., Y. Wang, R. Zhang, H. Zhang, and C. Gao. 2019. CRISPR/Cas Genome Editing and Precision Plant Breeding in Agriculture. Annu. Rev. Plant Biol. 70. doi:10.1146/annurev-arplant-050718-100049

Chen, L., W. Li, L. Katin-Grazzini, J. Ding, X. Gu, Y. Li, T. Gu, R. Wang, X. Lin, Z. Deng, R.J. McAvoy, F.G. Gmitter, Z. Deng, Y. Zhao, and Y. Li. 2018. A method for the production and expedient screening of CRISPR/Cas9-mediated non-transgenic mutant plants. Hortic. Res. 5. doi:10.1038/s41438-018-0023-4

Chen, L., D.J. Magliano, and P.Z. Zimmet. 2012. The worldwide epidemiology of type 2 diabetes mellitus - Present and future perspectives. Nat. Rev. Endocrinol. 8:228–236. doi:10.1038/nrendo.2011.183

Chen, M.H., L.F. Huang, H.M. Li, Y.R. Chen, and S.M. Yu. 2004. Signal peptide-dependent targeting of a rice α-amylase and cargo proteins to plastids and extracellular compartments of plant cells. Plant Physiol. 135. doi:10.1104/pp.104.042184

Cheng, N., and P.A. Nakata. 2020. Development of a rapid and efficient protoplast isolation

and transfection method for chickpea (Cicer arietinum). MethodsX 7. doi:10.1016/j.mex.2020.101025

Chow, R.D., J.S. Chen, J. Shen, and S. Chen. 2021. A web tool for the design of prime-editing guide RNAs. Nat. Biomed. Eng. 5. doi:10.1038/s41551-020-00622-8

Collier, R., K. Dasgupta, Y.P. Xing, B.T. Hernandez, M. Shao, D. Rohozinski, E. Kovak, J. Lin, M.L.P. de Oliveira, E. Stover, K.F. McCue, F.G. Harmon, A. Blechl, J.G. Thomson, and R. Thilmony. 2017. Accurate measurement of transgene copy number in crop plants using droplet digital PCR. Plant J. 90. doi:10.1111/tpj.13517

Conlon, M.A., C.A. Kerr, C.S. Mcsweeney, R.A. Dunne, J.M. Shaw, S. Kang, A.R. Bird, M.K. Morell, T.J. Lockett, P.L. Molloy, A. Regina, S. Toden, J.M. Clarke, and D.L. Topping. 2012. Resistant starches protect against colonic DNA damage and alter microbiota and gene expression in rats fed a western diet. J. Nutr. 142. doi:10.3945/jn.111.147660

Connelly, J.P., and S.M. Pruett-Miller. 2019. CRIS.py: A Versatile and High-throughput Analysis Program for CRISPR-based Genome Editing. Sci. Rep. 9. doi:10.1038/s41598-019-40896-w

Dash, S., E.K.S. Cannon, S.R. Kalberer, A.D. Farmer, and S.B. Cannon. 2016. PeanutBase and Other Bioinformatic Resources for Peanut. Elsevier Inc.

Dodo, H.W., K.N. Konan, F.C. Chen, M. Egnin, and O.M. Viquez. 2008. Alleviating peanut allergy using genetic engineering: The silencing of the immunodominant allergen Ara h 2 leads to its significant reduction and a decrease in peanut allergenicity. Plant Biotechnol. J. 6:135–145. doi:10.1111/j.1467-7652.2007.00292.x

Doyle, J.., and J.. Doyle. 1987. A rapid isolation procedure for small amounts of leaf tissue. Phytochem. Bull. 19

Fang, L., S.S.C. Hung, J. Yek, L. El Wazan, T. Nguyen, S. Khan, S.Y. Lim, A.W. Hewitt, and

R.C.B. Wong. 2019. A Simple Cloning-free Method to Efficiently Induce Gene Expression Using CRISPR/Cas9. Mol. Ther. - Nucleic Acids 14:184–191. doi:10.1016/j.omtn.2018.11.008

Gao, W., L. Long, X. Tian, F. Xu, J. Liu, P.K. Singh, J.R. Botella, and C. Song. 2017. Genome editing in cotton with the CRISPR/Cas9 system. Front. Plant Sci. 8:1–12. doi:10.3389/fpls.2017.01364

Gelvin, S.B. 2003. Agrobacterium -Mediated Plant Transformation: the Biology behind the "Gene-Jockeying" Tool . Microbiol. Mol. Biol. Rev. 67. doi:10.1128/mmbr.67.1.16-37.2003

Hassan, M.M., G. Yuan, J.-G. Chen, G.A. Tuskan, and X. Yang. 2020. Prime Editing Technology and Its Prospects for Future Applications in Plant Biology Research. BioDesign Res. 2020. doi:10.34133/2020/9350905

Hazard, B., X. Zhang, P. Colasuonno, C. Uauy, D.M. Beckles, and J. Dubcovsky. 2012. Induced mutations in the Starch Branching Enzyme II (SBEII) genes increase amylose and resistant starch content in durum wheat. Crop Sci. 52. doi:10.2135/cropsci2012.02.0126

Hedgecock, D., and J.P. Davis. 2007. Heterosis for yield and crossbreeding of the Pacific oyster Crassostrea gigas. Aquaculture 272. doi:10.1016/j.aquaculture.2007.07.226

Hiei, Y., and T. Komari. 2008. Agrobacterium-mediated transformation of rice using immature embryos or calli induced from mature seed. Nat. Protoc. 3. doi:10.1038/nprot.2008.46

Hudzieczek, V., R. Cegan, T. Cermak, N. Bacovska, Z. Machalkova, K. Dolezal, L. Plihalova, D. Voytas, R. Hobza, and B. Vyskot. 2019. Agrobacterium rhizogenes-mediated transformation of a dioecious plant model Silene latifolia. N. Biotechnol. 48:20–28. doi:10.1016/j.nbt.2018.04.001

Jacobs, T.B., P.R. LaFayette, R.J. Schmitz, and W.A. Parrott. 2015. Targeted genome modifications in soybean with CRISPR/Cas9. BMC Biotechnol. 15. doi:10.1186/s12896-015-0131-2

Janila, P., M.T. Variath, M.K. Pandey, H. Desmae, B.N. Motagi, P. Okori, S.S. Manohar, A.L. Rathnakumar, T. Radhakrishnan, B. Liao, and R.K. Varshney. 2016. Genomic tools in groundnut breeding program: Status and perspectives. Front. Plant Sci. 7:2004–2013. doi:10.3389/fpls.2016.00289

Jiang, Y.Y., Y.P. Chai, M.H. Lu, X.L. Han, Q. Lin, Y. Zhang, Q. Zhang, Y. Zhou, X.C. Wang, C. Gao, and Q.J. Chen. 2020. Prime editing efficiently generates W542L and S621I double mutations in two ALS genes in maize. Genome Biol. 21. doi:10.1186/s13059-020-02170-5

Johansen, I.E., Y. Liu, B. Jørgensen, E.P. Bennett, E. Andreasson, K.L. Nielsen, A. Blennow, and B.L. Petersen. 2019. High efficacy full allelic CRISPR/Cas9 gene editing in tetraploid potato. Sci. Rep. 9. doi:10.1038/s41598-019-54126-w

Jouanin, A., L.J.W.J. Gilissen, J.G. Schaart, F.J. Leigh, J. Cockram, E.J. Wallington, L.A. Boyd, H.C. van den Broeck, I.M. van der Meer, A.H.P. America, R.G.F. Visser, and M.J.M. Smulders. 2020. CRISPR/Cas9 Gene Editing of Gluten in Wheat to Reduce Gluten Content and Exposure—Reviewing Methods to Screen for Coeliac Safety. Front. Nutr. 7. doi:10.3389/fnut.2020.00051

Kang, B.C., J.Y. Yun, S.T. Kim, Y.J. Shin, J. Ryu, M. Choi, J.W. Woo, and J.S. Kim. 2018. Precision genome engineering through adenine base editing in plants. Nat. Plants 4. doi:10.1038/s41477-018-0178-x

Keshavareddy, G., S. Rohini, S. V. Ramu, S. Sundaresha, A.R.V. Kumar, P.A. Kumar, and M. Udayakumar. 2013. Transgenics in groundnut (Arachis hypogaea L.) expressing cry1AcF gene for resistance to Spodoptera litura (F.). Physiol. Mol. Biol. Plants 19:343–

352. doi:10.1007/s12298-013-0182-6

Komor, A.C., Y.B. Kim, M.S. Packer, J.A. Zuris, and D.R. Liu. 2016. Programmable editing of a target base in genomic DNA without double-stranded DNA cleavage. Nature 533. doi:10.1038/nature17946

Li, C., Y. Zong, Y. Wang, S. Jin, D. Zhang, Q. Song, R. Zhang, and C. Gao. 2018a. Expanded base editing in rice and wheat using a Cas9-adenosine deaminase fusion. Genome Biol. 19. doi:10.1186/s13059-018-1443-z

Li, J., Y. Sun, J. Du, Y. Zhao, and L. Xia. 2017. Generation of Targeted Point Mutations in Rice by a Modified CRISPR/Cas9 System. Mol. Plant 10. doi:10.1016/j.molp.2016.12.001

Li, J.F., J.E. Norville, J. Aach, M. McCormack, D. Zhang, J. Bush, G.M. Church, and J. Sheen. 2013. Multiplex and homologous recombination-mediated genome editing in Arabidopsis and Nicotiana benthamiana using guide RNA and Cas9. Nat. Biotechnol. 31. doi:10.1038/nbt.2654

Li, M., X. Li, Z. Zhou, P. Wu, M. Fang, X. Pan, Q. Lin, W. Luo, G. Wu, and H. Li. 2016a. Reassessment of the four yield-related genes Gn1a, DEP1, GS3, and IPA1 in rice using a CRISPR/Cas9 system. Front. Plant Sci. 7. doi:10.3389/fpls.2016.00377

Li, S., F. Gao, K. Xie, X. Zeng, Y. Cao, J. Zeng, Z. He, Y. Ren, W. Li, Q. Deng, S. Wang, A. Zheng, J. Zhu, H. Liu, L. Wang, and P. Li. 2016b. The OsmiR396c-OsGRF4-OsGIF1 regulatory module determines grain size and yield in rice. Plant Biotechnol. J. 14. doi:10.1111/pbi.12569

Li, X. 2011. A Transient Expression Assay Using Arabidopsis Mesophyll Protoplasts. BIO-PROTOCOL 1. doi:10.21769/bioprotoc.70

Li, X., Y. Wang, S. Chen, H. Tian, D. Fu, B. Zhu, Y. Luo, and H. Zhu. 2018b. Lycopene is enriched in tomato fruit by CRISPR/Cas9-mediated multiplex genome editing. Front.

Plant Sci. 9. doi:10.3389/fpls.2018.00559

Li, Z., R.L. Jarret, and J.W. Demski. 1995. Regeneration of Plants From Protoplasts of Arachis Species (Peanut)

Liang, Y., M. Baring, S. Wang, and E.M. Septiningsih. 2017. Mapping QTLs for Leafspot Resistance in Peanut Using SNP-Based Next-Generation Sequencing Markers. Plant Breed. Biotechnol. 5. doi:10.9787/pbb.2017.5.2.115

Liang, Y., M.R. Baring, and E.M. Septiningsih. 2018. Mapping of quantitative trait loci for yield and grade related traits in peanut (Arachis hypogaea L.) using high-resolution SNP markers. Plant Breed. Biotechnol. 6. doi:10.9787/PBB.2018.6.4.454

Liang, Y., S. Biswas, B. Kim, J. Bailey-Serres, and E.M. Septiningsih. 2021. Improved transformation and regeneration of Indica rice: disruption of sub1a as a test case via CRISPR-Cas9. Int. J. Mol. Sci. 22. doi:10.3390/ijms22136989

Liang, Y., J.M. Cason, M.R. Baring, and E.M. Septiningsih. 2020. Identification of QTLs associated with Sclerotinia blight resistance in peanut (Arachis hypogaea L.). Genet. Resour. Crop Evol.. doi:10.1007/s10722-020-01012-4

Lin, C.S., C.T. Hsu, L.H. Yang, L.Y. Lee, J.Y. Fu, Q.W. Cheng, F.H. Wu, H.C.W. Hsiao, Y. Zhang, R. Zhang, W.J. Chang, C.T. Yu, W. Wang, L.J. Liao, S.B. Gelvin, and M.C. Shih. 2018. Application of protoplast technology to CRISPR/Cas9 mutagenesis: from single-cell mutation detection to mutant plant regeneration. Plant Biotechnol. J. 16. doi:10.1111/pbi.12870

Lin, Q., S. Jin, Y. Zong, H. Yu, Z. Zhu, G. Liu, L. Kou, Y. Wang, J.L. Qiu, J. Li, and C. Gao. 2021. High-efficiency prime editing with optimized, paired pegRNAs in plants. Nat. Biotechnol. 39. doi:10.1038/s41587-021-00868-w

Lin, Q., Y. Zong, C. Xue, S. Wang, S. Jin, Z. Zhu, Y. Wang, A. V. Anzalone, A. Raguram, J.L. Doman, D.R. Liu, and C. Gao. 2020. Prime genome editing in rice and wheat. Nat.

Biotechnol. 38. doi:10.1038/s41587-020-0455-x

Liu, G., J. Li, and I.D. Godwin. 2019. Genome editing by CRISPR/Cas9 in sorghum through biolistic bombardment

Liu, H., Y. Ding, Y. Zhou, W. Jin, K. Xie, and L.L. Chen. 2017a. CRISPR-P 2.0: An Improved CRISPR-Cas9 Tool for Genome Editing in Plants. Mol. Plant 10:530–532. doi:10.1016/j.molp.2017.01.003

Liu, J., J. Chen, X. Zheng, F. Wu, Q. Lin, Y. Heng, P. Tian, Z.J. Cheng, X. Yu, K. Zhou, X. Zhang, X. Guo, J. Wang, H. Wang, and J. Wan. 2017b. GW5 acts in the brassinosteroid signalling pathway to regulate grain width and weight in rice. Nat. Plants 3. doi:10.1038/nplants.2017.43

Liu, S., L. Su, S. Liu, X. Zeng, D. Zheng, L. Hong, and L. Li. 2016. Agrobacterium rhizogenes-mediated transformation of Arachis hypogaea: an efficient tool for functional study of genes. Biotechnol. Biotechnol. Equip. 30. doi:10.1080/13102818.2016.1191972

Lu, K., B. Wu, J. Wang, W. Zhu, H. Nie, J. Qian, W. Huang, and Z. Fang. 2018. Blocking amino acid transporter OsAAP3 improves grain yield by promoting outgrowth buds and increasing tiller number in rice. Plant Biotechnol. J. 16. doi:10.1111/pbi.12907

Lu, Y., Y. Tian, R. Shen, Q. Yao, M. Wang, M. Chen, J. Dong, T. Zhang, F. Li, M. Lei, and J.K. Zhu. 2020. Targeted, efficient sequence insertion and replacement in rice. Nat. Biotechnol. 38. doi:10.1038/s41587-020-0581-5

Lu, Y., Y. Tian, R. Shen, Q. Yao, D. Zhong, X. Zhang, and J.K. Zhu. 2021. Precise genome modification in tomato using an improved prime editing system. Plant Biotechnol. J. 19. doi:10.1111/pbi.13497

Lu, Y., and J.K. Zhu. 2017. Precise Editing of a Target Base in the Rice Genome Using a Modified CRISPR/Cas9 System. Mol. Plant 10. doi:10.1016/j.molp.2016.11.013

Masani, M.Y.A., G.A. Noll, G.K.A. Parveez, R. Sambanthamurthi, and D. Prüfer. 2014.

Efficient transformation of oil palm protoplasts by PEG-mediated transfection and DNA microinjection. PLoS One 9. doi:10.1371/journal.pone.0096831

Mazzara, M.G.E.S.C. 2007. Event-specific method for the quantitation of rice line LLRICE62 using real-time PCR : validation report

McClung, A.. 2005. Presidio rice: A new long grain rice with improved ratoon crop potential and milling yield.. Texas Rice, Highlighting Res.

Mehta, R., T. Radhakrishnan, A. Kumar, R. Yadav, J.R. Dobaria, P.P. Thirumalaisamy, R.K. Jain, and P. Chigurupati. 2013. Coat protein-mediated transgenic resistance of peanut (Arachis hypogaea L.) to peanut stem necrosis disease through Agrobacterium-mediated genetic transformation. Indian J. Virol. 24:205–213. doi:10.1007/s13337-013-0157-9

Mishra, R., R.K. Joshi, and K. Zhao. 2018. Genome editing in rice: recent advances, challenges, and future implications. Front. Plant Sci. 9. doi:10.3389/fpls.2018.01361

Mishra, R., R.K. Joshi, and K. Zhao. 2020. Base editing in crops: current advances, limitations and future implications. Plant Biotechnol. J. 18. doi:10.1111/pbi.13225

Molina-Risco, M., O. Ibarra, M. Faion-Molina, B. Kim, E.M. Septiningsih, and M.J. Thomson. 2021. Optimizing agrobacterium-mediated transformation and crispr-cas9 gene editing in the tropical japonica rice variety presidio. Int. J. Mol. Sci. 22. doi:10.3390/ijms222010909

Molla, K.A., and Y. Yang. 2019. CRISPR/Cas-Mediated Base Editing: Technical Considerations and Practical Applications. Trends Biotechnol. 37. doi:10.1016/j.tibtech.2019.03.008

Molla, K.A., and Y. Yang. 2020. Predicting CRISPR/Cas9-Induced Mutations for Precise Genome Editing. Trends Biotechnol. 38. doi:10.1016/j.tibtech.2019.08.002

Morrison, W.R., and J. Karkalas. 1990. Methods in Plant Biochemistry. Elsevier.

Mueller, G.A., S.J. Maleki, and L.C. Pedersen. 2014. The Molecular Basis of Peanut Allergy.

Curr. Allergy Asthma Rep. 14. doi:10.1007/s11882-014-0429-5

Naito, Y., K. Hino, H. Bono, and K. Ui-Tei. 2015. CRISPRdirect: Software for designing CRISPR/Cas guide RNA with reduced off-target sites. Bioinformatics 31. doi:10.1093/bioinformatics/btu743

Nakamura, Y., Y. Utsumi, T. Sawada, S. Aihara, C. Utsumi, M. Yoshida, and S. Kitamura. 2010. Characterization of the reactions of starch branching enzymes from rice endosperm. Plant Cell Physiol. 51:776–794. doi:10.1093/pcp/pcq035

Nishida, K., T. Arazoe, N. Yachie, S. Banno, M. Kakimoto, M. Tabata, M. Mochizuki, A. Miyabe, M. Araki, K.Y. Hara, Z. Shimatani, and A. Kondo. 2016. Targeted nucleotide editing using hybrid prokaryotic and vertebrate adaptive immune systems. Science (80-.). 353. doi:10.1126/science.aaf8729

Oelck, M.M., V.A. Bapat, and O. Schieder. 1982. Protoplast Culture of Three Legumes: Arachis hypogaea, Melilotus officinalis, Trifolium resupinatum. Zeitschrift für Pflanzenphysiologie 106. doi:10.1016/s0044-328x(82)80080-9

Ozias-Akins, P., E.K.S. Cannon, and S.B. Cannon. 2017. Genomics Resources for Peanut Improvement

Pacher, M., and H. Puchta. 2017. From classical mutagenesis to nuclease-based breeding – directing natural DNA repair for a natural end-product. Plant J. 90. doi:10.1111/tpj.13469

Pandey, M.K., E. Monyo, P. Ozias-Akins, X. Liang, P. Guimarães, S.N. Nigam, H.D. Upadhyaya, P. Janila, X. Zhang, B. Guo, D.R. Cook, D.J. Bertioli, R. Michelmore, and R.K. Varshney. 2012a. Advances in Arachis genomics for peanut improvement. Biotechnol. Adv. 30. doi:10.1016/j.biotechadv.2011.11.001

Pandey, M.K., A.K. Pandey, R. Kumar, C.V. Nwosu, B. Guo, G.C. Wright, R.S. Bhat, X. Chen, S.K. Bera, M. Yuan, H. Jiang, I. Faye, T. Radhakrishnan, X. Wang, X. Liang, B.

Liao, X. Zhang, R.K. Varshney, and W. Zhuang. 2020. Translational genomics for achieving higher genetic gains in groundnut. Theor. Appl. Genet. 133. doi:10.1007/s00122-020-03592-2

Pandey, M.K., N.S. Rani, M.S. Madhav, R.M. Sundaram, G.S. Varaprasad, A.K.P. Sivaranjani, A. Bohra, G.R. Kumar, and A. Kumar. 2012b. Different isoforms of starch-synthesizing enzymes controlling amylose and amylopectin content in rice (Oryza sativa L.). Biotechnol. Adv. 30:1697–1706. doi:10.1016/j.biotechadv.2012.08.011

Prado, J.R., G. Segers, T. Voelker, D. Carson, R. Dobert, J. Phillips, K. Cook, C. Cornejo, J. Monken, L. Grapes, T. Reynolds, and S. Martino-Catt. 2014. Genetically engineered crops: From idea to product. Annu. Rev. Plant Biol. 65. doi:10.1146/annurev-arplant-050213-040039

Prasad, K., P. Bhatnagar-Mathur, F. Waliyar, and K.K. Sharma. 2013. Overexpression of a chitinase gene in transgenic peanut confers enhanced resistance to major soil borne and foliar fungal pathogens. J. Plant Biochem. Biotechnol. 22:222–233. doi:10.1007/s13562-012-0155-9

Prosekov, A.Y., and S.A. Ivanova. 2018. Food security: The challenge of the present. Geoforum 91:73–77. doi:10.1016/j.geoforum.2018.02.030

Qin, L., J. Li, Q. Wang, Z. Xu, L. Sun, M. Alariqi, H. Manghwar, G. Wang, B. Li, X. Ding, H. Rui, H. Huang, T. Lu, K. Lindsey, H. Daniell, X. Zhang, and S. Jin. 2020. High-efficient and precise base editing of C•G to T•A in the allotetraploid cotton (Gossypium hirsutum) genome using a modified CRISPR/Cas9 system. Plant Biotechnol. J. 18. doi:10.1111/pbi.13168

Razzaq, A., F. Saleem, M. Kanwal, G. Mustafa, S. Yousaf, H.M.I. Arshad, M.K. Hameed, M.S. Khan, and F.A. KhanJoyia. 2019. Modern trends in plant genome editing: An inclusive review of the CRISPR/Cas9 Toolbox. Int. J. Mol. Sci. 20.

doi:10.3390/ijms20164045

Reed, K.M., and B.O.R. Bargmann. 2021. Protoplast Regeneration and Its Use in New Plant Breeding Technologies. Front. Genome Ed. 3. doi:10.3389/fgeed.2021.734951

Rees, H.A., and D.R. Liu. 2018. Base editing: precision chemistry on the genome and transcriptome of living cells. Nat. Rev. Genet. 19. doi:10.1038/s41576-018-0059-1

Regina, A., P. Berbezy, B. Kosar-Hashemi, S. Li, M. Cmiel, O. Larroque, A.R. Bird, S.M. Swain, C. Cavanagh, S.A. Jobling, Z. Li, and M. Morell. 2015. A genetic strategy generating wheat with very high amylose content. Plant Biotechnol. J. 13. doi:10.1111/pbi.12345

Schönhofen, A., X. Zhang, and J. Dubcovsky. 2017. Combined mutations in five wheat STARCH BRANCHING ENZYME II genes improve resistant starch but affect grain yield and bread-making quality. J. Cereal Sci. 75. doi:10.1016/j.jcs.2017.03.028

Schwall, G.P., R. Safford, R.J. Westcott, R. Jeffcoat, A. Tayal, Y.C. Shi, M.J. Gidley, and S.A. Jobling. 2000. Production of very-high-amylose potato starch by inhibition of SBE A and B. Nat. Biotechnol. 18. doi:10.1038/75427

Shan, Q., Y. Wang, J. Li, and C. Gao. 2014. Genome editing in rice and wheat using the CRISPR/Cas system. Nat. Protoc. 9. doi:10.1038/nprot.2014.157

Shan, Q., Y. Zhang, K. Chen, K. Zhang, and C. Gao. 2015. Creation of fragrant rice by targeted knockout of the OsBADH2 gene using TALEN technology. Plant Biotechnol. J. 13. doi:10.1111/pbi.12312

Shimatani, Z., S. Kashojiya, M. Takayama, R. Terada, T. Arazoe, H. Ishii, H. Teramura, T. Yamamoto, H. Komatsu, K. Miura, H. Ezura, K. Nishida, T. Ariizumi, and A. Kondo. 2017. Targeted base editing in rice and tomato using a CRISPR-Cas9 cytidine deaminase fusion. Nat. Biotechnol. 35. doi:10.1038/nbt.3833

Stalker, H.T., S.P. Tallury, P. Ozias-Akins, D. Bertioli, and S.C.L. Bertioli. 2013. The Value

of Diploid Peanut Relatives for Breeding and Genomics. Peanut Sci. 40. doi:10.3146/ps13-6.1

Sun, L., R. Hu, G. Shen, and H. Zhang. 2013. Genetic Engineering Peanut for Higher Drought- and Salt-Tolerance. Food Nutr. Sci. 04. doi:10.4236/fns.2013.46a001

Sun, Y., G. Jiao, Z. Liu, X. Zhang, J. Li, X. Guo, W. Du, J. Du, F. Francis, Y. Zhao, and L. Xia. 2017. Generation of high-amylose rice through CRISPR/Cas9-mediated targeted mutagenesis of starch branching enzymes. Front. Plant Sci. 8:1–15. doi:10.3389/fpls.2017.00298

Svitashev, S., C. Schwartz, B. Lenderts, J.K. Young, and A. Mark Cigan. 2016. Genome editing in maize directed by CRISPR-Cas9 ribonucleoprotein complexes. Nat. Commun. 7. doi:10.1038/ncomms13274

Taiz, L., and R.L. Jones. 1971. The isolation of barley-aleurone protoplasts. Planta 101. doi:10.1007/BF00387620

Tang, X., S. Sretenovic, Q. Ren, X. Jia, M. Li, T. Fan, D. Yin, S. Xiang, Y. Guo, L. Liu, X. Zheng, Y. Qi, and Y. Zhang. 2020. Plant Prime Editors Enable Precise Gene Editing in Rice Cells. Mol. Plant 13. doi:10.1016/j.molp.2020.03.010

Tilman, D., C. Balzer, J. Hill, and B.L. Befort. 2011. Global food demand and the sustainable intensification of agriculture. Proc. Natl. Acad. Sci. U. S. A. 108. doi:10.1073/pnas.1116437108

Tuncel, A., K.R. Corbin, J. Ahn-Jarvis, S. Harris, E. Hawkins, M.A. Smedley, W. Harwood, F.J. Warren, N.J. Patron, and A.M. Smith. 2019. Cas9-mediated mutagenesis of potato starch-branching enzymes generates a range of tuber starch phenotypes. Plant Biotechnol. J. 17. doi:10.1111/pbi.13137

Veillet, F., M.P. Kermarrec, L. Chauvin, A. Guyon-Debast, J.E. Chauvin, J.L. Gallois, and F. Nogué. 2020. Prime editing is achievable in the tetraploid potato, but needs

improvement. bioRxiv. doi:10.1101/2020.06.18.159111

Veillet, F., L. Perrot, L. Chauvin, M.P. Kermarrec, A. Guyon-Debast, J.E. Chauvin, F. Nogué, and M. Mazier. 2019. Transgene-free genome editing in tomato and potato plants using Agrobacterium-mediated delivery of a CRISPR/Cas9 cytidine base editor. Int. J. Mol. Sci. 20. doi:10.3390/ijms20020402

Wang, J., P. Hu, Z. Chen, Q. Liu, and C. Wei. 2017. Progress in high-amylose cereal crops through inactivation of starch branching enzymes. Front. Plant Sci. 8. doi:10.3389/fpls.2017.00469

Wang, Q., G. Yu, Z. Chen, J. Han, Y. Hu, and K. Wang. 2021. Optimization of protoplast isolation, transformation and its application in sugarcane (Saccharum spontaneum L). Crop J. 9. doi:10.1016/j.cj.2020.05.006

Wilson, F.M., K. Harrison, A.D. Armitage, A.J. Simkin, and R.J. Harrison. 2019. CRISPR/Cas9-mediated mutagenesis of phytoene desaturase in diploid and octoploid strawberry. Plant Methods 15:1–13. doi:10.1186/s13007-019-0428-6

Wu, F., and Y. Hanzawa. 2018. A simple method for isolation of soybean protoplasts and application to transient gene expression analyses. J. Vis. Exp. 2018. doi:10.3791/57258

Xia, H., M. Yandeau-Nelson, D.B. Thompson, and M.J. Guiltinan. 2011. Deficiency of maize starch-branching enzyme i results in altered starch fine structure, decreased digestibility and reduced coleoptile growth during germination. BMC Plant Biol. 11. doi:10.1186/1471-2229-11-95

Xie, K., B. Minkenberg, and Y. Yang. 2015. Boosting CRISPR/Cas9 multiplex editing capability with the endogenous tRNA-processing system. Proc. Natl. Acad. Sci. U. S. A. 112:3570–3575. doi:10.1073/pnas.1420294112

Xu, R., J. Li, X. Liu, T. Shan, R. Qin, and P. Wei. 2020a. Development of Plant Prime-Editing Systems for Precise Genome Editing. Plant Commun. 1. doi:10.1016/j.xplc.2020.100043

Xu, R., Y. Yang, R. Qin, H. Li, C. Qiu, L. Li, P. Wei, and J. Yang. 2016. Rapid improvement of grain weight via highly efficient CRISPR/Cas9-mediated multiplex genome editing in rice. J. Genet. Genomics 43. doi:10.1016/j.jgg.2016.07.003

Xu, R.F., H. Li, R.Y. Qin, J. Li, C.H. Qiu, Y.C. Yang, H. Ma, L. Li, P.C. Wei, and J.B. Yang. 2015. Generation of inheritable and "transgene clean" targeted genome-modified rice in later generations using the CRISPR/Cas9 system. Sci. Rep. 5. doi:10.1038/srep11491

Xu, W., C. Zhang, Y. Yang, S. Zhao, G. Kang, X. He, J. Song, and J. Yang. 2020b. Versatile Nucleotides Substitution in Plant Using an Improved Prime Editing System. Mol. Plant 13. doi:10.1016/j.molp.2020.03.012

Yuan, M., J. Zhu, L. Gong, L. He, C. Lee, S. Han, C. Chen, and G. He. 2019. Mutagenesis of FAD2 genes in peanut with CRISPR/Cas9 based gene editing. BMC Biotechnol. 19:1–7. doi:10.1186/s12896-019-0516-8

Yue, J.-J., J.-L. Yuan, F.-H. Wu, Y.-H. Yuan, Q.-W. Cheng, C.-T. Hsu, and C.-S. Lin. 2021. Protoplasts: From Isolation to CRISPR/Cas Genome Editing Application. Front. Genome Ed. 3. doi:10.3389/fgeed.2021.717017

Zhang, H., J. Zhang, P. Wei, B. Zhang, F. Gou, Z. Feng, Y. Mao, L. Yang, H. Zhang, N. Xu, and J.K. Zhu. 2014. The CRISPR/Cas9 system produces specific and homozygous targeted gene editing in rice in one generation. Plant Biotechnol. J. 12. doi:10.1111/pbi.12200

Zhang, N., H.M. Roberts, J. Van Eck, and G.B. Martin. 2020. Generation and Molecular Characterization of CRISPR/Cas9-Induced Mutations in 63 Immunity-Associated Genes in Tomato Reveals Specificity and a Range of Gene Modifications. Front. Plant Sci. 11. doi:10.3389/fpls.2020.00010

Zhang, Y., D. Li, D. Zhang, X. Zhao, X. Cao, L. Dong, J. Liu, K. Chen, H. Zhang, C. Gao, and D. Wang. 2018. Analysis of the functions of TaGW2 homoeologs in wheat grain

weight and protein content traits. Plant J. 94. doi:10.1111/tpj.13903

Zhang, Y., Z. Liang, Y. Zong, Y. Wang, J. Liu, K. Chen, J.L. Qiu, and C. Gao. 2016. Efficient and transgene-free genome editing in wheat through transient expression of CRISPR/Cas9 DNA or RNA. Nat. Commun. 7. doi:10.1038/ncomms12617

Zhou, H., B. Liu, D.P. Weeks, M.H. Spalding, and B. Yang. 2014. Large chromosomal deletions and heritable small genetic changes induced by CRISPR/Cas9 in rice. Nucleic Acids Res. 42:10903–10914. doi:10.1093/nar/gku806

Zhu, L., M. Gu, X. Meng, S.C.K. Cheung, H. Yu, J. Huang, Y. Sun, Y. Shi, and Q. Liu. 2012. High-amylose rice improves indices of animal health in normal and diabetic rats. Plant Biotechnol. J. 10. doi:10.1111/j.1467-7652.2011.00667.x

Zhuang, W., H. Chen, M. Yang, J. Wang, M.K. Pandey, C. Zhang, W.C. Chang, L. Zhang, X. Zhang, R. Tang, V. Garg, X. Wang, H. Tang, C.N. Chow, J. Wang, Y. Deng, D. Wang, A.W. Khan, Q. Yang, T. Cai, P. Bajaj, K. Wu, B. Guo, X. Zhang, J. Li, F. Liang, J. Hu, B. Liao, S. Liu, A. Chitikineni, H. Yan, Y. Zheng, S. Shan, Q. Liu, D. Xie, Z. Wang, S.A. Khan, N. Ali, C. Zhao, X. Li, Z. Luo, S. Zhang, R. Zhuang, Z. Peng, S. Wang, G. Mamadou, Y. Zhuang, Z. Zhao, W. Yu, F. Xiong, W. Quan, M. Yuan, Y. Li, H. Zou, H. Xia, L. Zha, J. Fan, J. Yu, W. Xie, J. Yuan, K. Chen, S. Zhao, W. Chu, Y. Chen, P. Sun, F. Meng, T. Zhuo, Y. Zhao, C. Li, G. He, Y. Zhao, C. Wang, P.B. Kavikishor, R.L. Pan, A.H. Paterson, X. Wang, R. Ming, and R.K. Varshney. 2019. The genome of cultivated peanut provides insight into legume karyotypes, polyploid evolution and crop domestication. Nat. Genet. 51:865–876. doi:10.1038/s41588-019-0402-2

Zong, Y., Y. Wang, C. Li, R. Zhang, K. Chen, Y. Ran, J.L. Qiu, D. Wang, and C. Gao. 2017. Precise base editing in rice, wheat and maize with a Cas9-cytidine deaminase fusion. Nat. Biotechnol. 35. doi:10.1038/nbt.3811

APPENDIX

Appendix Table 1

Primer	**Sequence (5′-3′)**
CAS9_F	AGAAGATACACCAGACGGAAGAAC
CAS9_R	GGCTTGATGAACTTGTAGAACTCTT
tRNA_gRNA_F	AACTGTAGGAGAAAAGCATTTCGTAG
tRNA_gRNA_R	AGCTCTAAAACTCAGTCACATTTTCC
Ubiquitin_F	CCTTCGGAGACACCTTTTGA
Ubiquitin_R	TTGAAATGCACATTCGGGTG
SBE1_F	CAGCACTTTGGCTTTGTTTTC
SBE1_R	GATTCGGAACAAGAACATGGA
SBE2_F	ATAAAGCCGTAGGCCCACTAA
SBE2_R	CAGCCTGATTCTGGTGCTAAG
SBE3_F	AGGGTTTAGGTGGAAGCAGAG
SBE3_R	AATCCTACGCATATGGTGTGC
SBE4_F	CTGTTGGGCTACTGAAAACCA
SBE4_R	AATCACGTACCTGTGCTCCAG
SBE1_NGS_F	TCGTCGGCAGCGTCAGATGTGTATAAGAGACAGGACATCCGCCGCAATGCTGTGT
SBE1_NGS_R	GTCTCGTGGGCTCGGAGATGTGTATAAGAGACAGATCTTACCTTTCCAGGCCACGACC
SBE2_NGS_F	TCGTCGGCAGCGTCAGATGTGTATAAGAGACAGTCTCCAACAATGGATTCTTGCGCTC
SBE2_NGS_R	GTCTCGTGGGCTCGGAGATGTGTATAAGAGACAGAGATGCCGTGCTTGGCGAGGAA
SBE3_NGS_F	TCGTCGGCAGCGTCAGATGTGTATAAGAGACAGGTTTAGGTGGAAGCAGAGCGCG
SBE3_NGS_R	GTCTCGTGGGCTCGGAGATGTGTATAAGAGACAGCGGCGGACGAGAACAACAAGGT
SBE4_NGS_F	TCGTCGGCAGCGTCAGATGTGTATAAGAGACAGCCATCTATGTTCTGTGTAGATACCTGATGA
SBE4_NGS_R	GTCTCGTGGGCTCGGAGATGTGTATAAGAGACAGAATCCTTCCAGCATTGGGTCAATTT
HPT_F	CTATTTCTTTGCCCTCGGACGA
HPT_R	GGACCGATGGCTGTGTAGAAG
HPT_probe	CGCCGATAGTGGAAACCGACGCCC
OsPLD_F	TGGTGAGCGTTTTGCAGTCT
OsPLD_R	CTGATCCACTAGCAGGAGGTCC
OsPLD_probe	TGTTGTGCTGCCAATGTGGCCTG

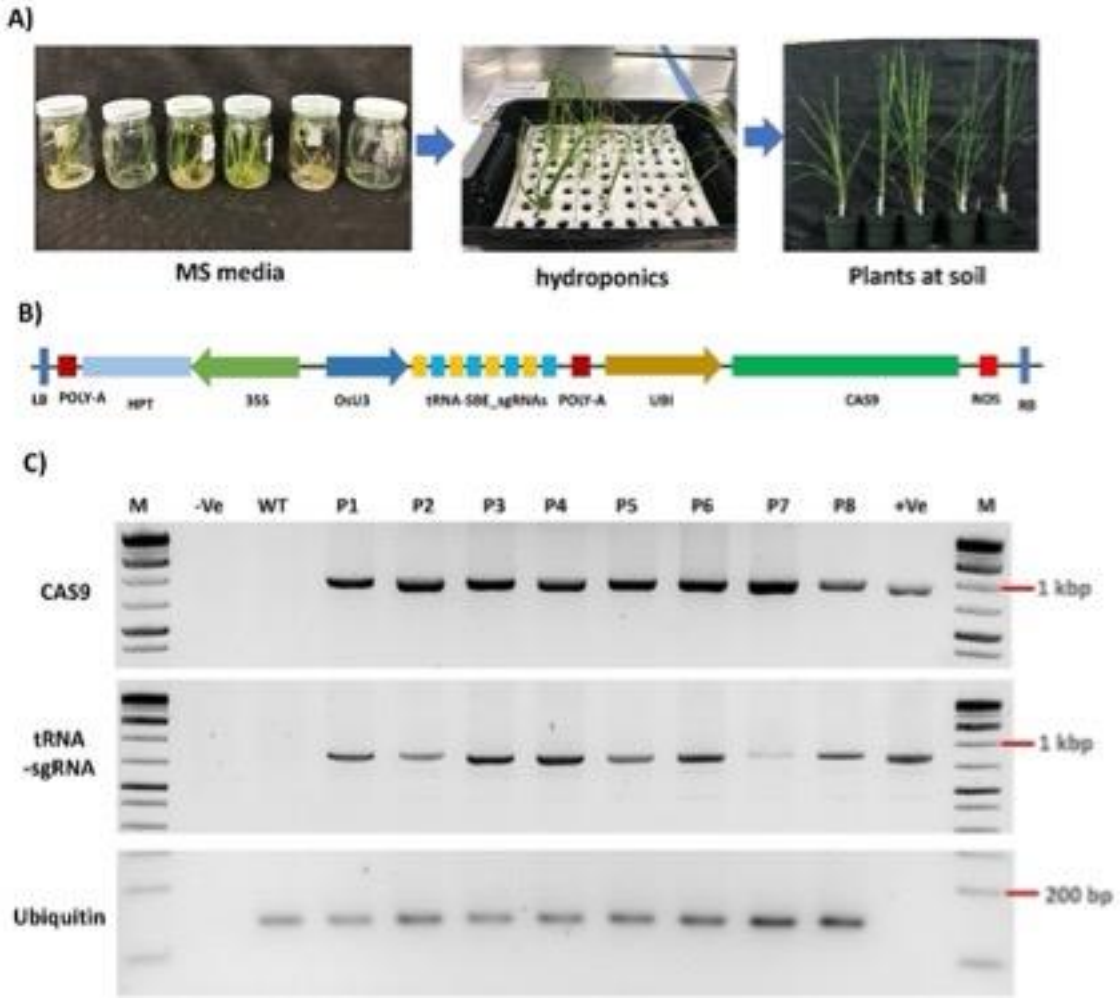

Appendix Figure 1. Transgenic plants maintenance and transgene detection in transformed plants. A) Cultivation of transformants in hydroponic and soil, B) Schematic diagram of T-DNA border of *pRGEB32_tRNA_SBE_gRNAs*, C) Confirmation of transgene presence in putative transformed rice plants with CAS9 and tRNA-gRNA overlapping primers. M = $1kb^{+}$ ladder, -Ve = H_2O control, WT= wild type control, P1-P8= transformed plants and +Ve = plasmid control.

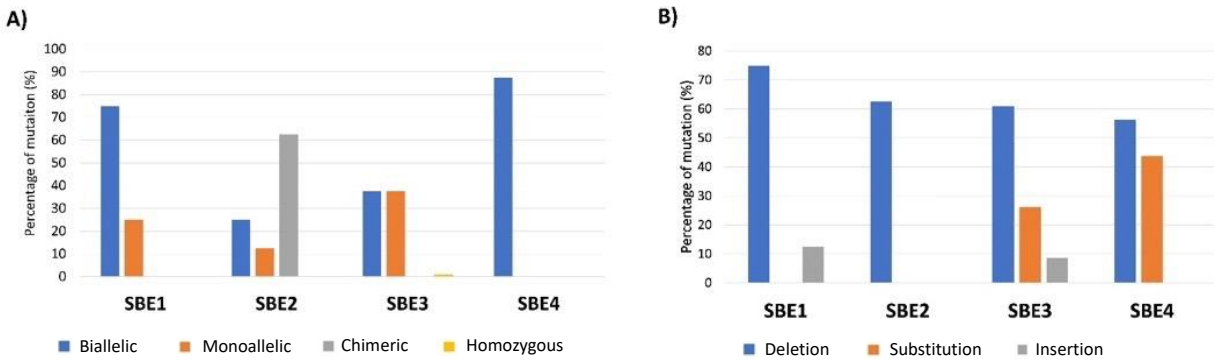

Appendix Figure 2. Edited mutation classes identified at the T_0 generation. (A) Percent mutation of edited SBE lines at each SBE gene by mutation zygosity. (B) Percent mutation of edited SBE lines by type of mutation.


A)
B)
C)
D)

Appendix Figure 3: Change in the coding sequence at A) *SBE1*, B) *SBE2*, C) *SBE3*, and D) *SBE4* due to deletions in the sgRNA regions (mutations identified in the P4-2 line at the T_1 generation; note: not all mutations are fixed homozygous yet). The red squares indicate the premature stop codon position in the coding region of four SBE genes.

Appendix Table 2A. CRISPR-Cas9 induced mutations in the transformed plants at T_0 generation for *SBE1*.

Plant no	Allele	Sequence	Percentage of mutation	Deletion/insertion/ Substitution	Mutant Zygosity
WT	Allele 1	CCGCTCCTTCCCTCTCTCGCTGATCGACCGAGCCCGGGAATCGCGGTCAG			
	Allele 2	CCGCTCCTTCCCTCTCTCGCTGATCGACCGAGCCCGGGAATCGCGGTCAG			
P1	Allele 1	CCGCTCCTT----------CCCGGGAATCGCGGTCAG	60%	23 bp deletion	Biallelic
	Allele 2	CCGCTCCTTCCCTCTCTCGCTGATCGACC-------CCCGGGAATCGCGGTCAG	39%	3 bp deletion	
P2	Allele 1	CCGCTCCTT----------CCCGGGAATCGCGGTCAG	45%	23 bp deletion	Biallelic
	Allele 2	CCGCTCCTTCCCTCTCTCGCTGATCGACC-------CCCGGGAATCGCGGTCAG	31%	3 bp deletion	
P3	Allele 1	CCGCTCCTT----------CCCGGGAATCGCGGTCAG	47%	23 bp deletion	Biallelic
	Allele 2	CCGCTCCTTCCCTCTCTCGCTGATCGACC-------CCCGGGAATCGCGGTCAG	31%	3 bp deletion	
P4	Allele 1	CCGCTCCTT----------CCCGGGAATCGCGGTCAG	42%	23 bp deletion	Biallelic
	Allele 2	CCGCTCCTTCCCTCTCTCGCTGATCGACC-------CCCGGGAATCGCGGTCAG	42%	3 bp deletion	
P5	Allele 1	CCGCTCCTTCCCTCTCTCGCTGATCGACCGAGCCCGGGAATCGCGGTCAG	55%	No edit	
	Allele 2	CCGCTCCTT----------CCCGGGAATCGCGGTCAG	8%	23 bp deletion	Monoallelic
P6	Allele 1	CCGCTCCTTCCCTCTCTCGCTGATCGACCGAGCCCGGGAATCGCGGTCAG	32%	No edit	
	Allele 2	CCGCTCCTTCCCTCTCTCGCT----------GTCAG	46%	24 bp deletion	Monoallelic
P7	Allele 1	CCGCTCCTTCCCTCTCTCGCTGATCGAC--------CCCGGGAATCGCGGTCAG	61%	4 bp deletion	Biallelic
	Allele 2	CCGCTCCTTCCCTCTCTCGCTGATCGACCGAGCTCCTCTTCCTCTTCCTCCTCCCCCGGGAATCGCGGTCAG	39%	22 bp insertion	
P8	Allele 1	CCGCTCCTTCCCTCTCTCGCTGATCGAC--------CCCGGGAATCGCGGTCAG	48%	4 bp deletion	Biallelic
	Allele 2	CCGCTCCTTCCCTCTCTCGCTGATCGACCGAGCTCCTCTTCCTCTTCCTCCTCCCCCGGGAATCGCGGTCAG	31%	22 bp insertion	

*Green fonts, dashes, and blue fonts represent gRNA region, deletion, and insertion, respectively

Appendix Table 2B. CRISPR-Cas9 induced mutations in the transformed plants at T_0 generation for *SBE2*.

Plant no	Allele	Sequence	Percentage of mutation	Deletion/insertion/ Substitution	Mutant Zygosity
WT	Allele 1	CTCAGGCCTCCGCCGCCGGGGAGGGTTGCCCCTGCAGCTGCGCCTCCTCCT			
	Allele 2	CTCAGGCCTCCGCCGCCGGGGAGGGTTGCCCCTGCAGCTGCGCCTCCTCCT			
P1	Allele 1	CTCAGGCCTCCGCCGCCGGGGAGGGTTGCCCCTGCAGCTGCGCCTCCTCCT	27%	No edit	Chimeric
	Allele 2	CTCAGGCCTCCGCCGCCGGGA...GGTTGCCCCTGCAGCTGCGCCTCCTCCT	41%	1 bp deletion	
	Allele 3	CTCAGGCCTCCGCCGCCGGGC...GGTTGCCCCTGCAGCTGCGCCTCCTCCT	4%	1 bp deletion and 1bp substitution	
	Allele 4	CTCAGGCCTCCGCCGCCGGGA.....GTTGCCCCTGCAGCTGCGCCTCCTCCT	4%	2 bp deletion	
P2	Allele 1	CTCAGGCCTCCGCCGCCGGGAAGGTTGCCCCTGCAGCTGCGCCTCCTCCT	57%	G to A substitution	Chimeric
	Allele 2	CTCAGGCCTCCGCCGCCGGGA—GGTTGCCCCTGCAGCTGCGCCTCCTCCT	25%	1 bp deletion	
	Allele 3	CTCAGGCCTCCGCCGCCGGGCAGGTTGCCCCTGCAGCTGCGCCTCCTCCT	8%	AG to CA substitution	
P3	Allele 1	CTCAGGCCTCCGCCGCCGGGA------TTGCCCCTGCAGCTGCGCCTCCTCCT	48%	3 bp deletion	Chimeric
	Allele 2	CTCAGGCCTCCGCCGCCGGGC------TTGCCCCTGCAGCTGCGCCTCCTCCT	4%	3 bp deletion and 1bp substitution	
	Allele 3	CTCAGGCCTCCGCCGCCGGGA-TCGCAGGTTGCCCCTGCAGCTGCGCCTCCTCCT	34%	1 bp deletion and 5 bp insertion	
	Allele 4	CTCAGGCCTCCGCCGCCGGGC-TCGCAGGTTGCCCCTGCAGCTGCGCCTCCTCCT	0.2%	1 bp deletion and substitution,	

				5 bp insertion	
P4	Allele 1	CTCAGGCCTCCGCCGCCGGGAGGGTTGCCCCTGCAGCTGCGCCTCCTCCT	45%	No edit	Monoallelic
	Allele 2	CTCAGGCCTCCGCCGCCGGG—GGGTTGCCCCTGCAGCTGCGCCTCCTCCT	25%	1 bp deletion	
P5	Allele 1	CTCAGGCCTCCGCCGCCGGGAGGGTTGCCCCTGCAGCTGCGCCTCCTCCT	22%	No edit	Chimeric
	Allele 2	CTCAG----------GCCTCCTCCT	57%	35 bp deletion	
	Allele 3	CTCAGGCCTCCGCCGCCGGGCGGGTTGCCCCTGCAGCTGCGCCTCCTCCT	2%	G to C substitution	
P6	Allele 1	CTCAGGCCTCCGCCGCCGGGAGGGTTGCCCCTGCAGCTGCGCCTCCTCCT	46%	No edit	Chimeric
	Allele 2	CTCAG----------GCCTCCTCCT	33%	35 bp deletion	
	Allele 3	CTCAGGCCTCCGCCGCCGGGCGGGTTGCCCCTGCAGCTGCGCCTCCTCCT	3%	G to C substitution	
P7	Allele 1	CTCAGGCCTCC----------GCCCCTGCAGCTGCGCCTCCTCCT	42%	15 bp deletion	Biallelic
	Allele 2	CTCAGGCCTCC----------GGTTGCCCCTGCAGCTGCGCCTCCTCCT	41%	11 bp deletion	
P8	Allele 1	CTCAGGCCTCC----------GCCCCTGCAGCTGCGCCTCCTCCT	43%	15 bp deletion	Biallelic
	Allele 2	CTCAGGCCTCC----------GGTTGCCCCTGCAGCTGCGCCTCCTCCT	42%	11 bp deletion	

*Green fonts, dashes, red fonts and blue fonts represent gRNA region, deletion, substitution and insertion, respectively

Appendix Table 2C. CRISPR-Cas9 induced mutations in the transformed plants at T_0 generation for *SBE3.*

Plant no	Allele	Sequence	Percentage of mutation	Deletion/insertion/ Substitution	Mutant Zygosity
WT	Allele 1	TACGGGCGGGGGCCGTGCGGTTCCCCGTGCCAGCCGGGGCCCGGAGCTGG			
	Allele 2	TACGGGCGGGGGCCGTGCGGTTCCCCGTGCCAGCCGGGGCCCGGAGCTGG			
P1	Allele 1	TACGGGCGGGGGCCGTGCGGTTCCCCGTGCCAGCCGGGGCCCGGAGCTGG	45%	No edited	Monoallelic
	Allele 2	TACGGGCGGGGGCCGTGC--GTTCCCCGTGCCAGCCGGGGCCCGGAGCTGG	41%	1 bp deletion	
P2	Allele 1	TACGGGCGGGGGCCGTGCGGTTCCCCGTGCCAGCCGGGGCCCGGAGCTGG	7%	No edited	Monoallelic
	Allele 2	TACGGGCGGGGGCCGTGC--GTTCCCCGTGCCAGCCGGGGCCCGGAGCTGG	31%	1 bp deletion	
P3	Allele 1	TACGGGCGGGGGCCGTGCGGTTCCCCGTGCCAGCCGGGGCCCGGAGCTGG	42%	No edited	Monoallelic
	Allele 2	TACGGGCGGGGGCCGTGC--GTTCCCCGTGCCAGCCGGGGCCCGGAGCTGG	38%	1 bp deletion	
P4	Allele 1	TACGGGCGGGGGCCGTGC--GTTCCCCGTGCCAGCCGGGGCCCGGAGCTGG	54%	1 bp deletion	Homozygous
	Allele 2	TACGGGCGGGGGCCGTGC--GTTCCCCGTGCCAGCCGGGGCCCGGAGCTGG			
P5	Allele 1	TACGGGCGGGGGCCGTGCG--TTCCCCGTGCCAGCCGGGGCCCGGAGCTGG	21%	1 bp deletion	Biallelic
	Allele 2	TACGGGCGGGGGCCGTGC--GTTCCCCGTGCCAGCCGGGGCCCGGAGCTGG	51%	1 bp deletion	
P6	Allele 1	TACGGGCGGGGGCCGTGCG--TTCCCCGTGCCAGCCGGGGCCCGGAGCTGG	39%	1 bp deletion	Biallelic
	Allele 2	TACGGGCGGGGGCCGTGC--GTTCCCCGTGCCAGCCGGGGCCCGGAGCTGG	17%	1 bp deletion	
P7	Allele 1	TACGGGCGGGGGCCGTGCG--TTCCCCGTGCCAGCCGGGGCCCGGAGCTGG	54%	1 bp deletion	Biallelic
	Allele 2	TACGGGCGGGGGCCGTGC--GTTCCCCGTGCCAGCCGGGGCCCGGAGCTGG	14%	1 bp deletion	
P8	Allele 1	TACGGGCGGGGGCCGTGCGGTTCCCCGTGCCAGCCGGGGCCCGGAGCTGG		No edit	
	Allele 2	TACGGGCGGGGGCCGTGCGGTTCCCCGTGCCAGCCGGGGCCCGGAGCTGG			

*Green fonts and dashes represent gRNA region and deletion, respectively

Appendix Table 2D. CRISPR-Cas9 induced mutations in the transformed plants at T_0 generation for *SBE4.*

Plant no	Allele	Sequence	Percentage of mutation	Deletion/insertion/ Substitution	Mutant Zygosity
WT	Allele 1	GAAGTGATTCAAGACATTGAGGAAAATGTGACTGAGGGTGTGATCAAAGA			
	Allele 2	GAAGTGATTCAAGACATTGAGGAAAATGTGACTGAGGGTGTGATCAAAGA			
P1	Allele 1	GAAGTGATTCAAGACATTGAGGAAAATGTGAGTGAGGGTGTGATCAAAGA	46%	C to G substitution	Biallelic
	Allele 2	GAAGTGATTCAAGACATTGAGGAAAATGTGA--TGAGGGTGTGATCAAAGA	45%	1 bp deletion	
P2	Allele 1	GAAGTGATTCAAGACATTGAGGAAAATGTGAGTGAGGGTGTGATCAAAGA	48%	C to G substitution	Biallelic
	Allele 2	GAAGTGATTCAAGACATTGAGGAAAATGTGA--TGAGGGTGTGATCAAAGA	45%	1 bp deletion	
P3	Allele 1	GAAGTGATTCAAGACATTGAGGAAAATGTGAGTGAGGGTGTGATCAAAGA	48%	C to G substitution	Biallelic
	Allele 2	GAAGTGATTCAAGACATTGAGGAAAATGTGA--TGAGGGTGTGATCAAAGA	45%	1 bp deletion	
P4	Allele 1	GAAGTGATTCAAGACATTGAGGAAAATGTGAGTGAGGGTGTGATCAAAGA	45%	C to G substitution	Biallelic

	Allele 2	GAAGTGATTCAAGACATTGAGGAAAATGTGA--TGAGGGTGTGATCAAAGA	47%	1 bp deletion	
P5	Allele 1	GAAGTGATTCAAGACATTGAGGAAAATGTGA--TGAGGGTGTGATCAAAGA	46%	1 bp deletion	Biallelic
	Allele 2	GAAGTGATTCAAGACATTGAGGAAAATGTGATTGAGGGTGTGATCAAAGA	39%	C to T substitution	
P6	Allele 1	GAAGTGATTCAAGACATTGAGGAAAATGTGACTGAGGGTGTGATCAAAGA		No edit	
	Allele 2	GAAGTGATTCAAGACATTGAGGAAAATGTGACTGAGGGTGTGATCAAAGA			
P7	Allele 1	GAAGTGATTCAAGACATTGAGGAAAATG-------TGAGGGTGTGATCAAAGA	43%	4 bp deletion	Biallelic
	Allele 2	GAAGTGATTCAAGACATTGAGGAAAATG-----GTGAGGGTGTGATCAAAGA	38%	4 bp deletion and C to G substitution	
P8	Allele 1	GAAGTGATTCAAGACATTGAGGAAAATG-------TGAGGGTGTGATCAAAGA	42%	4 bp deletion	Biallelic
	Allele 2	GAAGTGATTCAAGACATTGAGGAAAATG-----GTGAGGGTGTGATCAAAGA	40%	4 bp deletion and C to G substitution	

*Green fonts, dashes, and red fonts represent gRNA region, deletion, and substitution, respectively

Appendix Table 3A. CRISPR-Cas9 induced mutations in the transformed plants at T_1 generation of P1 for *SBE1*.

Plant no	Allele	Sequence	Percentage of mutation	Deletion/insertion/ Substitution	Mutant Zygosity
P1	Allele 1	CCGCTCCTT----------CCCGGGAATCGCGGTCAG	60%	23 bp deletion	Biallelic
	Allele 2	CCGCTCCTTCCCTCTCTCGCTGATCGACC-------CCCGGGAATCGCGGTCAG	39%	3 bp deletion	
P1-1	Allele 1	CCGCTCCTTCCCTCTCTCGCTGATCGACC-------CCCGGGAATCGCGGTCAG	88%	3 bp deletion	Homozygous
	Allele 2	CCGCTCCTTCCCTCTCTCGCTGATCGACC-------CCCGGGAATCGCGGTCAG		3 bp deletion	
P1-2	Allele 1	CCGCTCCTT----------CCCGGGAATCGCGGTCAG	88%	23 bp deletion	Biallelic
	Allele 2	CCGCTCCTTCCCTCTCTCGCTGATCGACC-------CCCGGGAATCGCGGTCAG	1.3%	3 bp deletion	
P1-3	Allele 1	CCGCTCCTT----------CCCGGGAATCGCGGTCAG	53%	23 bp deletion	Biallelic
	Allele 2	CCGCTCCTTCCCTCTCTCGCTGATCGACC-------CCCGGGAATCGCGGTCAG	34%	3 bp deletion	
P1-4	Allele 1	CCGCTCCTT----------CCCGGGAATCGCGGTCAG	88%	23 bp deletion	Biallelic
	Allele 2	CCGCTCCTTCCCTCTCTCGCTGATCGACC-------CCCGGGAATCGCGGTCAG	0.08%	3 bp deletion	
P1-5	Allele 1	CCGCTCCTT----------CCCGGGAATCGCGGTCAG	85%	23 bp deletion	Biallelic
	Allele 2	CCGCTCCTTCCCTCTCTCGCTGATCGACC-------CCCGGGAATCGCGGTCAG	1.1%	3 bp deletion	
P1-6	Allele 1	CCGCTCCTT----------CCCGGGAATCGCGGTCAG	49%	23 bp deletion	Biallelic
	Allele 2	CCGCTCCTTCCCTCTCTCGCTGATCGACC-------CCCGGGAATCGCGGTCAG	36%	3 bp deletion	
P1-7	Allele 1	CCGCTCCTT----------CCCGGGAATCGCGGTCAG	0.3%	23 bp deletion	Biallelic
	Allele 2	CCGCTCCTTCCCTCTCTCGCTGATCGACC-------CCCGGGAATCGCGGTCAG	89%	3 bp deletion	
P1-8	Allele 1	CCGCTCCTT----------CCCGGGAATCGCGGTCAG	54%	23 bp deletion	Biallelic
	Allele 2	CCGCTCCTTCCCTCTCTCGCTGATCGACC-------CCCGGGAATCGCGGTCAG	33%	3 bp deletion	
P1-9	Allele 1	CCGCTCCTTCCCTCTCTCGCTGATCGACC-------CCCGGGAATCGCGGTCAG	82%	3 bp deletion	Homozygous
	Allele 2	CCGCTCCTTCCCTCTCTCGCTGATCGACC-------CCCGGGAATCGCGGTCAG			
P1-10	Allele 1	CCGCTCCTT----------CCCGGGAATCGCGGTCAG	47%	23 bp deletion	Biallelic
	Allele 2	CCGCTCCTTCCCTCTCTCGCTGATCGACC-------CCCGGGAATCGCGGTCAG	36%	3 bp deletion	

Appendix Table 3B. CRISPR-Cas9 induced mutations in the transformed plants at T_1 generation of P1 for *SBE2*.

Plant no	Allele	Sequence	Percentage of mutation	Deletion/insertion/ Substitution	Mutant Zygosity
P1	Allele 1	CTCAGGCCTCCGCCGCCGGGAGGGTTGCCCCTGCAGCTGCGCCTCCTCCT	27%	No edit	Chimeric
	Allele 2	CTCAGGCCTCCGCCGCCGGGA--GGTTGCCCCTGCAGCTGCGCCTCCTCCT	41%	1 bp deletion	
	Allele 3	CTCAGGCCTCCGCCGCCGGGC--GGTTGCCCCTGCAGCTGCGCCTCCTCCT	4%	1 bp deletion and 1 bp substitution	
	Allele 4	CTCAGGCCTCCGCCGCCGGGA----GTTGCCCCTGCAGCTGCGCCTCCTCCT	4%	2 bp deletion	
P1-1	Allele 1	CTCAGGCCTCCGCCGCCGGGAGGGTTGCCCCTGCAGCTGCGCCTCCTCCT	33%	No edit	Chimeric
	Allele 2	CTCAGGCCTCCGCCGCCGGGA--GGTTGCCCCTGCAGCTGCGCCTCCTCCT	44%	1 bp deletion	
	Allele 3	CTCAGGCCTCCGCCGCCGGGA------TTGCCCCTGCAGCTGCGCCTCCTCCT	1.7%	3bp deletion	
P1-2	Allele 1	CTCAGGCCTCCGCCGCCGGGAGGGTTGCCCCTGCAGCTGCGCCTCCTCCT	41%	No edit	Monoallelic
	Allele 2	CTCAGGCCTCCGCCGCCGGGA--GGTTGCCCCTGCAGCTGCGCCTCCTCCT	42%	1 bp deletion	
P1-3	Allele 1	CTCAGGCCTCCGCCGCCGGGAGGGTTGCCCCTGCAGCTGCGCCTCCTCCT	29%	No edit	Chimeric
	Allele 2	CTCAGGCCTCCGCCGCCGGGATGGGTTGCCCCTGCAGCTGCGCCTCCTCCT	1.1%	1 bp insertion	
	Allele 3	CTCAGGCCTCCGCCGCCGGGTTGGGTTGCCCCTGCAGCTGCGCCTCCTCCT	1.3%	1 bp insertion and 1bp substitution	
	Allele 4	CTCAGGCCTCCGCCGCCGGGA--GGTTGCCCCTGCAGCTGCGCCTCCTCCT	44%	1 bp deletion	
	Allele 5	CTCAGGCCTCCGCCGCCGGGA----GTTGCCCCTGCAGCTGCGCCTCCTCCT	2.7%	2 bp deletion	
P1-4	Allele 1	CTCAGGCCTCCGCCGCCGGGAGGGTTGCCCCTGCAGCTGCGCCTCCTCCT	29%	No edit	Chimeric
	Allele 2	CTCAGGCCTCCGCCGCCGGGATGGGTTGCCCCTGCAGCTGCGCCTCCTCCT	16%	1 bp insertion	
	Allele 3	CTCAGGCCTCCGCCGCCGGGA--GGTTGCCCCTGCAGCTGCGCCTCCTCCT	44%	1 bp deletion	
	Allele 4	CTCAGGCCTCCGCCGCCGGGA----GTTGCCCCTGCAGCTGCGCCTCCTCCT	1.3	2 bp deletion	
P1-5				No edit	
	Allele 1	CTCAGGCCTCCGCCGCCGGGAGGGTTGCCCCTGCAGCTGCGCCTCCTCCT			
	Allele 2	CTCAGGCCTCCGCCGCCGGGAGGGTTGCCCCTGCAGCTGCGCCTCCTCCT			WT
P1-6	Allele 1	CTCAGGCCTCCGCCGCCGGGAGGGTTGCCCCTGCAGCTGCGCCTCCTCCT	27%	No edit	Chimeric
	Allele 2	CTCAGGCCTCCGCCGCCGGGAAGGGTTGCCCCTGCAGCTGCGCCTCCTCCT	2%	1 bp insertion	
	Allele 3	CTCAGGCCTCCGCCGCCGGGAGGGGTTGCCCCTGCAGCTGCGCCTCCTCCT	1.2%	1 bp insertion	
	Allele 4	CTCAGGCCTCCGCCGCCGGGA--GGTTGCCCCTGCAGCTGCGCCTCCTCCT	50%	1 bp deletion	
	Allele 5	CTCAGGCCTCCGCCGCCGGGA----GTTGCCCCTGCAGCTGCGCCTCCTCCT	0.6%	2 bp deletion	
P1-7	Allele 1	CTCAGGCCTCCGCCGCCGGGAGGGTTGCCCCTGCAGCTGCGCCTCCTCCT	24%	No edit	Chimeric
	Allele 2	CTCAGGCCTCCGCCGCCGGGAAGGGTTGCCCCTGCAGCTGCGCCTCCTCCT	0.9%	1 bp insertion	
	Allele 3	CTCAGGCCTCCGCCGCCGGGATGGGTTGCCCCTGCAGCTGCGCCTCCTCCT	1.5%	1 bp insertion	
	Allele 4	CTCAGGCCTCCGCCGCCGGGA--GGTTGCCCCTGCAGCTGCGCCTCCTCCT	54%	1 bp deletion	
	Allele 5	CTCAGGCCTCCGCCGCCGGGA----GTTGCCCCTGCAGCTGCGCCTCCTCCT	2%	2 bp deletion	
P1-8	Allele 1	CTCAGGCCTCCGCCGCCGGGAGGGTTGCCCCTGCAGCTGCGCCTCCTCCT		No edit	WT
	Allele 2	CTCAGGCCTCCGCCGCCGGGAGGGTTGCCCCTGCAGCTGCGCCTCCTCCT			
P1-9	Allele 1	CTCAGGCCTCCGCCGCCGGGA--GGTTGCCCCTGCAGCTGCGCCTCCTCCT	80%	1 bp deletion	Homozygous
	Allele 2	CTCAGGCCTCCGCCGCCGGGA--GGTTGCCCCTGCAGCTGCGCCTCCTCCT			
P1-10	Allele 1	CTCAGGCCTCCGCCGCCGGGA--GGTTGCCCCTGCAGCTGCGCCTCCTCCT	49%	1 bp deletion	Homozygous
	Allele 2	CTCAGGCCTCCGCCGCCGGGA--GGTTGCCCCTGCAGCTGCGCCTCCTCCT			

Appendix Table 3C. CRISPR-Cas9 induced mutations in the transformed plants at T_1 generation of P1 for *SBE3.*

Plant no	Allele	Sequence	Percentage of mutation	Deletion/insertion/ Substitution	Mutant Zygosity
P1	Allele 1	TACGGGCGGGGGCCGTGCGGTTCCCCGTGCCAGCCGGGGCCCGGAGCTGG		No edit	Monoallelic
	Allele 2	TACGGGCGGGGGCCGTGC--GTTCCCCGTGCCAGCCGGGGCCCGGAGCTGG		1 bp deletion	
P1-1	Allele 1	TACGGGCGGGGGCCGTGCGGTTCCCCGTGCCAGCCGGGGCCCGGAGCTGG	37%	No edit	Monoallelic
	Allele 2	TACGGGCGGGGGCCGTGC--GTTCCCCGTGCCAGCCGGGGCCCGGAGCTGG	47%	1 bp deletion	
P1-2	Allele 1	TACGGGCGGGGGCCGTGCGGTTCCCCGTGCCAGCCGGGGCCCGGAGCTGG	32%	No edit	Monoallelic
	Allele 2	TACGGGCGGGGGCCGTGC--GTTCCCCGTGCCAGCCGGGGCCCGGAGCTGG	44%	1 bp deletion	
P1-3	Allele 1	TACGGGCGGGGGCCGTGCGGTTCCCCGTGCCAGCCGGGGCCCGGAGCTGG	69%	No edit	Chimeric
	Allele 2	TACGGGCGGGGGCCGTGC--GTTCCCCGTGCCAGCCGGGGCCCGGAGCTGG	5%	1 bp deletion	
	Allele 3	TACGGGCGGGGGCC----------	04%	27 bp deletion	
P1-4	Allele 1	TACGGGCGGGGGCCGTGCGGTTCCCCGTGCCAGCCGGGGCCCGGAGCTGG	75%	No edit	Chimeric
	Allele 2	TACGGGCGGGGGCCGTGC--GTTCCCCGTGCCAGCCGGGGCCCGGAGCTGG	2.8%	1 bp deletion	
	Allele 3	TACGGGCGGGGGCC----------	0.4%	22 bp deletion	
P1-5	Allele 1	TACGGGCGGGGGCCGTGCGGTTCCCCGTGCCAGCCGGGGCCCGGAGCTGG	40%	No edit	Monoallelic
	Allele 2	TACGGGCGGGGGCCGTGC--GTTCCCCGTGCCAGCCGGGGCCCGGAGCTGG	42%	1 bp deletion	
P1-6	Allele 1	TACGGGCGGGGGCCGTGCGGTTCCCCGTGCCAGCCGGGGCCCGGAGCTGG	42%	No edit	Monoallelic
	Allele 2	TACGGGCGGGGGCCGTGC--GTTCCCCGTGCCAGCCGGGGCCCGGAGCTGG	36%	1 bp deletion	
P1-7	Allele 1	TACGGGCGGGGGCCGTGCGGTTCCCCGTGCCAGCCGGGGCCCGGAGCTGG	33%	No edit	Chimeric
	Allele 2	TACGGGCGGGGGCCGTGC--GTTCCCCGTGCCAGCCGGGGCCCGGAGCTGG	46%	1 bp deletion	
	Allele 3	TACGGGCGGGGGC----------	0.3%	48 bp deletion	
P1-8	Allele 1	TACGGGCGGGGGCCGTGCGGTTCCCCGTGCCAGCCGGGGCCCGGAGCTGG	41%	No edit	Chimeric
	Allele 2	TACGGGCGGGGGCCGTGC--GTTCCCCGTGCCAGCCGGGGCCCGGAGCTGG	41%	1 bp deletion	
	Allele 3	TACGGGCGGGGGCC----------	3.7%	27 bp deletion	
	Allele 4	TACGGGCGGGGGC----------	2.4%	48 bp deletion	
P1-9	Allele 1	TACGGGCGGGGGCCGTGCGGTTCCCCGTGCCAGCCGGGGCCCGGAGCTGG	39%	No edit	Monoallelic
	Allele 2	TACGGGCGGGGGCCGTGC--GTTCCCCGTGCCAGCCGGGGCCCGGAGCTGG	42%	1 bp deletion	
P1-10	Allele 1	TACGGGCGGGGGCCGTGCGGTTCCCCGTGCCAGCCGGGGCCCGGAGCTGG	0.3%	No edit	Monoallelic
	Allele 2	TACGGGCGGGGGCCGTGC--GTTCCCCGTGCCAGCCGGGGCCCGGAGCTGG	80%	1 bp deletion	

Appendix Table 3D. CRISPR-Cas9 induced mutations in the transformed plants at T_1 generation in P1 for *SBE4*.

Plant no	Allele	Sequence	Percentage of mutation	Deletion/insertion/ Substitution	Mutant Zygosity
P1	Allele 1	GAAGTGATTCAAGACATTGAGGAAAATGTGAGTGAGGGTGTGATCAAAGA	46%	C to G substitution	Biallelic
	Allele 2	GAAGTGATTCAAGACATTGAGGAAAATGTGA--TGAGGGTGTGATCAAAGA	45%	1 bp deletion	
P1-1	Allele 1	GAAGTGATTCAAGACATTGAGGAAAATGTGA--TGAGGGTGTGATCAAAGA	88%	1 bp deletion	Homozygous
	Allele 2	GAAGTGATTCAAGACATTGAGGAAAATGTGA--TGAGGGTGTGATCAAAGA			
P1-2	Allele 1	GAAGTGATTCAAGACATTGAGGAAAATGTGAGTGAGGGTGTGATCAAAGA	46%	C to G substitution	Biallelic
	Allele 2	GAAGTGATTCAAGACATTGAGGAAAATGTGA--TGAGGGTGTGATCAAAGA	45%	1 bp deletion	
P1-3	Allele 1	GAAGTGATTCAAGACATTGAGGAAAATGTGA--TGAGGGTGTGATCAAAGA	89%	1 bp deletion	Homozygous
	Allele 2	GAAGTGATTCAAGACATTGAGGAAAATGTGA--TGAGGGTGTGATCAAAGA			
P1-4	Allele 1	GAAGTGATTCAAGACATTGAGGAAAATGTGAGTGAGGGTGTGATCAAAGA	42%	C to G substitution	Biallelic
	Allele 2	GAAGTGATTCAAGACATTGAGGAAAATGTGA--TGAGGGTGTGATCAAAGA	45%	1 bp deletion	
P1-5	Allele 1	GAAGTGATTCAAGACATTGAGGAAAATGTGA--TGAGGGTGTGATCAAAGA	88%	1 bp deletion	Homozygous
	Allele 2	GAAGTGATTCAAGACATTGAGGAAAATGTGA--TGAGGGTGTGATCAAAGA			
P1-6	Allele 1	GAAGTGATTCAAGACATTGAGGAAAATGTGAGTGAGGGTGTGATCAAAGA	42%	C to G substitution	Biallelic
	Allele 2	GAAGTGATTCAAGACATTGAGGAAAATGTGA--TGAGGGTGTGATCAAAGA	46%	1 bp deletion	
P1-7	Allele 1	GAAGTGATTCAAGACATTGAGGAAAATGTGA--TGAGGGTGTGATCAAAGA	88%	1 bp deletion	Homozygous
	Allele 2	GAAGTGATTCAAGACATTGAGGAAAATGTGA--TGAGGGTGTGATCAAAGA			
P1-8	Allele 1	GAAGTGATTCAAGACATTGAGGAAAATGTGAGTGAGGGTGTGATCAAAGA	47%	C to G substitution	Biallelic
	Allele 2	GAAGTGATTCAAGACATTGAGGAAAATGTGA--TGAGGGTGTGATCAAAGA	41%	1 bp deletion	
P1-9	Allele 1	GAAGTGATTCAAGACATTGAGGAAAATGTGAGTGAGGGTGTGATCAAAGA	78%	C to G substitution	Homozygous
	Allele 2	GAAGTGATTCAAGACATTGAGGAAAATGTGAGTGAGGGTGTGATCAAAGA			
P1-10	Allele 1	GAAGTGATTCAAGACATTGAGGAAAATGTGAGTGAGGGTGTGATCAAAGA	39%	1 bp deletion	Biallelic
	Allele 2	GAAGTGATTCAAGACATTGAGGAAAATGTGA--TGAGGGTGTGATCAAAGA	40%	C to G substitution	

Appendix Table 3E. CRISPR-Cas9 induced mutations in the transformed plants at T_1 generation of P2 for *SBE1*.

Plant no	Allele	Sequence	Percentage of mutation	Deletion/insertion/ Substitution	Mutant Zygosity
P2	Allele 1	CCGCTCCTT----------CCCGGGAATCGCGGTCAG			
	Allele 2	CCGCTCCTTCCCTCTCTCGCTGATCGACC-------CCCGGGAATCGCGGTCAG			
P2-1	Allele 1	CCGCTCCTT----------CCCGGGAATCGCGGTCAG	87%	23 bp deletion	Homozygous
	Allele 2	CCGCTCCTT----------CCCGGGAATCGCGGTCAG			
P2-2	Allele 1	CCGCTCCTT----------CCCGGGAATCGCGGTCAG	59%	23 bp deletion	Biallelic
	Allele 2	CCGCTCCTTCCCTCTCTCGCTGATCGACC-------CCCGGGAATCGCGGTCAG	29%	3 bp deletion	
P2-3	Allele 1	CCGCTCCTT----------CCCGGGAATCGCGGTCAG	74%	23 bp deletion	Biallelic
	Allele 2	CCGCTCCTTCCCTCTCTCGCTGATCGACC-------CCCGGGAATCGCGGTCAG	13%	3 bp deletion	
P2-4	Allele 1	CCGCTCCTT----------CCCGGGAATCGCGGTCAG	51%	23 bp deletion	Biallelic
	Allele 2	CCGCTCCTTCCCTCTCTCGCTGATCGACC-------CCCGGGAATCGCGGTCAG	36%	3 bp deletion	
P2-5	Allele 1	CCGCTCCTT----------CCCGGGAATCGCGGTCAG	51%	23 bp deletion	Biallelic
	Allele 2	CCGCTCCTTCCCTCTCTCGCTGATCGACC-------CCCGGGAATCGCGGTCAG	36%	3 bp deletion	
P2-6	Allele 1	CCGCTCCTT----------CCCGGGAATCGCGGTCAG	0.4%	23 bp deletion	Biallelic
	Allele 2	CCGCTCCTTCCCTCTCTCGCTGATCGACC-------CCCGGGAATCGCGGTCAG	87%	3 bp deletion	
P2-7	Allele 1	CCGCTCCTTCCCTCTCTCGCTGATCGACC-------CCCGGGAATCGCGGTCAG	84%	3 bp deletion	Homozygous
	Allele 2	CCGCTCCTTCCCTCTCTCGCTGATCGACC-------CCCGGGAATCGCGGTCAG			
P2-8	Allele 1	CCGCTCCTTCCCTCTCTCGCTGATCGACC-------CCCGGGAATCGCGGTCAG	51%	23 bp deletion	Biallelic
	Allele 2	CCGCTCCTT----------CCCGGGAATCGCGGTCAG	32%	3 bp deletion	
P2-9	Allele 1	CCGCTCCTT----------CCCGGGAATCGCGGTCAG	86%	23 bp deletion	Homozygous
	Allele 2	CCGCTCCTT----------CCCGGGAATCGCGGTCAG			
P2-10	Allele 1	CCGCTCCTT----------CCCGGGAATCGCGGTCAG	94%	3 bp deletion	Biallelic
	Allele 2	CCGCTCCTTCCCTCTCTCGCTGATCGACC-------CCCGGGAATCGCGGTCAG	0.4%	23 bp deletion	
P2-11	Allele 1	CCGCTCCTT----------CCCGGGAATCGCGGTCAG	86%	23 bp deletion	Homozygous
	Allele 2	CCGCTCCTT----------CCCGGGAATCGCGGTCAG			
P2-12	Allele 1	CCGCTCCTT----------CCCGGGAATCGCGGTCAG	0.7%	3 bp deletion	Biallelic
	Allele 2	CCGCTCCTTCCCTCTCTCGCTGATCGACC-------CCCGGGAATCGCGGTCAG	85%	23 bp deletion	
P2-13	Allele 1	CCGCTCCTTCCCTCTCTCGCTGATCGACC-------CCCGGGAATCGCGGTCAG	83%	3 bp deletion	Homozygous
	Allele 2	CCGCTCCTTCCCTCTCTCGCTGATCGACC-------CCCGGGAATCGCGGTCAG			
P2-14	Allele 1	CCGCTCCTT----------CCCGGGAATCGCGGTCAG	82%	23 bp deletion	Biallelic
	Allele 2	CCGCTCCTTCCCTCTCTCGCTGATCGACC-------CCCGGGAATCGCGGTCAG	0.6%	3 bp deletion	
P2-15	Allele 1	CCGCTCCTT----------CCCGGGAATCGCGGTCAG	46%	23 bp deletion	Biallelic
	Allele 2	CCGCTCCTTCCCTCTCTCGCTGATCGACC-------CCCGGGAATCGCGGTCAG	46%	3 bp deletion	

Appendix Table 3F. CRISPR-Cas9 induced mutations in the transformed plants at T_1 generation of P2 for *SBE2.*

Plant no	Allele	Sequence	Percentage of mutation	Deletion/insertion/ Substitution	Mutant Zygosity
P2	Allele 1	CTCAGGCCTCCGCCGCCGGGAAGGTTGCCCCTGCAGCTGCGCCTCCTCCT		G to A substitution	Chimeric
	Allele 2	CTCAGGCCTCCGCCGCCGGGA—GGTTGCCCCTGCAGCTGCGCCTCCTCCT		1 bp deletion	
	Allele 3	CTCAGGCCTCCGCCGCCGGGCAGGTTGCCCCTGCAGCTGCGCCTCCTCCT		AG to CA substitution	
P2-1	Allele 1	CTCAGGCCTCCGCCGCCGGGA—GGTTGCCCCTGCAGCTGCGCCTCCTCCT	93%	1bp deletion	Homozygous
	Allele 2	CTCAGGCCTCCGCCGCCGGGA—GGTTGCCCCTGCAGCTGCGCCTCCTCCT			
P2-2	Allele 1	CTCAGGCCTCCGCCGCCGGGAAGGTTGCCCCTGCAGCTGCGCCTCCTCCT	43%	G to A substitution	Biallelic
	Allele 2	CTCAGGCCTCCGCCGCCGGGA—GGTTGCCCCTGCAGCTGCGCCTCCTCCT		1 bp deletion	
P2-3	Allele 1	CTCAGGCCTCCGCCGCCGGGAAGGTTGCCCCTGCAGCTGCGCCTCCTCCT	44%	G to A substitution	Biallelic
	Allele 2	CTCAGGCCTCCGCCGCCGGGA—GGTTGCCCCTGCAGCTGCGCCTCCTCCT	41%	1 bp deletion	
P2-4	Allele 1	CTCAGGCCTCCGCCGCCGGGAAGGTTGCCCCTGCAGCTGCGCCTCCTCCT	85%	G to A substitution	Homozygous
	Allele 2	CTCAGGCCTCCGCCGCCGGGAAGGTTGCCCCTGCAGCTGCGCCTCCTCCT			
P2-5	Allele 1	CTCAGGCCTCCGCCGCCGGGAAGGTTGCCCCTGCAGCTGCGCCTCCTCCT	83%	G to A substitution	Homozygous
	Allele 2	CTCAGGCCTCCGCCGCCGGGAAGGTTGCCCCTGCAGCTGCGCCTCCTCCT			
P2-6	Allele 1	CTCAGGCCTCCGCCGCCGGGAAGGTTGCCCCTGCAGCTGCGCCTCCTCCT	83%	G to A substitution	Homozygous
	Allele 2	CTCAGGCCTCCGCCGCCGGGAAGGTTGCCCCTGCAGCTGCGCCTCCTCCT			
P2-7	Allele 1	CTCAGGCCTCCGCCGCCGGGAAGGTTGCCCCTGCAGCTGCGCCTCCTCCT	41%	G to A substitution	Biallelic
	Allele 2	CTCAGGCCTCCGCCGCCGGGA—GGTTGCCCCTGCAGCTGCGCCTCCTCCT	43%	1 bp deletion	
P2-8	Allele 1	CTCAGGCCTCCGCCGCCGGGAAGGTTGCCCCTGCAGCTGCGCCTCCTCCT	41%	G to A substitution	Biallelic
	Allele 2	CTCAGGCCTCCGCCGCCGGGA—GGTTGCCCCTGCAGCTGCGCCTCCTCCT	40%	1 bp deletion	
P2-9	Allele 1	CTCAGGCCTCCGCCGCCGGGAAGGTTGCCCCTGCAGCTGCGCCTCCTCCT	79%	G to A substitution	Biallelic
	Allele 2	CTCAGGCCTCCGCCGCCGGGA—GGTTGCCCCTGCAGCTGCGCCTCCTCCT	0.4%	1 bp deletion	
P2-10	Allele 1	CTCAGGCCTCCGCCGCCGGGAAGGTTGCCCCTGCAGCTGCGCCTCCTCCT	41%	G to A substitution	Biallelic
	Allele 2	CTCAGGCCTCCGCCGCCGGGA—GGTTGCCCCTGCAGCTGCGCCTCCTCCT	43%	1 bp deletion	
P2-11	Allele 1	CTCAGGCCTCCGCCGCCGGGAAGGTTGCCCCTGCAGCTGCGCCTCCTCCT	38%	G to A substitution	Biallelic
	Allele 2	CTCAGGCCTCCGCCGCCGGGA—GGTTGCCCCTGCAGCTGCGCCTCCTCCT	40%	1 bp deletion	
P2-12	Allele 1	CTCAGGCCTCCGCCGCCGGGAAGGTTGCCCCTGCAGCTGCGCCTCCTCCT	40%	G to A substitution	Biallelic
	Allele 2	CTCAGGCCTCCGCCGCCGGGA—GGTTGCCCCTGCAGCTGCGCCTCCTCCT	42%	1 bp deletion	
P2-13	Allele 1	CTCAGGCCTCCGCCGCCGGGAAGGTTGCCCCTGCAGCTGCGCCTCCTCCT	83%	G to A substitution	Homozygous
	Allele 2	CTCAGGCCTCCGCCGCCGGGAAGGTTGCCCCTGCAGCTGCGCCTCCTCCT			
P2-14	Allele 1	CTCAGGCCTCCGCCGCCGGGA—GGTTGCCCCTGCAGCTGCGCCTCCTCCT	80%	1 bp deletion	Homozygous
	Allele 2	CTCAGGCCTCCGCCGCCGGGA—GGTTGCCCCTGCAGCTGCGCCTCCTCCT			
P2-15	Allele 1	CTCAGGCCTCCGCCGCCGGGA—GGTTGCCCCTGCAGCTGCGCCTCCTCCT	81%	1 bp deletion	Homozygous
	Allele 2	CTCAGGCCTCCGCCGCCGGGA—GGTTGCCCCTGCAGCTGCGCCTCCTCCT			

Appendix Table 3G. CRISPR-Cas9 induced mutations in the transformed plants at T_1 generation of P2 for *SBE3*.

Plant no	Allele	Sequence	Percentage of mutation	Deletion/insertion/ Substitution	Mutant Zygosity
P2	Allele 1	TACGGGCGGGGGCCGTGCGGTTCCCCGTGCCAGCCGGGGCCCGGAGCTGG		No edit	Monoallelic
	Allele 2	TACGGGCGGGGGCCGTGC--GTTCCCCGTGCCAGCCGGGGCCCGGAGCTGG		1 bp deletion	
P2-1	Allele 1	TACGGGCGGGGGCCGTGCGGTTCCCCGTGCCAGCCGGGGCCCGGAGCTGG	42%	No edit	Monoallelic
	Allele 2	TACGGGCGGGGGCCGTGC--GTTCCCCGTGCCAGCCGGGGCCCGGAGCTGG	41%	1 bp deletion	
P2-2	Allele 1	TACGGGCGGGGGCCGTGCGGTTCCCCGTGCCAGCCGGGGCCCGGAGCTGG	74%	No edit	Chimeric
	Allele 2	TACGGGCGGGGGCCGTGC--GTTCCCCGTGCCAGCCGGGGCCCGGAGCTGG	2%	1 bp deletion	
	Allele 3	TACGGGCGGGGGCCGTGCGGGTTCCCCGTGCCAGCCGGGGCCCGGAGCTGG	1%	1 bp insertion	
P2-3	Allele 1	TACGGGCGGGGGCCGTGCGGTTCCCCGTGCCAGCCGGGGCCCGGAGCTGG	57%	No edit	Chimeric
	Allele 2	TACGGGCGGGGGCCGTGC--GTTCCCCGTGCCAGCCGGGGCCCGGAGCTGG	3%	1 bp deletion	
	Allele 3	TACGGGCGGGGGCC----------	1%	27 bp deletion	
	Allele 4	TACGGGCGGGG----------	1%	33 bp deletion	
P2-4	Allele 1	TACGGGCGGGGGCCGTGCGGTTCCCCGTGCCAGCCGGGGCCCGGAGCTGG	94%	No edit	WT
	Allele 2	TACGGGCGGGGGCCGTGCGGTTCCCCGTGCCAGCCGGGGCCCGGAGCTGG			
P2-5	Allele 1	TACGGGCGGGGGCCGTGC--GTTCCCCGTGCCAGCCGGGGCCCGGAGCTGG	94%	1 bp deletion	Homozygous
	Allele 2	TACGGGCGGGGGCCGTGC--GTTCCCCGTGCCAGCCGGGGCCCGGAGCTGG			
P2-6	Allele 1	TACGGGCGGGGGCCGTGCGGTTCCCCGTGCCAGCCGGGGCCCGGAGCTGG	13%	No edit	Monoallelic
	Allele 2	TACGGGCGGGGGCCGTGC--GTTCCCCGTGCCAGCCGGGGCCCGGAGCTGG	47%	1 bp deletion	
P2-7	Allele 1	TACGGGCGGGGGCCGTGCGGTTCCCCGTGCCAGCCGGGGCCCGGAGCTGG	74%	No edit	Monoallelic
	Allele 2	TACGGGCGGGGGCCGTGC--GTTCCCCGTGCCAGCCGGGGCCCGGAGCTGG	5%	1 bp deletion	
P2-8	Allele 1	TACGGGCGGGGGCCGTGC--GTTCCCCGTGCCAGCCGGGGCCCGGAGCTGG	84%	1 bp deletion	Chimeric
	Allele 2	TACGGGCGGGGGCCGTGC--ATTCCCCGTGCCAGCCGGGGCCCGGAGCTGG	4%	1 bp deletion and 1 bp substitution	
	Allele 3	TACGGGCGGGGGCCGTGT--GTTCCCCGTGCCAGCCGGGGCCCGGAGCTGG	3%	1 bp deletion and 1 bp substitution	
P2-9	Allele 1	TACGGGCGGGGGCCGTGCGGTTCCCCGTGCCAGCCGGGGCCCGGAGCTGG	36%	No edit	Monoallelic
	Allele 2	TACGGGCGGGGGCCGTGC--GTTCCCCGTGCCAGCCGGGGCCCGGAGCTGG	45%	1 bp deletion	
P2-10	Allele 1	TACGGGCGGGGGCCGTGCGGTTCCCCGTGCCAGCCGGGGCCCGGAGCTGG	3%	No edit	Chimeric
	Allele 2	TACGGGCGGGGGCCGTGC--GTTCCCCGTGCCAGCCGGGGCCCGGAGCTGG	17%	1 bp deletion	
	Allele 3	----------	39%	63 bp deletion	
	Allele 4	TACGGGCGGGGG----------	4%	48 bp deletion	
P2-11	Allele 1	TACGGGCGGGGGCCGTGCGGTTCCCCGTGCCAGCCGGGGCCCGGAGCTGG	45%	No edit	Chimeric
	Allele 2	TACGGGCGGGGGCCGTGC--GTTCCCCGTGCCAGCCGGGGCCCGGAGCTGG	30%	1 bp deletion	
	Allele 3	TACGGGCGGGGGCC----------	0.4%	27 bp deletion	
P2-12	Allele 1	TACGGGCGGGGGCCGTGCGGTTCCCCGTGCCAGCCGGGGCCCGGAGCTGG	69%	No edit	Monoallelic
	Allele 2	TACGGGCGGGGGCCGTGC--GTTCCCCGTGCCAGCCGGGGCCCGGAGCTGG	8%	1 bp deletion	
P2-13	Allele 1	TACGGGCGGGGGCCGTGCGGTTCCCCGTGCCAGCCGGGGCCCGGAGCTGG	70%	No edit	Monoallelic
	Allele 2	TACGGGCGGGGGCCGTGC--GTTCCCCGTGCCAGCCGGGGCCCGGAGCTGG	4%	1 bp deletion	
P2-14	Allele 1	TACGGGCGGGGGCCGTGCGGTTCCCCGTGCCAGCCGGGGCCCGGAGCTGG	33%	No edit	Chimeric
	Allele 2	TACGGGCGGGGGCCGTGC--GTTCCCCGTGCCAGCCGGGGCCCGGAGCTGG	43%	1 bp deletion	
	Allele 3	TACGGGCGGGGGCC----------	1%	27 bp deletion	
P2-15	Allele 1	TACGGGCGGGGGCCGTGCGGTTCCCCGTGCCAGCCGGGGCCCGGAGCTGG		No edit	WT
	Allele 2	TACGGGCGGGGGCCGTGCGGTTCCCCGTGCCAGCCGGGGCCCGGAGCTGG			

Appendix Table 3H. CRISPR-Cas9 induced mutations in the transformed plants at T_1 generation of P2 for *SBE4*.

Plant no	Allele	Sequence	Percentage of mutation	Deletion/insertion/ Substitution	Mutant Zygosity
P2	Allele 1	GAAGTGATTCAAGACATTGAGGAAAATGTGAGTGAGGGTGTGATCAAAGA	48%	C to G substitution	Biallelic
	Allele 2	GAAGTGATTCAAGACATTGAGGAAAATGTGA--TGAGGGTGTGATCAAAGA	45%	1 bp deletion	
P2-1	Allele 1	GAAGTGATTCAAGACATTGAGGAAAATGTGAGTGAGGGTGTGATCAAAGA	0.2%	C to G substitution	Biallelic
	Allele 2	GAAGTGATTCAAGACATTGAGGAAAATGTGA--TGAGGGTGTGATCAAAGA	84%	1 bp deletion	
P2-2	Allele 1	GAAGTGATTCAAGACATTGAGGAAAATGTGAGTGAGGGTGTGATCAAAGA	85%	C to G substitution	Homozygous
	Allele 2	GAAGTGATTCAAGACATTGAGGAAAATGTGAGTGAGGGTGTGATCAAAGA			
P2-3	Allele 1	GAAGTGATTCAAGACATTGAGGAAAATGTGAGTGAGGGTGTGATCAAAGA	85%	C to G substitution	Biallelic
	Allele 2	GAAGTGATTCAAGACATTGAGGAAAATGTGGGTGAGGGTGTGATCAAAGA	0.3%	AC to CG substitution	
P2-4	Allele 1	GAAGTGATTCAAGACATTGAGGAAAATGTGAGTGAGGGTGTGATCAAAGA	47%	C to G substitution	Biallelic
	Allele 2	GAAGTGATTCAAGACATTGAGGAAAATGTGA--TGAGGGTGTGATCAAAGA	42%	1 bp deletion	
P2-5	Allele 1	GAAGTGATTCAAGACATTGAGGAAAATGTGAGTGAGGGTGTGATCAAAGA	53%	C to G substitution	Biallelic
	Allele 2	GAAGTGATTCAAGACATTGAGGAAAATGTGA--TGAGGGTGTGATCAAAGA	41%	1 bp deletion	
P2-6	Allele 1	GAAGTGATTCAAGACATTGAGGAAAATGTGAGTGAGGGTGTGATCAAAGA	43%	C to G substitution	Biallelic
	Allele 2	GAAGTGATTCAAGACATTGAGGAAAATGTGA--TGAGGGTGTGATCAAAGA	44%	1 bp deletion	
P2-7	Allele 1	GAAGTGATTCAAGACATTGAGGAAAATGTGAGTGAGGGTGTGATCAAAGA	52%	C to G substitution	Biallelic
	Allele 2	GAAGTGATTCAAGACATTGAGGAAAATGTGA--TGAGGGTGTGATCAAAGA	33%	1 bp deletion	
P2-8	Allele 1	GAAGTGATTCAAGACATTGAGGAAAATGTGAGTGAGGGTGTGATCAAAGA	84%	C to G substitution	Homozygous
	Allele 2	GAAGTGATTCAAGACATTGAGGAAAATGTGAGTGAGGGTGTGATCAAAGA			
P2-9	Allele 1	GAAGTGATTCAAGACATTGAGGAAAATGTGAGTGAGGGTGTGATCAAAGA	40%	C to G substitution	Biallelic
	Allele 2	GAAGTGATTCAAGACATTGAGGAAAATGTGA--TGAGGGTGTGATCAAAGA	40%	1 bp deletion	
P2-10	Allele 1	GAAGTGATTCAAGACATTGAGGAAAATGTGAGTGAGGGTGTGATCAAAGA	42%	C to G substitution	Biallelic
	Allele 2	GAAGTGATTCAAGACATTGAGGAAAATGTGA--TGAGGGTGTGATCAAAGA	45%	1 bp deletion	
P2-11	Allele 1	GAAGTGATTCAAGACATTGAGGAAAATGTGAGTGAGGGTGTGATCAAAGA	42%	C to G substitution	Biallelic
	Allele 2	GAAGTGATTCAAGACATTGAGGAAAATGTGA--TGAGGGTGTGATCAAAGA	45%	1 bp deletion	
P2-12	Allele 1	GAAGTGATTCAAGACATTGAGGAAAATGTGAGTGAGGGTGTGATCAAAGA	42%	C to G substitution	Biallelic
	Allele 2	GAAGTGATTCAAGACATTGAGGAAAATGTGA--TGAGGGTGTGATCAAAGA	47%	1 bp deletion	
P2-13	Allele 1	GAAGTGATTCAAGACATTGAGGAAAATGTGAGTGAGGGTGTGATCAAAGA	40%	C to G substitution	Biallelic
	Allele 2	GAAGTGATTCAAGACATTGAGGAAAATGTGA--TGAGGGTGTGATCAAAGA	43%	1 bp deletion	
P2-14	Allele 1	GAAGTGATTCAAGACATTGAGGAAAATGTGAGTGAGGGTGTGATCAAAGA	37%	C to G substitution	Biallelic
	Allele 2	GAAGTGATTCAAGACATTGAGGAAAATGTGA--TGAGGGTGTGATCAAAGA	39%	1 bp deletion	
P2-15	Allele 1	GAAGTGATTCAAGACATTGAGGAAAATGTGAGTGAGGGTGTGATCAAAGA	80%	C to G substitution	Homozygous
	Allele 2	GAAGTGATTCAAGACATTGAGGAAAATGTGAGTGAGGGTGTGATCAAAGA			

Appendix Table 3I. CRISPR-Cas9 induced mutations in the transformed plants at T_1 generation of P3 for *SBE1*.

Plant no	Allele	Sequence	Percentage of mutation	Deletion/insertion/ Substitution	Mutant Zygosity
P3	Allele 1	CCGCTCCTT----------CCCGGGAATCGCGGTCAG	47%	23 bp deletion	Biallelic
	Allele 2	CCGCTCCTTCCCTCTCTCGCTGATCGACC-------CCCGGGAATCGCGGTCAG	32%	3 bp deletion	
P3-1	Allele 1	CCGCTCCTT----------CCCGGGAATCGCGGTCAG	1%	23 bp deletion	Biallelic
	Allele 2	CCGCTCCTTCCCTCTCTCGCTGATCGACC-------CCCGGGAATCGCGGTCAG	85%	3 bp deletion	
P3-2	Allele 1	CCGCTCCTT----------CCCGGGAATCGCGGTCAG	53%	23 bp deletion	Biallelic
	Allele 2	CCGCTCCTTCCCTCTCTCGCTGATCGACC-------CCCGGGAATCGCGGTCAG	32%	3 bp deletion	
P3-3	Allele 1	CCGCTCCTT----------CCCGGGAATCGCGGTCAG	51%	23 bp deletion	Biallelic
	Allele 2	CCGCTCCTTCCCTCTCTCGCTGATCGACC-------CCCGGGAATCGCGGTCAG	35%	3 bp deletion	
P3-4	Allele 1	CCGCTCCTT----------CCCGGGAATCGCGGTCAG	48%	23 bp deletion	Biallelic
	Allele 2	CCGCTCCTTCCCTCTCTCGCTGATCGACC-------CCCGGGAATCGCGGTCAG	37%	3 bp deletion	
P3-5	Allele 1	CCGCTCCTT----------CCCGGGAATCGCGGTCAG	84%	23 bp deletion	Homozygous
	Allele 2	CCGCTCCTT----------CCCGGGAATCGCGGTCAG			
P3-6	Allele 1	CCGCTCCTT----------CCCGGGAATCGCGGTCAG	87%	23 bp deletion	Homozygous
	Allele 2	CCGCTCCTT----------CCCGGGAATCGCGGTCAG			
P3-7	Allele 1	CCGCTCCTT----------CCCGGGAATCGCGGTCAG	87%	23 bp deletion	Homozygous
	Allele 2	CCGCTCCTT----------CCCGGGAATCGCGGTCAG			
P3-8	Allele 1	CCGCTCCTT----------CCCGGGAATCGCGGTCAG	87%	23 bp deletion	Homozygous
	Allele 2	CCGCTCCTT----------CCCGGGAATCGCGGTCAG			
P3-9	Allele 1	CCGCTCCTTCCCTCTCTCGCTGATCGACC-------CCCGGGAATCGCGGTCAG	87%	3 bp deletion	Homozygous
	Allele 2	CCGCTCCTTCCCTCTCTCGCTGATCGACC-------CCCGGGAATCGCGGTCAG			
P3-10	Allele 1	CCGCTCCTT----------CCCGGGAATCGCGGTCAG	50%	23 bp deletion	Biallelic
	Allele 2	CCGCTCCTTCCCTCTCTCGCTGATCGACC-------CCCGGGAATCGCGGTCAG	35%	3 bp deletion	
P3-11	Allele 1	CCGCTCCTT----------CCCGGGAATCGCGGTCAG	55%	23 bp deletion	Biallelic
	Allele 2	CCGCTCCTTCCCTCTCTCGCTGATCGACC-------CCCGGGAATCGCGGTCAG	31%	3 bp deletion	
P3-12	Allele 1	CCGCTCCTT----------CCCGGGAATCGCGGTCAG	53%	23 bp deletion	Biallelic
	Allele 2	CCGCTCCTTCCCTCTCTCGCTGATCGACC-------CCCGGGAATCGCGGTCAG	28%	3 bp deletion	
P3-13	Allele 1	CCGCTCCTTCCCTCTCTCGCTGATCGACC-------CCCGGGAATCGCGGTCAG	84%	3 bp deletion	Biallelic
	Allele 2	CCGCTCCTTCCCTCTCTCGCTGATCGACC-------CCCGGGAATCGCGGTCAG			

Appendix Table 3J. CRISPR-Cas9 induced mutations in the transformed plants at T_1 generation of P3 for *SBE2*.

Plant no	Allele	Sequence	Percentage of mutation	Deletion/insertion/ Substitution	Mutant Zygosity
P3	Allele 1	CTCAGGCCTCCGCCGCCGGGGA------TTGCCCCTGCAGCTGCGCCTCCTCCT	48%	3 bp deletion	Chimeric
	Allele 2	CTCAGGCCTCCGCCGCCGGGGC------TTGCCCCTGCAGCTGCGCCTCCTCCT	4%	3 bp deletion and 1bp substitution	
	Allele 3	CTCAGGCCTCCGCCGCCGGGA-TCGCAGGTTGCCCCTGCAGCTGCGCCTCCTCCT	34%	1 bp deletion and 5 bp insertion	
	Allele 4	CTCAGGCCTCCGCCGCCGGGC-TCGCAGGTTGCCCCTGCAGCTGCGCCTCCTCCT	0.2%	1 bp deletion and substitution, 5 bp insertion	
P3-1	Allele 1	CTCAGGCCTCCGCCGCCGGGA------TTGCCCCTGCAGCTGCGCCTCCTCCT	80%	3 bp deletion	Homozygous
	Allele 2	CTCAGGCCTCCGCCGCCGGGA------TTGCCCCTGCAGCTGCGCCTCCTCCT			
P3-2	Allele 1	CTCAGGCCTCCGCCGCCGGGA------TTGCCCCTGCAGCTGCGCCTCCTCCT	44%	3 bp deletion	Biallelic
	Allele 2	CTCAGGCCTCCGCCGCCGGGA-TCGCAGGTTGCCCCTGCAGCTGCGCCTCCTCCT	40%	1 bp deletion and 5 bp insertion	
P3-3	Allele 1	CTCAGGCCTCCGCCGCCGGGA------TTGCCCCTGCAGCTGCGCCTCCTCCT	47%	3 bp deletion	Biallelic
	Allele 2	CTCAGGCCTCCGCCGCCGGGA-TCGCAGGTTGCCCCTGCAGCTGCGCCTCCTCCT	35%	1 bp deletion and 5 bp insertion	
P3-5	Allele 1	CTCAGGCCTCCGCCGCCGGGA------TTGCCCCTGCAGCTGCGCCTCCTCCT	45%	3 bp deletion	Biallelic
	Allele 2	CTCAGGCCTCCGCCGCCGGGA-TCGCAGGTTGCCCCTGCAGCTGCGCCTCCTCCT	41%	1 bp deletion and 5 bp insertion	
P3-6	Allele 1	CTCAGGCCTCCGCCGCCGGGA------TTGCCCCTGCAGCTGCGCCTCCTCCT	37%	3 bp deletion	Biallelic
	Allele 2	CTCAGGCCTCCGCCGCCGGGA-TCGCAGGTTGCCCCTGCAGCTGCGCCTCCTCCT	35%	1 bp deletion and 5 bp insertion	
P3-7	Allele 1	CTCAGGCCTCCGCCGCCGGGA------TTGCCCCTGCAGCTGCGCCTCCTCCT	84%	3 bp deletion	Homozygous
	Allele 2	CTCAGGCCTCCGCCGCCGGGA------TTGCCCCTGCAGCTGCGCCTCCTCCT			
P3-8	Allele 1	CTCAGGCCTCCGCCGCCGGGA------TTGCCCCTGCAGCTGCGCCTCCTCCT	45%	3 bp deletion	Biallelic
	Allele 2	CTCAGGCCTCCGCCGCCGGGA-TCGCAGGTTGCCCCTGCAGCTGCGCCTCCTCCT	38%	1 bp deletion and 5 bp insertion	
P3-9	Allele 1	CTCAGGCCTCCGCCGCCGGGA------TTGCCCCTGCAGCTGCGCCTCCTCCT	67%	3 bp deletion	Biallelic
	Allele 2	CTCAGGCCTCCGCCGCCGGGA-TCGCAGGTTGCCCCTGCAGCTGCGCCTCCTCCT	16%	1 bp deletion and 5 bp insertion	
P3-10	Allele 1	CTCAGGCCTCCGCCGCCGGGA------TTGCCCCTGCAGCTGCGCCTCCTCCT	84%	3 bp deletion	Homozygous
	Allele 2	CTCAGGCCTCCGCCGCCGGGA------TTGCCCCTGCAGCTGCGCCTCCTCCT			
P3-11	Allele 1	CTCAGGCCTCCGCCGCCGGGA------TTGCCCCTGCAGCTGCGCCTCCTCCT	84%	3 bp deletion	Homozygous
	Allele 2	CTCAGGCCTCCGCCGCCGGGA------TTGCCCCTGCAGCTGCGCCTCCTCCT			
P3-12	Allele 1	CTCAGGCCTCCGCCGCCGGGA-TCGCAGGTTGCCCCTGCAGCTGCGCCTCCTCCT	39%	1 bp deletion and 5 bp insertion	Homozygous
	Allele 2	CTCAGGCCTCCGCCGCCGGGA-TCGCAGGTTGCCCCTGCAGCTGCGCCTCCTCCT			
P3-13	Allele 1	CTCAGGCCTCCGCCGCCGGGA-TCGCAGGTTGCCCCTGCAGCTGCGCCTCCTCCT	81%	1 bp deletion and 5 bp insertion	Homozygous
	Allele 2	CTCAGGCCTCCGCCGCCGGGA-TCGCAGGTTGCCCCTGCAGCTGCGCCTCCTCCT			

Appendix Table 3K. CRISPR-Cas9 induced mutations in the transformed plants at T_1 generation of P3 for *SBE3*.

Plant no	Allele	Sequence	Percentage of mutation	Deletion/insertion/ Substitution	Mutant Zygosity
P3	Allele 1	TACGGGCGGGGGCCGTGCGGTTCCCCGTGCCAGCCGGGGCCCGGAGCTGG			
	Allele 2	TACGGGCGGGGGCCGTGC--GTTCCCCGTGCCAGCCGGGGCCCGGAGCTGG			
P3-1	Allele 1	TACGGGCGGGGGCCGTGCGGTTCCCCGTGCCAGCCGGGGCCCGGAGCTGG		No edit	WT
	Allele 2	TACGGGCGGGGGCCGTGCGGTTCCCCGTGCCAGCCGGGGCCCGGAGCTGG			
P3-2	Allele 1	TACGGGCGGGGGCCGTGCGGTTCCCCGTGCCAGCCGGGGCCCGGAGCTGG		No edit	WT
	Allele 2	TACGGGCGGGGGCCGTGCGGTTCCCCGTGCCAGCCGGGGCCCGGAGCTGG			
P3-3	Allele 1	TACGGGCGGGGGCCGTGCGGTTCCCCGTGCCAGCCGGGGCCCGGAGCTGG	35%	No edit	Chimeric
	Allele 2	TACGGGCGGGGGCCGTGC--GTTCCCCGTGCCAGCCGGGGCCCGGAGCTGG	6.8%	1 bp deletion	
	Allele 3	TACGGGCGGGGGCCGTGCGGGTTCCCCGTGCCAGCCGGGGCCCGGAGCTGG	37%	1 bp insertion	
P3-4	Allele 1	TACGGGCGGGGGCCGTGC--GTTCCCCGTGCCAGCCGGGGCCCGGAGCTGG	80%	1 bp deletion	Homozygous
	Allele 2	TACGGGCGGGGGCCGTGC--GTTCCCCGTGCCAGCCGGGGCCCGGAGCTGG			
P3-5	Allele 1	TACGGGCGGGGGCCGTGCGGTTCCCCGTGCCAGCCGGGGCCCGGAGCTGG	69%	No edit	Monoallelic
	Allele 2	TACGGGCGGGGGCCGTGC--GTTCCCCGTGCCAGCCGGGGCCCGGAGCTGG	5.4%	1 bp deletion	
P3-6	Allele 1	TACGGGCGGGGGCCGTGCGGTTCCCCGTGCCAGCCGGGGCCCGGAGCTGG	78%	No edit	Monoallelic
	Allele 2	TACGGGCGGGGGCCGTGC--GTTCCCCGTGCCAGCCGGGGCCCGGAGCTGG	3%	1 bp deletion	
P3-7	Allele 1	TACGGGCGGGGGCCGTGCGGTTCCCCGTGCCAGCCGGGGCCCGGAGCTGG	69%	No edit	Monoallelic
	Allele 2	TACGGGCGGGGGCCGTGC--GTTCCCCGTGCCAGCCGGGGCCCGGAGCTGG	5.8%	1 bp deletion	
P3-8	Allele 1	TACGGGCGGGGGCCGTGCGGTTCCCCGTGCCAGCCGGGGCCCGGAGCTGG		No edit	WT
	Allele 2	TACGGGCGGGGGCCGTGCGGTTCCCCGTGCCAGCCGGGGCCCGGAGCTGG			
P3-9	Allele 1	TACGGGCGGGGGCCGTGCGGTTCCCCGTGCCAGCCGGGGCCCGGAGCTGG	33%	No edit	Chimeric
	Allele 2	TACGGGCGGGGGCCGTGC--GTTCCCCGTGCCAGCCGGGGCCCGGAGCTGG	4%	1 bp deletion	
	Allele 3	TACGGGCGGGGGCC----------	5%	28 bp deletion	
	Allele 4	TACGGGCGGGGGCC----------	4%	29 bp deletion	
P3-10	Allele 1	TACGGGCGGGGGCCGTGCGGTTCCCCGTGCCAGCCGGGGCCCGGAGCTGG	27%	No edit	Chimeric
	Allele 2	TACGGGCGGGGGCCGTGC--GTTCCCCGTGCCAGCCGGGGCCCGGAGCTGG	2%	1 bp deletion	
	Allele 3	----------	3%	59 bp deletion	
	Allele 4	TACGGGCGGGGGCC----------	3%	28 bp deletion	
	Allele 5	TACGGGCGGGGGCC----------	2%	29 bp deletion	
P3-11	Allele 1	TACGGGCGGGGGCCGTGCGGTTCCCCGTGCCAGCCGGGGCCCGGAGCTGG	35%	No edit	Chimeric
	Allele 2	TACGGGCGGGGGCCGTGC--GTTCCCCGTGCCAGCCGGGGCCCGGAGCTGG	3%	1 bp deletion	
	Allele 3	TACGGGCGGGGGCCGTGC----TTCCCCGTGCCAGCCGGGGCCCGGAGCTGG	39%	2 bp deletion	
P3-12	Allele 1	TACGGGCGGGGGCCGTGCGGTTCCCCGTGCCAGCCGGGGCCCGGAGCTGG		No edit	WT
	Allele 2	TACGGGCGGGGGCCGTGCGGTTCCCCGTGCCAGCCGGGGCCCGGAGCTGG			
P3-13	Allele 1	TACGGGCGGGGGCCGTGCGGTTCCCCGTGCCAGCCGGGGCCCGGAGCTGG	73%	No edit	Chimeric
	Allele 2	TACGGGCGGGGGCCGTGC--GTTCCCCGTGCCAGCCGGGGCCCGGAGCTGG	1.5%	1 bp deletion	
	Allele 3	TACGGGCGGGGGCC----------	0.4%	27 bp deletion	

Appendix Table 3L. CRISPR-Cas9 induced mutations in the transformed plants at T_1 generation of P3 for *SBE4*.

Plant no	Allele	Sequence	Percentage of mutation	Deletion/insertion/ Substitution	Mutant Zygosity
P3	Allele 1	GAAGTGATTCAAGACATTGAGGAAAATGTGAGTGAGGGTGTGATCAAAGA	48%	C to G substitution	Biallelic
	Allele 2	GAAGTGATTCAAGACATTGAGGAAAATGTGA--TGAGGGTGTGATCAAAGA	45%	1 bp deletion	
P3-1	Allele 1	GAAGTGATTCAAGACATTGAGGAAAATGTGAGTGAGGGTGTGATCAAAGA	43%	C to G substitution	Biallelic
	Allele 2	GAAGTGATTCAAGACATTGAGGAAAATGTGA--TGAGGGTGTGATCAAAGA	45%	1 bp deletion	
P3-2	Allele 1	GAAGTGATTCAAGACATTGAGGAAAATGTGAGTGAGGGTGTGATCAAAGA	88%	C to G substitution	Homozygous
	Allele 2	GAAGTGATTCAAGACATTGAGGAAAATGTGAGTGAGGGTGTGATCAAAGA			
P3-3	Allele 1	GAAGTGATTCAAGACATTGAGGAAAATGTGAGTGAGGGTGTGATCAAAGA	84%	C to G substitution	Homozygous
	Allele 2	GAAGTGATTCAAGACATTGAGGAAAATGTGAGTGAGGGTGTGATCAAAGA			
P3-4	Allele 1	GAAGTGATTCAAGACATTGAGGAAAATGTGAGTGAGGGTGTGATCAAAGA	40%	C to G substitution	Biallelic
	Allele 2	GAAGTGATTCAAGACATTGAGGAAAATGTGA--TGAGGGTGTGATCAAAGA	39%	1 bp deletion	
P3-5	Allele 1	GAAGTGATTCAAGACATTGAGGAAAATGTGAGTGAGGGTGTGATCAAAGA	39%	C to G substitution	Biallelic
	Allele 2	GAAGTGATTCAAGACATTGAGGAAAATGTGA--TGAGGGTGTGATCAAAGA	49%	1 bp deletion	
P3-6	Allele 1	GAAGTGATTCAAGACATTGAGGAAAATGTGAGTGAGGGTGTGATCAAAGA	42%	C to G substitution	Biallelic
	Allele 2	GAAGTGATTCAAGACATTGAGGAAAATGTGA--TGAGGGTGTGATCAAAGA	42%	1 bp deletion	
P3-7	Allele 1	GAAGTGATTCAAGACATTGAGGAAAATGTGAGTGAGGGTGTGATCAAAGA	41%	C to G substitution	Biallelic
	Allele 2	GAAGTGATTCAAGACATTGAGGAAAATGTGA--TGAGGGTGTGATCAAAGA	43%	1 bp deletion	
P3-8	Allele 1	GAAGTGATTCAAGACATTGAGGAAAATGTGAGTGAGGGTGTGATCAAAGA	0.3%	C to G substitution	Biallelic
	Allele 2	GAAGTGATTCAAGACATTGAGGAAAATGTGA--TGAGGGTGTGATCAAAGA	83%	1 bp deletion	
P3-9	Allele 1	GAAGTGATTCAAGACATTGAGGAAAATGTGAGTGAGGGTGTGATCAAAGA	42%	C to G substitution	Biallelic
	Allele 2	GAAGTGATTCAAGACATTGAGGAAAATGTGA--TGAGGGTGTGATCAAAGA	43%	1 bp deletion	
P3-10	Allele 1	GAAGTGATTCAAGACATTGAGGAAAATGTGAGTGAGGGTGTGATCAAAGA	41%	C to G substitution	Biallelic
	Allele 2	GAAGTGATTCAAGACATTGAGGAAAATGTGA--TGAGGGTGTGATCAAAGA	44%	1 bp deletion	
P3-11	Allele 1	GAAGTGATTCAAGACATTGAGGAAAATGTGACTGAGGGTGTGATCAAAGA		No edit	WT
	Allele 2	GAAGTGATTCAAGACATTGAGGAAAATGTGACTGAGGGTGTGATCAAAGA			
P3-12	Allele 1	GAAGTGATTCAAGACATTGAGGAAAATGTGAGTGAGGGTGTGATCAAAGA	37%	C to G substitution	Biallelic
	Allele 2	GAAGTGATTCAAGACATTGAGGAAAATGTGA--TGAGGGTGTGATCAAAGA	40%	1 bp deletion	
P3-13	Allele 1	GAAGTGATTCAAGACATTGAGGAAAATGTGAGTGAGGGTGTGATCAAAGA	38%	C to G substitution	Biallelic
	Allele 2	GAAGTGATTCAAGACATTGAGGAAAATGTGA--TGAGGGTGTGATCAAAGA	40%	1 bp deletion	

Appendix Table 3M. CRISPR-Cas9 induced mutations in the transformed plants at T_1 generation of P4 for *SBE1*.

Plant no	Allele	Sequence	Percentage of mutation	Deletion/insertion/ Substitution	Mutant Zygosity
P4	Allele 1	CCGCTCCTT----------CCCGGGAATCGCGGTCAG	42%	23 bp deletion	Biallelic
	Allele 2	CCGCTCCTTCCCTCTCTCGCTGATCGACC-------CCCGGGAATCGCGGTCAG	42%	3 bp deletion	
P4-1	Allele 1	CCGCTCCTTCCCTCTCTCGCTGATCGACC-------CCCGGGAATCGCGGTCAG	85%	3 bp deletion	Homozygous
	Allele 2	CCGCTCCTTCCCTCTCTCGCTGATCGACC-------CCCGGGAATCGCGGTCAG			
P4-2	Allele 1	CCGCTCCTT----------CCCGGGAATCGCGGTCAG	2.5%	23 bp deletion	Biallelic
	Allele 2	CCGCTCCTTCCCTCTCTCGCTGATCGACC-------CCCGGGAATCGCGGTCAG	84%	3 bp deletion	
P4-3	Allele 1	CCGCTCCTT----------CCCGGGAATCGCGGTCAG	0.2%	23 bp deletion	Biallelic
	Allele 2	CCGCTCCTTCCCTCTCTCGCTGATCGACC-------CCCGGGAATCGCGGTCAG	86%	3 bp deletion	
P4-4	Allele 1	CCGCTCCTTCCCTCTCTCGCTGATCGACC-------CCCGGGAATCGCGGTCAG	86%	3 bp deletion	Homozygous
	Allele 2	CCGCTCCTTCCCTCTCTCGCTGATCGACC-------CCCGGGAATCGCGGTCAG			
P4-5	Allele 1	CCGCTCCTTCCCTCTCTCGCTGATCGACC-------CCCGGGAATCGCGGTCAG	89%	3 bp deletion	Homozygous
	Allele 2	CCGCTCCTTCCCTCTCTCGCTGATCGACC-------CCCGGGAATCGCGGTCAG			
P4-6	Allele 1	CCGCTCCTTCCCTCTCTCGCTGATCGACC-------CCCGGGAATCGCGGTCAG	86%	3 bp deletion	Homozygous
	Allele 2	CCGCTCCTTCCCTCTCTCGCTGATCGACC-------CCCGGGAATCGCGGTCAG			
P4-8	Allele 1	CCGCTCCTTCCCTCTCTCGCTGATCGACC-------CCCGGGAATCGCGGTCAG	82%	3 bp deletion	Homozygous
	Allele 2	CCGCTCCTTCCCTCTCTCGCTGATCGACC-------CCCGGGAATCGCGGTCAG			
P4-10	Allele 1	CCGCTCCTT----------CCCGGGAATCGCGGTCAG	50%	23 bp deletion	Biallelic
	Allele 2	CCGCTCCTTCCCTCTCTCGCTGATCGACC-------CCCGGGAATCGCGGTCAG	30%	3 bp deletion	
P4-11	Allele 1	CCGCTCCTT----------CCCGGGAATCGCGGTCAG	50%	23 bp deletion	Biallelic
	Allele 2	CCGCTCCTTCCCTCTCTCGCTGATCGACC-------CCCGGGAATCGCGGTCAG	34%	3 bp deletion	

Appendix Table 3N. CRISPR-Cas9 induced mutations in the transformed plants at T_1 generation of P4 for *SBE2*.

Plant no	Allele	Sequence	Percentage of mutation	Deletion/insertion/ Substitution	Mutant Zygosity
P4	Allele 1	CTCAGGCCTCCGCCGCCGGGAGGGTTGCCCCTGCAGCTGCGCCTCCTCCT	45%	No edit	Monoallelic
	Allele 2	CTCAGGCCTCCGCCGCCGGG—GGGTTGCCCCTGCAGCTGCGCCTCCTCCT	25%	1 bp deletion	
P4-1	Allele 1	CTCAGGCCTCCGCCGCCGGGAGGGTTGCCCCTGCAGCTGCGCCTCCTCCT	42%	No edit	Monoallelic
	Allele 2	CTCAGGCCTCCGCCGCCGGG—GGGTTGCCCCTGCAGCTGCGCCTCCTCCT	43%	1 bp deletion	
P4-2	Allele 1	CTCAGGCCTCCGCCGCCGGGAGGGTTGCCCCTGCAGCTGCGCCTCCTCCT	43%	No edit	Monoallelic
	Allele 2	CTCAGGCCTCCGCCGCCGGG—GGGTTGCCCCTGCAGCTGCGCCTCCTCCT	42%	1 bp deletion	
P4-3	Allele 1	CTCAGGCCTCCGCCGCCGGGAGGGTTGCCCCTGCAGCTGCGCCTCCTCCT	34%	No edit	Chimeric
	Allele 2	CTCAGGCCTCCGCCGCCGGG—GGGTTGCCCCTGCAGCTGCGCCTCCTCCT	42%	1 bp deletion	
	Allele 3	CTCAGGCCTCCGCCGCCGGGA---GGTTGCCCCTGCAGCTGCGCCTCCTCCT	2.6%	1 bp deletion	
	Allele 4	CTCAGGCCTCCGCCGCCGGGATGGGTTGCCCCTGCAGCTGCGCCTCCTCCT	1.7%	1 bp insertion	
	Allele 5	CTCAGGCCTCCGCCGCCGGGAAGGGTTGCCCCTGCAGCTGCGCCTCCTCCT	1.5%	1 bp insertion	
P4-4	Allele 1	CTCAGGCCTCCGCCGCCGGGAGGGTTGCCCCTGCAGCTGCGCCTCCTCCT	56%	No edit	Chimeric
	Allele 2	CTCAGGCCTCCGCCGCCGGG—GGGTTGCCCCTGCAGCTGCGCCTCCTCCT	9.6%	1 bp deletion	
	Allele 3	CTCAGGCCTCCGCCGCCGGGA---GGTTGCCCCTGCAGCTGCGCCTCCTCCT	9%	1 bp deletion	
	Allele 4	CTCAGGCCTCCGCCGCCGGGATGGGTTGCCCCTGCAGCTGCGCCTCCTCCT	5.5%	1 bp insertion	
	Allele 5	CTCAGGCCTCCGCCGCCGGGAAGGGTTGCCCCTGCAGCTGCGCCTCCTCCT	1.6%	1 bp insertion	
P4-5	Allele 1	CTCAGGCCTCCGCCGCCGGGAGGGTTGCCCCTGCAGCTGCGCCTCCTCCT	44%	No edit	Monoallelic
	Allele 2	CTCAGGCCTCCGCCGCCGGG—GGGTTGCCCCTGCAGCTGCGCCTCCTCCT	42%	1 bp deletion	
P4-6	Allele 1	CTCAGGCCTCCGCCGCCGGGAGGGTTGCCCCTGCAGCTGCGCCTCCTCCT	33%	No edit	Chimeric
	Allele 2	CTCAGGCCTCCGCCGCCGGG—GGGTTGCCCCTGCAGCTGCGCCTCCTCCT	46%	1 bp deletion	
	Allele 3	CTCAGGCCTCCGCCGCCGGGA---GGTTGCCCCTGCAGCTGCGCCTCCTCCT	1.5%	1 bp deletion	
	Allele 4	CTCAGGCCTCCGCCGCCGGGATGGGTTGCCCCTGCAGCTGCGCCTCCTCCT	1%	1 bp insertion	
	Allele 5	CTCAGGCCTCCGCCGCCGGGAAGGGTTGCCCCTGCAGCTGCGCCTCCTCCT	0.4%	1 bp insertion	
P4-8	Allele 1	CTCAGGCCTCCGCCGCCGGGAGGGTTGCCCCTGCAGCTGCGCCTCCTCCT	35%	No edit	Chimeric
	Allele 2	CTCAGGCCTCCGCCGCCGGG—GGGTTGCCCCTGCAGCTGCGCCTCCTCCT	41%	1 bp deletion	
	Allele 3	CTCAGGCCTCCGCCGCCGGGA---GGTTGCCCCTGCAGCTGCGCCTCCTCCT	2.3%	1 bp deletion	
	Allele 4	CTCAGGCCTCCGCCGCCGGGATGGGTTGCCCCTGCAGCTGCGCCTCCTCCT	3.7%	1 bp insertion	
	Allele 5	CTCAGGCCTCCGCCGCCGGGAAGGGTTGCCCCTGCAGCTGCGCCTCCTCCT	0.3%	1 bp insertion	
P4-10	Allele 1	CTCAGGCCTCCGCCGCCGGG—GGGTTGCCCCTGCAGCTGCGCCTCCTCCT	76%	1 bp deletion	Homozygous
	Allele 2	CTCAGGCCTCCGCCGCCGGG—GGGTTGCCCCTGCAGCTGCGCCTCCTCCT			
P4-11	Allele 1	CTCAGGCCTCCGCCGCCGGG—GGGTTGCCCCTGCAGCTGCGCCTCCTCCT	24%	1 bp deletion	Biallelic
	Allele 2	CTCAGGCCTCCGCCGCCGGGAAGGGTTGCCCCTGCAGCTGCGCCTCCTCCT	59%	1 bp insertion	

Appendix Table 3O. CRISPR-Cas9 induced mutations in the transformed plants at T_1 generation of P4 for *SBE3*.

Plant no	Allele	Sequence	Percentage of mutation	Deletion/insertion/ Substitution	Mutant Zygosity
P4	Allele 1	TACGGGCGGGGGCCGTGC--GTTCCCCGTGCCAGCCGGGGCCCGGAGCTGG	54%	1 bp deletion	Homozygous
	Allele 2	TACGGGCGGGGGCCGTGC--GTTCCCCGTGCCAGCCGGGGCCCGGAGCTGG			
P4-1	Allele 1	TACGGGCGGGGGCCGTGC--GTTCCCCGTGCCAGCCGGGGCCCGGAGCTGG	79%	1 bp deletion	Homozygous
	Allele 2	TACGGGCGGGGGCCGTGC--GTTCCCCGTGCCAGCCGGGGCCCGGAGCTGG			
P4-2	Allele 1	TACGGGCGGGGGCCGTGC--GTTCCCCGTGCCAGCCGGGGCCCGGAGCTGG	78%	1 bp deletion	Homozygous
	Allele 2	TACGGGCGGGGGCCGTGC--GTTCCCCGTGCCAGCCGGGGCCCGGAGCTGG			
P4-3	Allele 1	TACGGGCGGGGGCCGTGC--GTTCCCCGTGCCAGCCGGGGCCCGGAGCTGG	82%	1 bp deletion	Homozygous
	Allele 2	TACGGGCGGGGGCCGTGC--GTTCCCCGTGCCAGCCGGGGCCCGGAGCTGG			
P4-4	Allele 1	TACGGGCGGGGGCCGTGC--GTTCCCCGTGCCAGCCGGGGCCCGGAGCTGG	82%	1 bp deletion	Homozygous
	Allele 2	TACGGGCGGGGGCCGTGC--GTTCCCCGTGCCAGCCGGGGCCCGGAGCTGG			
P4-5	Allele 1	TACGGGCGGGGGCCGTGC--GTTCCCCGTGCCAGCCGGGGCCCGGAGCTGG	77%	1 bp deletion	Homozygous
	Allele 2	TACGGGCGGGGGCCGTGC--GTTCCCCGTGCCAGCCGGGGCCCGGAGCTGG			
P4-6	Allele 1	TACGGGCGGGGGCCGTGC--GTTCCCCGTGCCAGCCGGGGCCCGGAGCTGG	83%	1 bp deletion	Homozygous
	Allele 2	TACGGGCGGGGGCCGTGC--GTTCCCCGTGCCAGCCGGGGCCCGGAGCTGG			
P4-8	Allele 1	TACGGGCGGGGGCCGTGC--GTTCCCCGTGCCAGCCGGGGCCCGGAGCTGG	83%	1 bp deletion	Homozygous
	Allele 2	TACGGGCGGGGGCCGTGC--GTTCCCCGTGCCAGCCGGGGCCCGGAGCTGG			
P4-10	Allele 1	TACGGGCGGGGGCCGTGC--GTTCCCCGTGCCAGCCGGGGCCCGGAGCTGG	79%	1 bp deletion	Homozygous
	Allele 2	TACGGGCGGGGGCCGTGC--GTTCCCCGTGCCAGCCGGGGCCCGGAGCTGG			
P4-11	Allele 1	TACGGGCGGGGGCCGTGC--GTTCCCCGTGCCAGCCGGGGCCCGGAGCTGG	81%	1 bp deletion	Homozygous
	Allele 2	TACGGGCGGGGGCCGTGC--GTTCCCCGTGCCAGCCGGGGCCCGGAGCTGG			

Appendix Table 3P. CRISPR-Cas9 induced mutations in the transformed plants at T_1 generation of P4 for *SBE4.*

Plant no	Allele	Sequence	Percentage of mutation	Deletion/insertion/ Substitution	Mutant Zygosity
P4	Allele 1	GAAGTGATTCAAGACATTGAGGAAAATGTGAGTGAGGGTGTGATCAAAGA	45%	C to G substitution	Biallelic
	Allele 2	GAAGTGATTCAAGACATTGAGGAAAATGTGA--TGAGGGTGTGATCAAAGA	47%	1 bp deletion	
P4-1	Allele 1	GAAGTGATTCAAGACATTGAGGAAAATGTGAGTGAGGGTGTGATCAAAGA	81%	C to G substitution	Homozygous
	Allele 2	GAAGTGATTCAAGACATTGAGGAAAATGTGAGTGAGGGTGTGATCAAAGA			
P4-2	Allele 1	GAAGTGATTCAAGACATTGAGGAAAATGTGAGTGAGGGTGTGATCAAAGA	44%	C to G substitution	Biallelic
	Allele 2	GAAGTGATTCAAGACATTGAGGAAAATGTGA--TGAGGGTGTGATCAAAGA	45%	1 bp deletion	
P4-3	Allele 1	GAAGTGATTCAAGACATTGAGGAAAATGTGAGTGAGGGTGTGATCAAAGA	85%	C to G substitution	Homozygous
	Allele 2	GAAGTGATTCAAGACATTGAGGAAAATGTGAGTGAGGGTGTGATCAAAGA			
P4-4	Allele 1	GAAGTGATTCAAGACATTGAGGAAAATGTGAGTGAGGGTGTGATCAAAGA	83%	C to G substitution	Homozygous
	Allele 2	GAAGTGATTCAAGACATTGAGGAAAATGTGAGTGAGGGTGTGATCAAAGA			
P4-5	Allele 1	GAAGTGATTCAAGACATTGAGGAAAATGTGAGTGAGGGTGTGATCAAAGA	87%	C to G substitution	Homozygous
	Allele 2	GAAGTGATTCAAGACATTGAGGAAAATGTGAGTGAGGGTGTGATCAAAGA			
P4-6	Allele 1	GAAGTGATTCAAGACATTGAGGAAAATGTGAGTGAGGGTGTGATCAAAGA	42%	C to G substitution	Biallelic
	Allele 2	GAAGTGATTCAAGACATTGAGGAAAATGTGA--TGAGGGTGTGATCAAAGA	43%	1 bp deletion	
P4-8	Allele 1	GAAGTGATTCAAGACATTGAGGAAAATGTGAGTGAGGGTGTGATCAAAGA	84%	C to G substitution	Homozygous
	Allele 2	GAAGTGATTCAAGACATTGAGGAAAATGTGAGTGAGGGTGTGATCAAAGA			
P4-10	Allele 1	GAAGTGATTCAAGACATTGAGGAAAATGTGAGTGAGGGTGTGATCAAAGA	77%	C to G substitution	Homozygous
	Allele 2	GAAGTGATTCAAGACATTGAGGAAAATGTGAGTGAGGGTGTGATCAAAGA			
P4-11	Allele 1	GAAGTGATTCAAGACATTGAGGAAAATGTGAGTGAGGGTGTGATCAAAGA	80%	C to G substitution	Homozygous
	Allele 2	GAAGTGATTCAAGACATTGAGGAAAATGTGAGTGAGGGTGTGATCAAAGA			

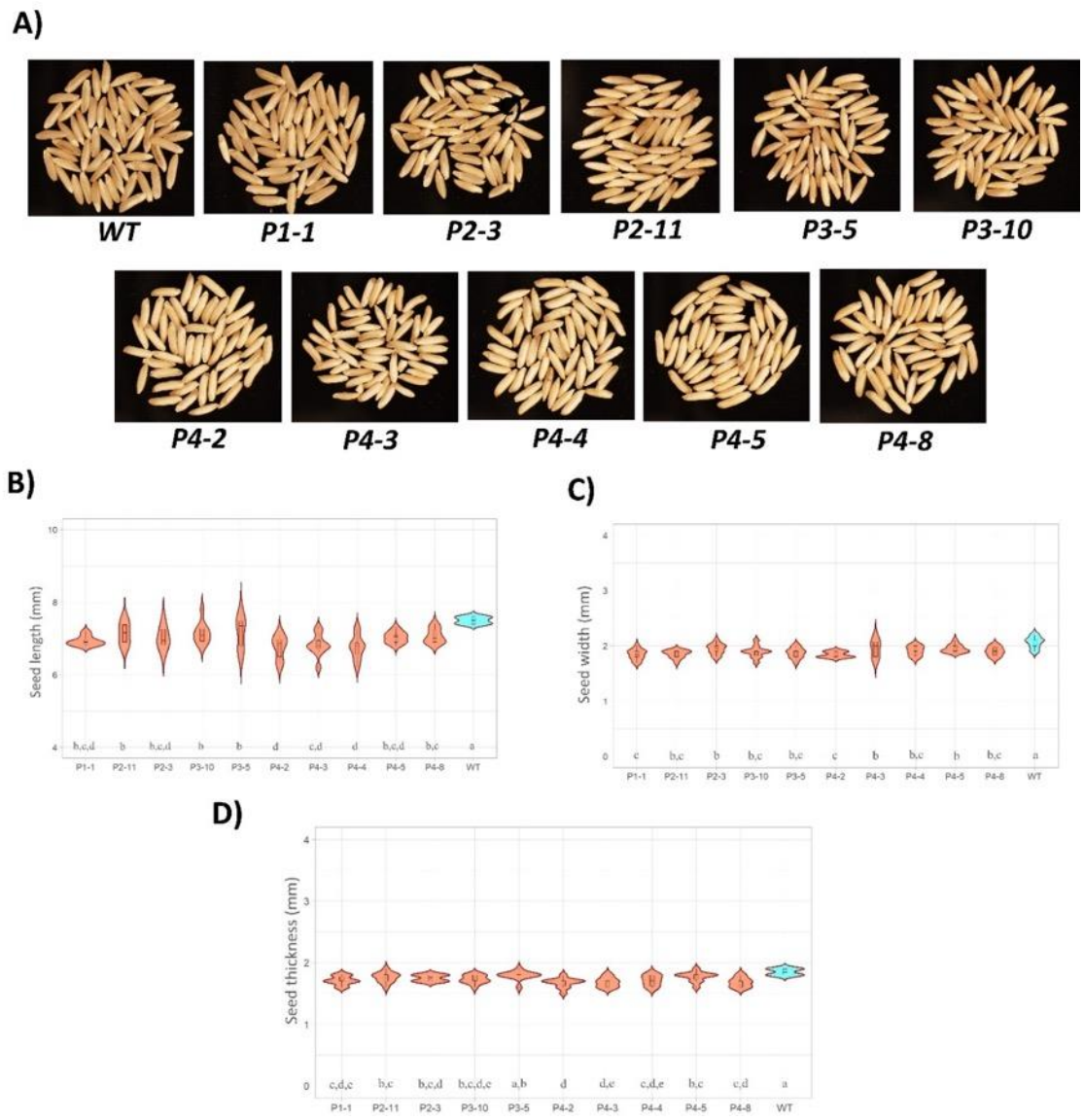

Appendix Figure 4. Seed morphology of WT and *SBE* edited plants (T_2 generation); A) Seed morphology of WT and *SBE* mutants (T_2 generation) B) seed length, C) Seed width D) Seed thickness of WT and edited SBE plants. In all three seed parameters, the edited *SBE* plants showed significantly lower value compared to WT. Values represent means ± SE (n = 10). The different letters indicate significant differences at $p < 0.05$.

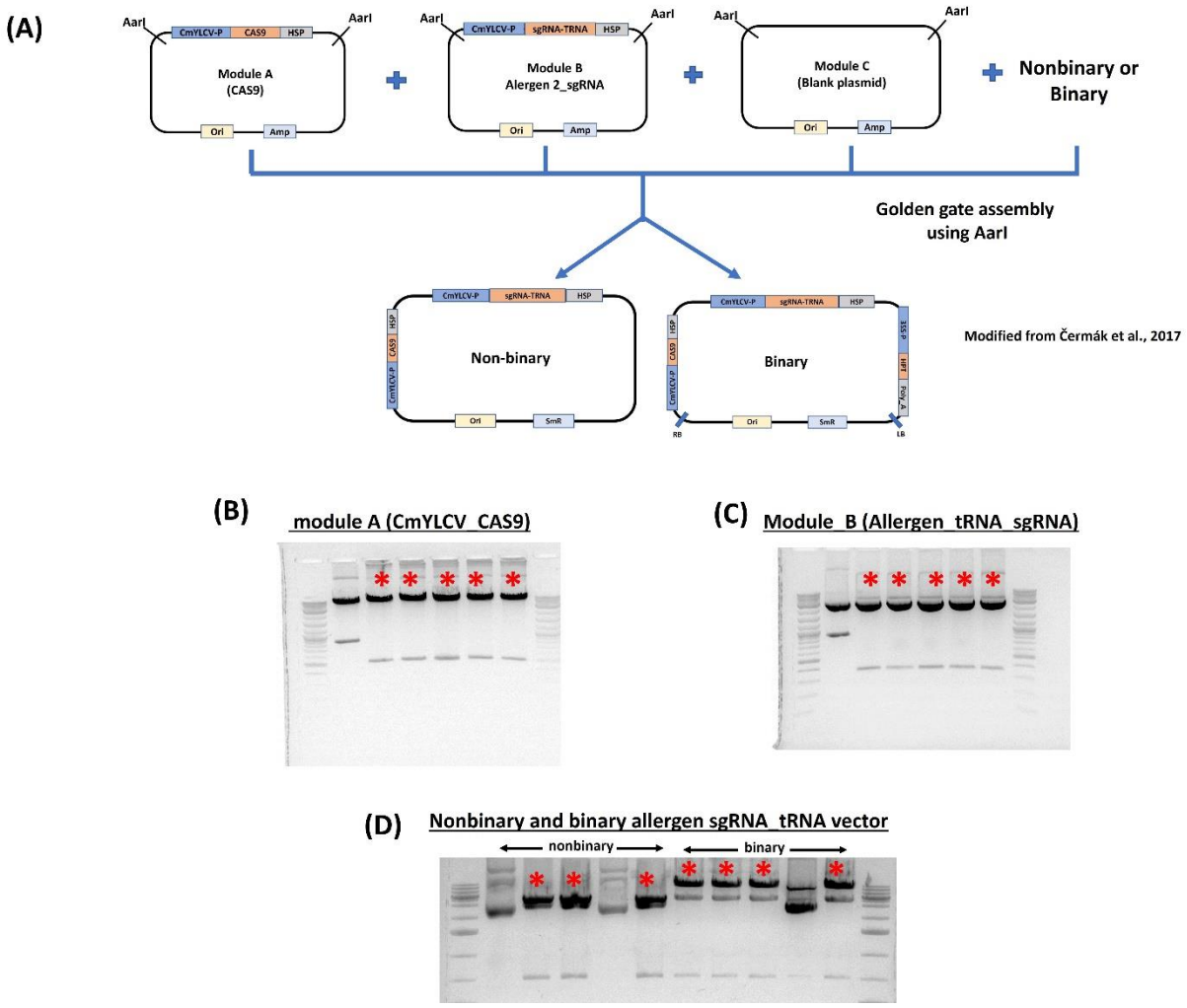

Appendix Figure 5: Cloning of Polycistronic tRNA_gRNAs (PTG) of *Ara h 2* gene into destination vector (non-binary and binary); A) Schematic diagram of golden gate assemble assembly for making CRISPR-CAS9 vector; B), C) and D) confirmation of positive clones by digestion with specific restriction enzymes. "*" indicates the positive clones of respective vectors.

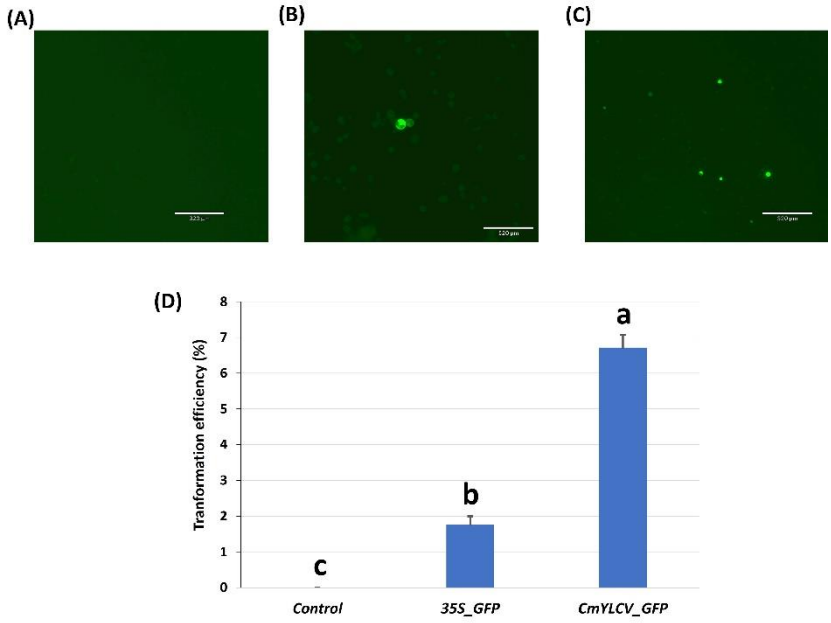

Appendix Figure 6. GFP expression under 35S and CmYLCV promoter in peanut protoplast. Micrograph of A) control protoplast (no GFP plasmid) B) protoplast with GFP expression under 35S; C) protoplast with GFP expression under CmYLCV promoter D) The transformation efficiency (TE) of protoplasts transformed with 35S: GFP and CmYLCV:GFP plasmid. The protoplasts TE was evaluated after incubation in 50% PEG solution. Values represent means ± SE (n = 7). The different letters indicate significant differences at $P < 0.05$.

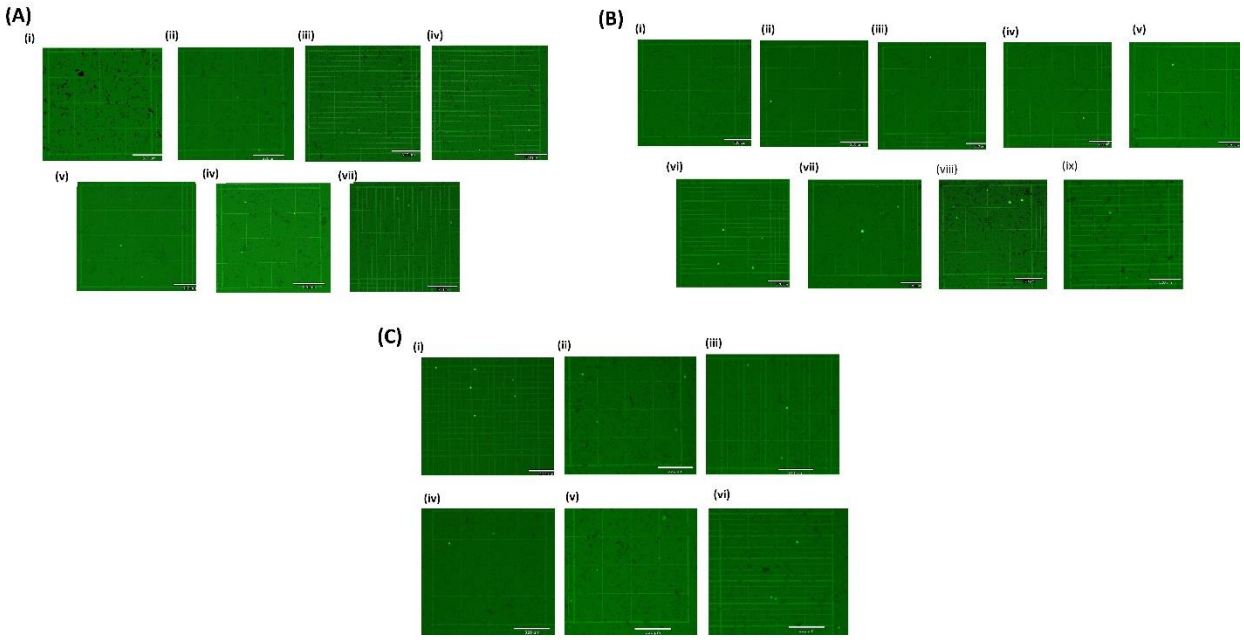

Appendix Figure 7. Effect of PEG concentration, plasmid concentrations and PEG incubation time on protoplast transfection; A) (i)-(vii) Micrographs of protoplasts expressing *CmYLCV: GFP* under GFP field treated with 20%, 30%, 40%, 50%, 60%, 70% and 80% PEG concentrations respectively. The protoplasts were treated with 250 µg of *CmYLCV: GFP* plasmid for 5 min. B) (i)-(ix) Micrographs of protoplasts expressing *CmYLCV: GFP* under GFP field treated with 0 µg , 20 µg, 40 µg, 80 µg, 100 µg, 150 µg, 200 µg, 250 µg and 300 µg plasmid concentrations respectively. In this case, the condition was 50% PEG and 5 min PEG incubation time. C) (i)-(vi) Micrographs of protoplasts expressing *CmYLCV: GFP* under GFP field treated with 5 min, 10 min, 20 min, 30 min, 40 min and 50 min PEG incubation time respectively. Here, the protoplasts were incubated with 250 µg of *CmYLCV: GFP* plasmid and 50% PEG.

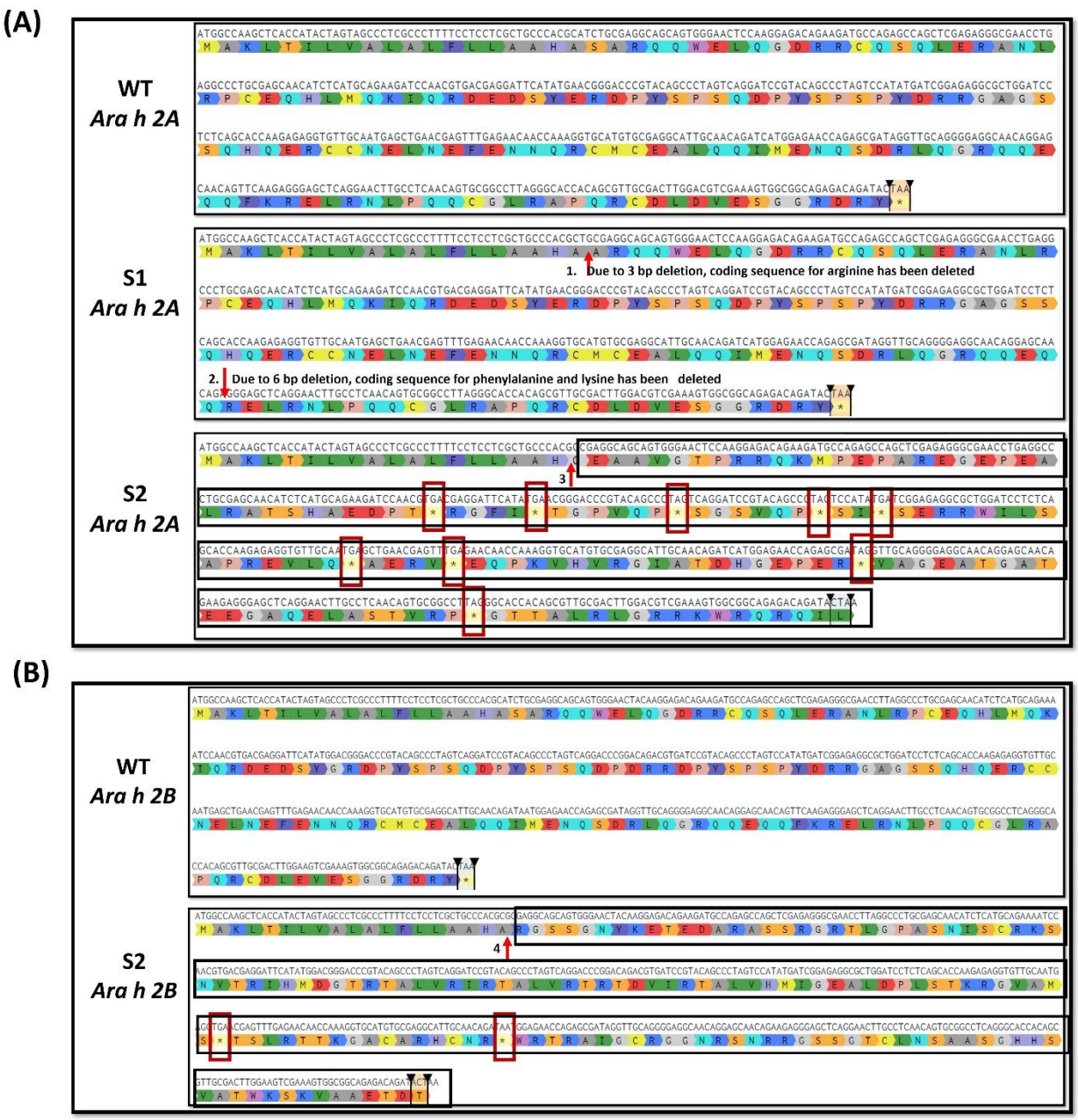

Appendix Figure 8. Change in the coding sequence at *Arah 2* gene due to deletion in two sgRNA region*:* A) Coding sequence of *Ara h 2A* in WT and edited sample S1 and S2. B) Coding sequence of *Ara h 2B* in WT and edited sample S1 and S2.

1 ↑ indicates where due to 3 bp deletion, coding sequence of arginine has been removed and 2 ↑ indicates where due to 6 bp deletion, coding sequence of phenylalanine and lysin has been removed in *Ara h 2A* of S2

Frameshift mutation (black block) occurred due to the mutation in the two gRNA region for S2 samples. 3↑ and 4↑ indicates the frameshift start site in *Ara h 2A* and *Ara h 2B* of S2 edited sample. However, premature stop codons were generated in the coding sequence of both gene copies in edited sample S2. Red block indicates the premature stop codon position in the coding region of *Ara h 2A* and *Ara h 2B* in S2.

Appendix Table 4

Primers used in this study.

Primer	Sequence (5′-3′)
Arah 2AF	GAAGGTGCATTAAACATTGAACATGTG
Arah 2AR	ATGATCTTTATTATTACCAAAACTAACATAA
Arah 2BF	GAAGGTGCATTAAACATTGAACATCTC
Arah 2BR	ATGATCTTTATTATTACCAAAACTAACATTA
Arah2A_NGS_1F	TCGTCGGCAGCGTCAGATGTGTATAAGAGACAGCACCACACACTCTTCAATACACATTC
Arah2A_NGS_1R	GTCTCGTGGGCTCGGAGATGTGTATAAGAGACAGTCCTGACTAGGGCTGTACGGG
Arah2A_NGS_2F	TCGTCGGCAGCGTCAGATGTGTATAAGAGACAGGATCCTCTCAGCACCAAGAGAGGT
Arah2A_NGS_2R	GTCTCGTGGGCTCGGAGATGTGTATAAGAGACAGCAAGTCGCAACGCTGTGGTG
Arah2B_NGS_1F	TCGTCGGCAGCGTCAGATGTGTATAAGAGACAGTACCTCACATGCAAAATCCCTC
Arah2B_NGS_1R	GTCTCGTGGGCTCGGAGATGTGTATAAGAGACAGGCCTAAGGTTCGCCCTCTCG
Arah2B_NGS_2F	TCGTCGGCAGCGTCAGATGTGTATAAGAGACAGAAGGTGCATGTGCGAGGCAT
Arah2B_NGS_2R	GTCTCGTGGGCTCGGAGATGTGTATAAGAGACAGTAGCTTATATATAAGCTATTTTCTTT